Sorption kinetics and equilibrium isotherms of phosphine and evaluation of chlorine dioxide gas during wheat fumigation

by

Rania Marie Buenavista

B.S., University of the Philippines – Los Baños, 2018

A THESIS

submitted in partial fulfillment of the requirements for the degree

MASTER OF SCIENCE

Department of Grain Science and Industry
College of Agriculture

KANSAS STATE UNIVERSITY
Manhattan, Kansas

2022

Approved by:

Co-Major Professor
Dr. Mark E. Casada

Approved by:

Co-Major Professor
Dr. Kaliramesh Siliveru

Copyright

Abstract

Increased genetic-based resistance to widely used fumigant phosphine among stored-product insect species is a result of fumigating challenges in leaky pest management practices. Phosphine can be prolonged for use as a fumigant through proper fumigation practices and efficient insect resistance monitoring. Along with prolonging the use of phosphine, it is also critical to find potential fumigant alternatives that could effectively control stored-product insects once phosphine is no longer effective.

In the first study, fumigation flasks, half-filled with hard red winter wheat, were fumigated to achieve desired phosphine concentration levels of 400, 700, 1000, 1500, 2000, and 2400 ppm at 25°C. Gas chromatographic analysis of headspace gas showed the change in concentration through time until it reached an equilibrium. Pseudo-first order and pseudo-second order kinetic models were fitted to phosphine sorption data and sorption isotherms were plotted fitting Langmuir, Freundlich, and Redlich-Peterson sorption isotherm models. All three models showed good fit (standard error of prediction = 0.46-0.47). Higher equilibrium concentration was observed at the maximum phosphine concentration (2400 ppm), indicating that maximum adsorption capacity of wheat kernels was still not met. Total sorbed phosphine at equilibrium was important in determining the rate and maximum quantity of phosphine uptake in wheat.

The second objective of this study focused on further evaluation of chlorine dioxide as a potential fumigant in terms of wheat kernel and flour characteristics. Hard red spring wheat kernels were exposed to varying levels of gaseous ClO_2 concentrations (200, 300, 400, and 500 ppm) and held in a gas-tight bucket assembly for 24 h after achieving the nominal concentration. Three vials containing 20 unsexed adults of lesser grain borer (*Rhyzopertha dominica* (Fabricius)) were placed at top, middle, and bottom layers of wheat mass during fumigation to assess insect mortality. ClO_2

gas treatment achieved complete insect mortality at 500 ppm across all vial locations. Adult progeny reduction was found to be highest for 500 ppm treatment ranging from 96 to 99%. Significant reduction (37.7-51.1%) in germination rate resulted after exposure to 300-500 ppm. In terms of flour color, lightness value significantly increased after treatment of 200-500 ppm. The pH value of wheat flour had significant reduction from 6.2 to 6.1 after 500 ppm treatment. In terms of pasting characteristics, peak and final viscosities of ClO_2-treated wheat flour at 200-500 ppm significantly decreased from 3303.7 to 3073.3 cP and from 3515.0 to 3208.3 cP, respectively. No significant difference was observed in flour quality and functionality parameters, including falling number, trough viscosity, breakdown viscosity, starch damage, and mixolab dough behavior properties. Overall, ClO_2 gas treatment at 500 ppm was effective in killing adult lesser grain borers without negatively affecting wheat flour quality parameters but affected wheat kernel viability.

Table of Contents

List of Figures

List of Tables

Acknowledgements

I would like to express my gratitude and heartfelt appreciation to the following people who have extended their help and support in completion of this manuscript.

• To Dr. Kaliramesh Siliveru, my major professor, for his mentorship, guidance, patience, valuable inputs, and support in my research. I would have not surpassed all my setbacks without his support and words of encouragement.

• To Dr. Mark Casada, my co-major professor, for allowing me to work in USDA-ARS CGAHR as part of my research work. I am grateful for his guidance, valuable inputs, and patience in my research.

• To Dr. Bhadriraju Subramanyam for accepting to be part of my supervisory committee and helping me improve my manuscript and experimental protocol, for allowing me to use his resources and chlorine dioxide gas generator for my experiments.

• To Dr. Tom Phillips for allowing me to work in his laboratory to perform my gas chromatograph experiments and guiding me throughout my phosphine research work.

• To Jamie Aikins and Dr. Erin Scully for their hands-on support and for answering all my questions regarding gas chromatography. I also would like to thank Xiao Li for sharing her space in the environmental chamber so I can proceed with my experiments.

• To Dr. Xinyi E for helping me with my experiments and sharing her expertise on chlorine dioxide gas.

• To Scott Graber for fabricating my gas-tight buckets and for ensuring my safety for my chlorine dioxide gas experiments.

• To Dr. Dennis Tilley and Dianna Halcumb for helping me with material procurement. I would also like to thank Dr. Paul Armstrong and Dr. Dan Brabec for sharing their laboratory materials.

• To Roselle Barretto for helping me with my experiments, improving my manuscript, and his suggestions to improve my presentation skills. I would also like to express my gratitude for his endless encouragement and support in my research.

• To Clayton Van Meter and Clay Thomas for their help during troubleshooting and plumbing of the gas chromatograph.

• To Sherif Elsayed for his advice in my phosphine work and for helping me during applicator licensure examination.

• To Dr. Marvin Petingco and Manivannan Selladurai for providing transportation and for their help during material hauling.

• To Dr. Li for allowing me to use his instruments for my wheat quality analysis and to Dr. Greg Aldrich for allowing me to use his laboratory for my milling experiments.

• To Elizabeth Maghirang for introducing the opportunity of pursuing graduate studies in KState. Special thanks to all PhilSA members for their warm welcome.

• To my labmates (Jared Rivera, Manoj Pulivarthi, Shivaprasad Prakash, Anu Suprabha Raj, Roselle Barretto, Mohana Yoganandan) and lab interns (Stanzin Chosdon and Maddy Rosenthal) for their help in conducting my experiments and for providing constructive feedback on my manuscript and presentation. I appreciate their words of encouragement and support.

• To USDA-ARS Center for Grain and Animal Health for funding my research and to all faculty, staff, and graduate students of the Department of Grain Science and Industry for their assistance and support.

Chapter 1 - Introduction

1.1 Problem Statement

In the United States, wheat is one of the major staple food crops that ranks third in terms of annual production, planted acreage, and gross farm receipts only next to corn and soybeans. In total, 34.8 million metric tons of wheat from 37.2 million acres of harvested land was recorded for marketing year 2021-2022 in the U.S. (USDA, 2022). Wheat production varies in quantity from year to year based on environmental conditions, and planting and harvesting practices. Storing grains during over-production is a strategic way to meet the demand for wheat during under-production seasons (Neethirajan et al., 2007).

Fumigation is a widely used pest control method for stored commodities against various insect pests. Historically, phosphine has been widely used fumigant for both static and in-transit application (USDA, 2020). In 1970s, first global survey revealed incidence of phosphine resistance among major stored-grain insect pests. Two phenotypes of phosphine resistance – strong and weak – among insect pests requires about 10- to 50-fold and ≥ 100-fold concentrations higher than the concentrations needed to suppress susceptible strains of insect pests, respectively (Nayak et al., 2015; Afful et al., 2020; Afful et al., 2021). This resistance problem has been exacerbated by overuse of phosphine due to lack of fumigant alternatives. Phosphine is preferred because it is easy to apply, has low cost, and suitable in a wide range of storage conditions and does not leave residue.

With the growing concerns of phosphine-resistance insect pests in the U.S. and across the globe, the sustainability of phosphine as an effective fumigant has been put at risk. Research efforts have been made to prolong the use of phosphine and to find alternative fumigants for chemical stored product pest management. Several researchers have established the relationship of selected engineering variables and ecosystem conditions, but these studies were insufficient to fully

understand why fumigant concentrations in the grain bin are not consistent during treatments (Agrafioti et al., 2020). Sorption is one of the important factors needed to be accounted as equilibrium sorption data is missing in these studies. Sorption equilibrium data is critical in improving the accuracy of modelling studies for phosphine-wheat fumigation systems. Only few studies have investigated phosphine sorption effects of phosphine fumigation efficacy and other factors affecting phosphine sorption in wheat (Berck, 1968; Dumas, 1980; Soma et al., 1996; Xiaoping et al., 2004; Daglish & Pavic, 2008). There is also a lack of equilibrium data for phosphine sorption in wheat kernels that would be helpful in understanding phosphine uptake and sorption capacity of wheat.

Chlorine dioxide is a potential alternative fumigant to phosphine that has been proven to be effective in killing major stored product insect pests in recent research studies (E et al., 2017). However, there is still limited research published regarding its effect on wheat kernel and flour quality parameters. It is important to determine specific concentrations that can achieve complete insect mortality but not cause any negative effects on the product quality of wheat. Wheat kernel and flour characteristics are important considerations as it relates to final product quality and consumer acceptability.

1.2 Research Objectives

This research focused on understanding sorption of phosphine into wheat kernels during fumigation and evaluation of chlorine dioxide as a potential alternative fumigant to phosphine in terms of wheat quality parameters. Specific objectives of this study are listed below:

1. Develop sorption kinetic and isotherm models for phosphine-wheat system.
2. Determine effective chlorine dioxide concentration for complete mortality of adult lesser grain borers during wheat fumigation with non-continuous gas supply.

3. Determine influence of chlorine dioxide treatment on wheat kernel quality and flour characteristics.

1.3 Outline

This thesis consists of four chapters excluding the current chapter. Chapter 2 provides comprehensive literature review of wheat storage and fumigation using phosphine and chlorine dioxide gas. Development of sorption kinetics and equilibrium isotherm models of phosphine into wheat kernels are discussed in Chapter 3. The effects of chlorine dioxide gas treatment on mortality of adult lesser grain borers and wheat kernel and flour characteristics are described in Chapter 4. Lastly, summary of findings, conclusions, and recommendations for future work based on the two presented studies are reported in Chapter 5.

1.4 References

Afful, E., Cato, A., Nayak, M. K., & Phillips, T. W. (2021). A rapid assay for the detection of resistance to phosphine in the lesser grain borer, Rhyzopertha dominica (F.) (Coleoptera: Bostrichidae). Journal of Stored Products Research, 91, 101776.

Afful, E., Tadesse, T. M., Nayak, M. K., & Phillips, T. W. (2020). High-dose strategies for managing phosphine-resistant populations of Rhyzopertha dominica (F.) (Coleoptera: Bostrichidae). Pest management science, 76(5), 1683-1690.

Agrafioti, P., Kaloudis, E., Bantas, S., Sotiroudas, V., & Athanassiou, C. G. (2020). Modeling the distribution of phosphine and insect mortality in cylindrical grain silos with computational fluid dynamics: validation with field trials. Computers and electronics in agriculture, 173, 105383.

Berck, B. (1968). Sorption of phosphine by cereal products. Journal Of Agricultural and Food Chemistry, 16(3), 419-425. doi: 10.1021/jf60157a009.

Daglish, G. J., & Pavic, H. (2008). Effect of phosphine dose on sorption in wheat. Pest Management Science: formerly Pesticide Science, 64(5), 513-518.

Dumas, T. (1980). Phosphine sorption and desorption by stored wheat and corn. Journal of agricultural and food chemistry, 28(2), 337-339.

E, X., Subramanyam, B., & Li, B. (2017). Efficacy of ozone against phosphine susceptible and resistant strains of four stored-product insect species. Insects, 8(2), 42.

Nayak, M. K., Daglish, G. J., & Phillips, T. W. (2015). Managing resistance to chemical treatments in stored products pests. Stewart Postharvest Rev, 11(3).

Neethirajan, S., Karunakaran, C., Jayas, D. S., & White, N. D. G. (2007). Detection techniques for stored-product insects in grain. Food control, 18(2), 157-162.

Soma, Y., Kishino, H., & Akagawa, T. (1996). Sorption of phosphine in cereal grains and beans. Research Bulletin of the Plant Protection Service (Japan).

Xiaoping, Y., Zhanggui, Q., Daolin, G., & Wanwu, L. (2004, August). Adsorption of phosphine by wheat, paddy and corn. In Proceedings of the International Conference on Controlled Atmosphere and Fumigation in Stored Products. Gold-Coast Australia (pp. 8-13).

US Department of Agriculture (USDA). (2022). Retrieved 23 July 2022 from https://www.ers.usda.gov/topics/crops/wheat/.

US Department of Agriculture (USDA). (2020). Fumigation handbook. Retrieved 26 July 2022 from https://www.ams.usda.gov/sites/default/files/media/FumigationHB.pdf.

Chapter 2 - Wheat Storage and Fumigation using Phosphine and Chlorine Dioxide: Literature Review

2.1 Grain Storage

Harvested wheat grains primarily have a high moisture content of 14-16% and are susceptible to spoilage by insects and microorganisms in storage. Since wheat is seasonally produced in the United States, the surplus wheat grains during high production season should be stored under favorable environmental conditions by maintaining a low moisture content to prevent deterioration and attack of insect pests. In this way, an adequate supply of grains will be available during low production periods.

In farms, wheat grains may be stored temporarily or for long-term. Temporary storage techniques are often done to keep the harvested grains from rodents, insects, and molds prior to drying. Grains are also stored short-term after drying when all bins suitable for long-term storage are still occupied by the harvest from the previous season (FAO, 2002). Dry, cooled grains can be stored for long-term if managed properly. Although drying grains would lead to low moisture content, various physical, biological, and chemical factors can still influence the rate of deterioration of grains, which include temperature, moisture, carbon dioxide, oxygen, insects, rodents, birds, storage structure, geographical location, and grain characteristics (Jayas & White, 2003).

For wheat used as livestock feed, the freshly harvested grains are usually transferred in gas-tight silos. Sealed storage is an effective method for reducing the deterioration rate of grains due to the increase in oxygen levels in the structure brought by the respiration of the grain and insect pests (FAO, 2002). According to Brooker et al. (1992), the air in the interstitial space during storage experiences an oxygen reduction from 21% down to 0.02%. In addition, the pH level of

the grain also decreases as fermentation occurs. These phenomena make the environment less conducive for the growth and survival of insect pests and microorganisms.

In general, storage aim to maintaining the quality of grains within standard for human consumption is necessary. To achieve this goal, the presence of molds and insects should be minimized. The proliferation of insects leads to the secretion of wastes that can contaminate the grains. When grains are milled, the presence of insects and molds remains in the final product in the form of fragments. In most postharvest facilities, grains pass through a piece of cleaning equipment to separate the impurities and insects from the grains before milling. However, this process fails to remove the insects thriving inside wheat grains; thus, contamination can still exist (Reed et al., 1989).

2.1.1 US Steel Corrugated Silo

On January 2020, the National Agricultural Statistics Service (NASS) reported a total of 39.8 million metric tons of wheat stored across the U.S. which is 9% lower than the previous year's wheat grain stocks. Of these, 11.3 million metric tons represent on-farm stored grains, while 28.3 million metric tons correspond to off-farm storage stocks. The on-farm stored grains increased by 3%, while the off-farm stocks decreased by 13% as compared to the previous year. Within the period of September to November 2019, U.S. experienced a decrease of about 11.1 million metric tons or 35% within the same span of the previous year's stocks (NASS, 2020). Total wheat and other cereal production have been decreasing since the late 1990s mainly due to the increase in corn and soybean production and decrease in total planted acres for wheat and sorghum. Another factor was the unfavorable weather during the previous years that caused relatively lower yields. During this peak in late 1990s, the total production had exceeded the storage capacity of Kansas, which led to the establishment of more storage bins in 2000. Although Kansas is relying more on

off-farm storage facilities, various factors influence the increase in on-farm storage for cereal crops, which may be seen in trends in the coming years. These include a) production flexibility leading to varying crop combinations, b) procurement of larger hauling vehicles allowing the operators to haul grains straight to its client without the use of local grain elevators, c) the increase in acres of land planted with specialty crops, d) bottleneck concerns during harvest period, and e) grain quality issues (Dhuyvetter et al., 2007).

These on-farm and off-farm storage structures are often made of overlapping corrugated steel sheets overlapped, either welded or bolted, to form the wall and roof ridges. With the use of corrugated sheets, the wall strength of the silo is reinforced due to less contact of the metal sheets against the pressure induced by the grain mass against the wall. The typical grain silo in the U.S. has an open-eave roof design that lessens the buildup of moisture in the headspace. The base of the silo may either be conical or flat, with a pathway for grain unloading. A hopper-bottom silo allows the operator to achieve lower material handling expenditures due to easier grain unloading. On average, a U.S. silo can store about 10.9 metric tons to over 21.8 thousand metric tons of wheat grains (Cook, 2016). Figure 2.1 shows the research grain storage bins at the USDA Center for Grain and Animal Health Research (CGAHR) in Manhattan, Kansas.

Figure 2.1 Research grain storage bins at USDA CGAHR, Manhattan, Kansas

The common parts of a silo include walk-in door, ladder system inside and outside the bin, inspection hatch at the roof, and cap and rib roof panels (Cook, 2016). The bulk of grains is loaded into the silo using a grain elevator rather than using inclined conveyor systems as it is more cost-efficient due to the extreme height of most silos. If the grains are intended for livestock, a blower system is used to ease the loading of grains. However, this supplemental system does not apply to grains intended for human consumption due to the high incidence of grain cracking caused by the blowers. On the other hand, the unloading of grains is usually exhibited under the influence of gravity wherein the grains exit at the bottom of the silo. An auger is utilized to catch the unloaded grains and to transfer it to a truck or a nearby grain storage bin. In the absence of auger, farm managers opt to use grain vacuum to facilitate the unloading of grains (Lee, 2018).

2.1.2 Mold and other Deterioration Issues

Deterioration, usually due to mold or insect activity, is generally avoided by maintaining proper moisture and temperature levels of the grain safely stored in concrete or metal bins. Schroth et al. (1998) stated that the moisture content of the grain determines its storage life before spoilage and deterioration occurs. In order to achieve higher efficiency in harvesting with the use of a combine harvester, wheat grains are usually harvested at 16 to 20% moisture content which is not ideal for storage. Wheat grains should be dried to a moisture content of at most 14.5% wet basis to prevent the proliferation of mycotoxins and the occurrence of spoilage (Megan et al., 2010). Nithya et al. found that at 15 to 16% moisture content (wet basis), durum wheat can last up to 13 weeks in storage at 10 and 20 °C and 4 weeks in storage at 30 °C; at 17%, 18%, 19%, and 20% moisture content (wet basis), durum wheat can last up to 2 weeks. In the research of Karunakaran et al. (2001), safe storage was studied in relation to the germination capacity of the grain. Storage is considered ‘safe’ when the conditions would decrease the germination capacity to not less than

90%. The length of storage is considered in determining the maximum moisture content of the grains for safe storage. For wheat, maximum moisture content of 14% wet basis should be observed for storing up to 6 months, and 13% m.c. wet basis when storing for more than 6 months (McKenzie & Fossen, 2002).

When the moisture content of wheat grains has been reduced to the recommended moisture content for safe storage, potential quality deterioration could be caused by factors such as lack of adequate observation, insufficient insect control, improper grain cooling, and poor initial grain quality. Although drying is usually done prior to storage, the moisture content of grains can still fluctuate due to varying environmental conditions which influence grain temperature. The temperature gradient across the bin, as well as that of the internal and external parts of the bin, causes moisture migration. In effect, accumulation of moisture leads to grain spoilage. The bulk of grain has the same temperature as that of its surrounding air. The outside temperature during cold season decreases to 20 °F on the average, which causes the walls of the bin and the grains at its periphery to decrease in temperature (McKenzie & Fossen, 2002). As the center of the grain mass retains its initial temperature while the outer part of the grain mass becomes cooler, both air and moisture circulate in the bin due to temperature difference. The convection currents of air aid moisture migration, increasing the moisture at the top part of the bin. The opposite direction of convection currents can be observed during summer, wherein the bottom part of the bin accumulates moisture. Figure 2.2 shows the direction of convection currents of air and moisture during late fall and winter.

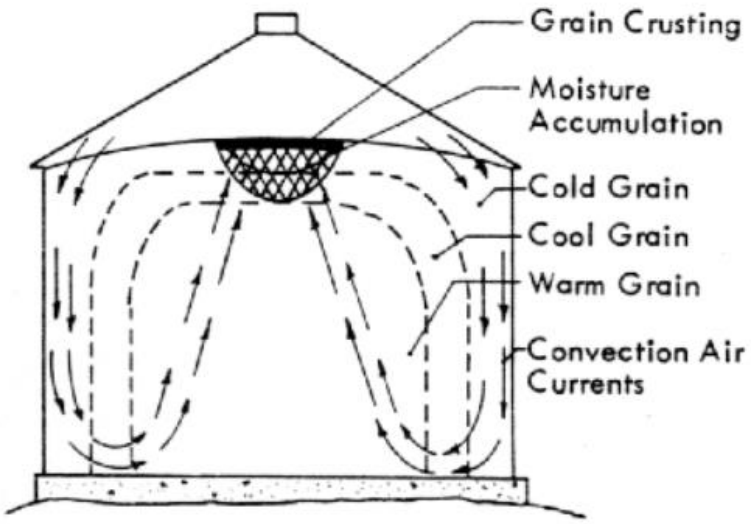

Figure 2.2 Direction of convection currents of air and moisture during late fall and winter (McKenzie & Fossen, 2005)

Besides moisture migration, condensation is also a major problem in grain storage. It occurs as the amount of moisture in the surrounding air exceeds the capacity of air to absorb, which is observed when the temperature of grain is lower than the dew point temperature of the air passing through it. Excess moisture condenses on the grain and silo wall (Shelton & Jones, 1998). The varying headspace conditions also influence the occurrence of condensation. Headspace temperature exceeds ambient temperature during the daytime when the sun's solar radiation directly heats the steel silos and approaches the ambient temperature at night. Aside from direct heat from the sunlight, natural convection currents induce air infiltration through the roof leak points such as the eave and vents. Water holding capacity of the air in the headspace rises as its temperature increases (Lawrence & Maier, 2011).

To prevent condensation, aeration should be done when the air temperature is the same or lower than that of the grain mass (Shelton & Jones, 1998). Aeration is different from drying. Cooling the grains through aeration is a grain management technique to prevent condensation and moisture migration, which can result to insect activity and mold development. Due to varying air

temperatures outside the bin, different storage temperatures should be maintained throughout the year. The direction of moving air can be upward or downward, but for practical purposes, upward aeration is preferred. In an upward aeration system, the endpoint of the stream is at the top of the bin. The operators can easily monitor the headspace if the air has completely cooled the grain mass. In the study of Morales-Quiros et al. (2019), chilled aeration of grain bulk during summer was explored in pursuit of lowering the average temperature across a silo. Through this mechanism, the average temperature of 1350-ton wheat grains were decreased by 11 ℃ in a span of 175 hours for their first trial and 20.4 ℃ in a span of 245 hours for their second trial. In comparison to normal aeration using ambient air, the average temperature inside the silo was above 25 ℃ for both Trial 1 and Trial 2. This research concluded that grain chilling down to a temperature below 20 ℃ poses a viable solution for controlling insect activity and population during the high-temperature season. Through the chilled aeration, the insect population was observed to decrease drastically. Table 2.1 shows the target grain storage temperatures in the United States (Buschermohle & Wilhelm, 2005). Relatively lower target grain storage temperature is observed during cold seasons during the months of November to February. Meanwhile, Table 2.2 shows the estimated aeration cooling and warming cycles (hours) in the United States. Lower airflow rates translate to longer time of aeration cycle. Moreover, increasing airflow rate requires less time to perform aeration to achieve target grain storage temperature. Longer aeration cycle is observed during winter, followed by fall and spring, respectively.

Table 2.1 Target grain storage temperatures in the United States (Buschermohle & Wilhelm, 2005)

Month	Temperature (° F)
September	55-65
October	55-65
November	40-50
December - February	35-45
April	60

Table 2.2 Estimated aeration cooling and warming cycles (hours) (Buschermohle & Wilhelm, 2005)

Airflow (cfm/bu)	Aeration Cycles (hours)		
	Fall	Winter	Spring
1/10	150	200	120
1/4	60	80	48
1/2	30	40	24
3/4	20	27	16
1	15	20	12

Localized high-temperature zones, often referred as hot spots, usually form within the bulk of grains, which is primarily experienced during winter season as heat is trapped within the inner part of the bin. The two types of hot spots include insect-induced and fungi-induced hot spots that are commonly seen in dry and damp grains, respectively (Sinha, 1967). Damp grain pockets often result from filling wet grains over dry grains, moisture migration between a damp cracked floor, snow melting upon ventilator blowing, and rain seep in roof leak entry (Manickavasagan et al., 2006). In fungi-induced hot spots, microorganisms exist after mixing damp grains with dry grains. The activity of these microorganisms that develop and thrive in these high moisture zones leads to an increase in temperature in this specific area of the bin. It could reach up to 64 ℃ that could last up to 3 months. In the case of insect-induced hot spots, molds formed in high-temperature pockets are precursor of increasing temperature, carbon dioxide, and moisture, which are beneficial to the insect growth and grain respiration (Sinha, 1961).

2.1.3 Stored-Product Insect Issues

Grains stored in large storage structures are usually infested by stored-product insects, which contribute about 9% up to 20% of postharvest losses in most developing and under-developed countries (Phillips & Throne, 2010). Aside from losses, grains are contaminated by the chemical secretion, insect fragments, and dead insects. These contaminants may accumulate in the structures and further contaminate the next batch of grains to be stored.

Insects infest stored grains during their larval and adult stages (Mason & Obermeyer, 2010). An insect infestation may happen in the internal or external surroundings of the grain. Internal insect pests, also known as internal developers or primary invaders, proliferate and feed within the grains. Common internal developers in stored products include lesser grain borer (*Rhyzopertha dominica* (Fabricius)), granary weevil (*Sitophilus granarius*), Australian wheat weevil, rice weevil (*Sitophilus oryzae*), and Angoumois grain moth (*Sitotroga cerealella*) (US Department of Agriculture, 2015). Meanwhile, external insect pests, also referred to as external developers or secondary invaders, contaminate and feed on fragments and dust produced from grains. These secondary invaders are also present in bulk of grains, but most detected in flour and other by-products of wheat kernels. Common external insect species in stored product pests include Indianmeal moth, red and confused flour beetles, cadelle, sawtoothed grain beetle, and flat grain beetle. These secondary invaders can be separated from the grains through cleaning operations (Mason & Obermeyer, 2010). Among these insects, the rice weevil and the lesser grain borer are regarded as the most damaging pests to wheat grains during storage in the United States (Hagstrum et al., 1999).

Internal infestations may not be visible to the naked eye as it only sees the surface of the grain. Grain safety is a primary concern in many countries as it is used in most food products. Published studies have focused on developing methods for the detection of internal infestations on stored products. These methods include trap catching, computer vision recognition, screening, electronic nose, and voice detection. However, such methods can be subjective, inaccurate, and destructive to grains. A recent detection technique which utilizes the principle of nuclear magnetic resonance spectroscopy (NMR), near-infrared reflectance spectroscopy (NIR), and x-ray image analysis has been developed. Both NMR and X-ray methods are costly and pose radioactivity. On

the other hand, NIR is still not widely used due to its costly and inconvenient implementation. A group of researchers from the School of Information Science and Technology in China explored the application of Biophoton Analytical Technology and pattern recognition in detecting internal infestation in wheat. The results from their study were able to distinguish differences in extracted feature vectors between good quality and insect-infested wheat grain which was produced by biophoton emission (Shi et al., 2015). Biophoton emission is performed by emitting ultraweak light from any object, which is within the range of ultraviolet and low visible light (Cohen & Popp, 1997). The emitted light is characterized to determine the significant difference among the objects.

By altering the environmental conditions, the stored-product insect population can be controlled. The ideal temperature for insect growth and reproduction is within the range of 25 to 33°C. Outside this range, insects can barely survive. Aeration can be performed to lower the temperature and cease insect activity, which is a common activity during summer. On average, aeration fans lower grain temperature by 4 °C. In the United States, aeration has not provided consistent results in lowering grain temperature, which may be attributed to fluctuating grain surface temperature (Phillips & Throne, 2010). Table 2.3 shows responses of store-product insect pests to various temperature ranges.

Table 2.3 Responses of stored-product insect pests to various temperature ranges (Fields, 1992; as cited in Tang et al., 2007)

Zone	Temperature Range (°C)	Effect(s)
Lethal	>62	Death in < 1 min
	50-62	Death in < 1 h
	45-50	Death in < 1 day
	35-42	Populations die out, mobile insects seek a cooler environment
Suboptimal	35	The maximum temperature for reproduction
	2-35	Slow population increase
Optimal	25-32	The maximum rate of population increase
Suboptimal	13-25	Slow population increase
Lethal	5-13	Slowly lethal
	1-5	Movement ceases
	-10 to -5	Death in weeks, or months if acclimated
	-25 to -15	Death in < 1h

Insects obtain water through grain consumption while some insects could absorb water from the surrounding air at a relative humidity level of at least 55%. The amount of water that the insects can get from the food and environment dictates its growth, development, and reproduction. For instance, rice weevil has a 10% mortality at 14% moisture content, allowing it to produce 344 eggs on the average, while it has a 75% mortality if the moisture content decreases to 10.5% moisture content with the ability to lay about 10 eggs (Fields, 2006). The Federal Grain Inspection Service established a list of standards for grading bulk of grains as “infested”, as shown in Table 2.4.

Table 2.4 Federal Grain Inspection Service Standards for grain that is graded “infested” (Mason & Obermeyer, 2010)

Grain (1000 g sample)	Number and Type of Insects
Wheat, triticale, rye	• 2 or more live weevils • 1 live weevil and 1 other live insect injurious to stored grain, or • 2 other live insects injurious to stored grain
All other grains	• 2 or more live weevils • 1 live weevil and five other live insects injurious to stored grain, or • 10 other live insects injurious to stored grain

2.2 Fumigation for Insect Pest Management

Fumigation has been done to reduce insect activity in various stored products. It is applicable to a variety of types of storage such as silo bags, chambers, silo bins, warehouses, containers, ships, gas-proof sheets, railway boxcars, and enclosures (Bell, 2000). Fumigants are toxic chemical gases that may be applied in the form of pellets, tablets, liquid formulations, or gaseous stream. Exposure to fumigants are hazardous to both insects and workers. Hence, fumigation is done when the insects are no longer reachable by biological or pesticide control. For instance, the grain mass is already inside a large bin wherein other insect control techniques could no longer reach the center of the grain mass (Utah Department of Agriculture, 1996). Fumigants are volatile and can easily diffuse into separate molecules which allow each molecule to penetrate the grains. Fumigant components such as carbon dioxide and inert gases displaces oxygen molecules in the interstitial air space. This lack of oxygen in the air makes it more difficult for the insects to respire (Nevada State Department of Agriculture, 2005).

The efficacy of fumigation depends on the lethal concentration of chemicals exposed to the insects. The diffusion of fumigant is an important factor to achieve even distribution and to reach all points in a large storage bin. By Graham's law of diffusion of gases, "the velocity of diffusion of a gas is inversely proportional to the square root of its density" while the "density of a gas is proportional to its molecular weight" (FAO, 1985). Hence, gases with lower density or molecular weight will traverse an open space faster than denser or lighter gases. In addition, the temperature inside the storage bin also affects the diffusion of gas wherein diffusion will happen at faster rate in hotter temperatures compared to colder temperatures (FAO, 1985). Phosphine, a commonly used fumigant in the United States, has a specific gravity of 1.21 (US Department of Agriculture, 2006), which means that phosphine is denser than air. A specific gravity greater than 1 means that

the gas needs an external force to be diffused into a bin filled with grains and air. For instance, if phosphine is introduced at the top of the bin along with the headspace or at the surface of the grains, the gravitational force pulls its molecules to diffuse downwards. However, in cases wherein phosphine is introduced at the bottom of the bin, then a thermosiphon or fan should be implemented to aid the process of diffusion.

Apart from diffusion, the adsorption and absorption of fumigant molecules into the grain kernels affect the availability of fumigant in the air as it diffuses. Adsorption occurs when fumigant molecules adhere to the surface of a grain kernel, while absorption occurs when the fumigant penetrates within the grain kernel up to a certain depth. Sorption which is the combination of adsorption and absorption is often considered in most fumigation studies since it is difficult to account for the specific quantities of adsorbed and absorbed fumigant. The reverse of sorption is known as desorption. After fumigation, the storage bin is usually opened at the top to vent the fumigant until it reaches the acceptable residue that is safe for human exposure (FAO, 1985).

With the increasing population of insect pests, the use of various chemical fumigants and pesticides is observed in grain storage starting the late half of the 20th century. However, the use of most fumigants and pesticides is already prohibited by the U.S. EPA due to risks of toxicity, hazardous exposure to workers, and detrimental effects on the environment. Currently, phosphine (PH_3) is the most used fumigant in the U.S. due to its low price, ease of use, and wide accessibility. The increasing insect resistance to currently used fumigants and pesticides is a major problem in the United States. The increasing number of populations of insect pests that are resistant to phosphine has also been observed throughout the globe. To account for this, farm operators are forced to increase phosphine concentration and length of the fumigation period to sufficiently kill insect pests. However, this approach is hazardous to the environment and farm workers while also

resulting in longer venting periods. The main reason for the development of resistance among insect pests is the repeated application of chemicals (Cook & Maier, 2016). The insect species with high resistance to phosphine includes maize weevil (Daglish et al., 2002), lesser grain borer (Opit et al., 2015; Chen et al., 2015), red flour beetle (Opit et al., 2015; Koçak et al., 2015; Chen et al., 2015), and rusty grain beetle (Nayak et al., 2013; Konemann et al., 2017).

2.2.1 Fumigation Methods

According to Isa et al. (2016), two of the most common fumigation methods across the globe are the tablet and forced-convection fumigation systems. Tablet fumigation is a type of fumigation wherein tablets or pellets are placed in a basket at the top of the grain bin along the headspace or at the surface of the grain bin. These pellets and tablets are volatile and vaporize through sublimation as it reacts with air and moisture. On the other hand, a forced-convection fumigation system involves a gaseous stream being injected near or at the bottom of the silo with or without mechanical means (Isa et al., 2016). Mechanical fans may be attached to the grain silo to draw air from the headspace and circulate it throughout the bin. Another alternative to induce air currents is to install a thermosiphon, which is usually painted with black to absorb heat from the sun. A thermosiphon consists of a pipe with ends connected to the headspace and the base of the silo. The difference with the temperatures inside the thermosiphon and the outside environment causes the air inside the pipe to expand due to the excited movement of molecules due to heat exchange. As the molecules in air expand, its molecules become more distant, causing the air to be less dense and buoyant. Hot air is displaced by the cold air as hot air moves upward. This process continues creating continuous air currents (Newman et al., 2012). The direction and velocity of air current vary as the temperature outside the grain bin changes throughout the day

(Cook, 2016). Figure 2.3 shows a schematic diagram for the forced-convection fumigation system using a fan (a) and a thermosiphon (b).

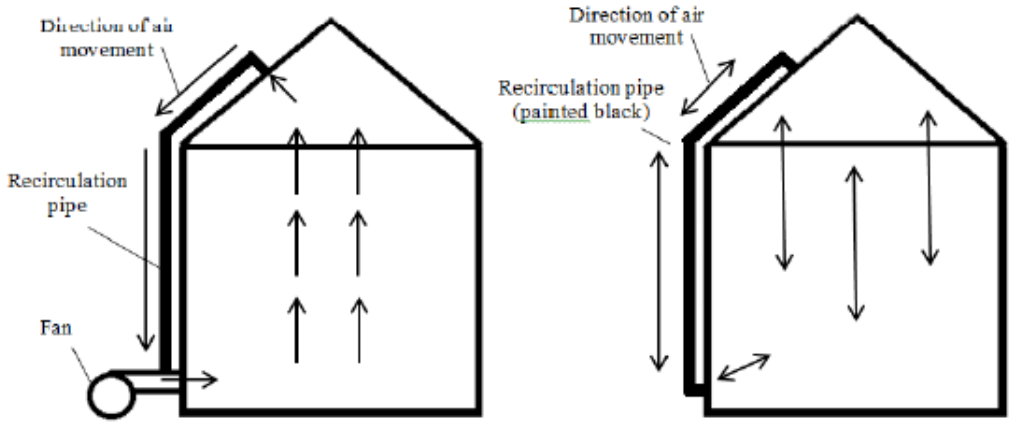

Figure 2.3 A schematic diagram for the fan-forced system using a fan (a) and a thermosiphon (b) (Cook, 2016)

2.2.2 Fumigants approved by U.S. Environmental Protection Agency (EPA)

In the U.S., chemical substances such as sulfuryl fluoride (SO_2F_2), methyl bromide (CH_3Br), and phosphine (PH_3) are highly considered for effective fumigation. Sulfuryl fluoride is a colorless, odorless gas known for its application for insect control in grain storage since 1959 (National Pesticide Information Center, 2017). It is registered to kill insect pests in the storage of dried fruits, coffee, cocoa beans, tree nuts, and stored grains. Based on the assessment of U.S. EPA in 2011, sulfuryl fluoride leaves a minute amount of fluoride in stored grains and other food products, but its effect on human health can be exacerbated by its interaction with other fluoride sources. The EPA claimed that the residue of sulfuryl fluoride in food exceeded the threshold limit for safety standards established by the 1947 Federal Food, Drug, and Cosmetic Act (FFDCA). Hence, sulfuryl fluoride is being proposed for phase-out in the fumigation industry (Environmental Working Group, 2011). On the other hand, methyl bromide is also colorless, odorless gas mainly

utilized in killing agricultural pests such as rodents, nematodes, fungi, weeds, and insects. The use of methyl bromide leads to the depletion of the ozone layer which results in increased passage of ultraviolet radiation (UV) through it. Based on its adverse effects on the ozone layer, methyl bromide is classified under Class I ozone-depleting substance (Environmental Protection Agency, 2018). Furthermore, due to its high toxicity levels to the atmosphere, it has been completely phased out through Montreal Protocol in 2005 stating that the United States and other developed countries are prohibiting the production and importation of this chemical formulation for domestic use (U.S. Department of Agriculture, 2003).

Phosphine is currently the most commonly used fumigant in the U.S. mainly because of its low price, ease of use, and minimal residue. Compounds such as Aluminum phosphide (AlP) and magnesium phosphide (Mg_3P_2) are used in fumigation to release phosphine, with formulations that may consist of urea, paraffin, ammonium bicarbonate, and ammonium carbamate. These components of AlP aids in suppressing ignition. Aluminum phosphide weighs approximately 0.60 grams per pellet and about 3 grams per tablet. Both pellets and tablets could release 30% phosphine by weight (US Department of Agriculture, 2006). In terms of toxicity, both AlP and Mg_3P_2 fall under Toxic Category I, which corresponds to the highest out of 4 levels. Possible risk of exposure during fumigation is through inhalation. Based on inhalation experiments in rats, the threshold limit for inhalation is 0.0113 mg/kg/day for magnesium phosphide and aluminum phosphide (US Environmental Protection Agency, 1994). Table 2.5 shows the essential properties of phosphine (US Department of Agriculture, 2006).

Table 2.5 Essential properties of phosphine (US Department of Agriculture, 2006)

Molecular weight[1]	34.0
Boiling point (at 760 mm pressure)[1]	-87.4 °C (-125.3 °F)
Specific gravity (at 39.2 °F) [1]	1.21
Flammability/Lower explosion limit (% by volume of gas in air)[1]	1.79%
Water solubility (ppm) at 63 °F[2]	416
Odor as gas[2]	Garlic-like odor due to contaminant; ammonia in certain formulations

[1] U.S. Department of Agriculture (2006)
[2] Phillips et al. (2014)

2.2.3 Factors affecting Fumigation Efficacy

For achieving a successful fumigation, three conditions must be maintained which are: a) the maximum phosphine concentration in the bin should be at least half of the applied phosphine on the average, b) the ratio of minimum to maximum phosphine concentration should be at least 0.24, and c) phosphine concentration after the fumigation period must be greater than or equal to the minimum effective lethal concentration against insect pests (Banks & Annis, 1984). Plumier & Maier (2018) reported that fumigant concentration is dependent on various ecosystem conditions (moisture content and temperature of the grain mass, difference between the temperatures of the grain mass and ambient air, and wind speed) and engineering variables (fumigation circulation rate, rate of evolution of phosphine into gaseous form, leakage rate, and amount of phosphine applied in the bin). Hence, it is important to know the factors affecting phosphine concentration throughout the fumigation period to determine possible ways to maintain maximum efficacy of the process.

2.2.3.1 Half-life pressure decay and leakage

In Australia, a half-life pressure decay test is performed to check if the fabricated silo meets the standard for sealing for effective fumigation. Half-life pressure decay test is measuring the

time needed for an applied pressure in a silo to decrease by 50%. In the early 1980s, Western Australia established the minimum effective half-life pressure decay time of 3 minutes for small farm silos with a structural volume of less than 300 m3 (Andrews et al., 1994). Based on the 2010 Australian Government standard, AS 2628, a "sealed" silo has a half-life pressure decay time of 3 minutes for older silos and 5 minutes for new silos (Banks & Ripp, 1984; Newman, 1990; Cook, 2016). In performing the test, Warrick (2010) stated that once the oil level in the pressure relief valve changes from 25-mm to 12.5-mm difference, it means that the pressure inside the structure falls by 50% of its initial pressure. It is suggested that farm operators should perform a half-life pressure decay test regularly prior to fumigation. If the pressure takes less than the required time to drop by half, then the silo is considered "leaky". For leaky silos, farm operators often isolate the leaks by applying soapy water to possible areas of leakage. The appearance of bubbles in the soapy water applied to a silo part indicates air leaks. Additional sealing may then be applied in the identified "leaky" areas if applicable. Common areas where air leaks are likely to occur include aeration inlet seal stretched springs on latches, the junction between the bottom and wall, the junction between the wall and roof, and overlapping metal sheets.

2.2.3.2 Concentration-time product

Successful fumigation involves exposing insect pests to a lethal concentration of toxic chemicals for a sufficient period of time to kill all of its life stages. The amount of fumigant exposed to insects is a function of concentration and time of exposure (F.A.O., 1985). It is expressed as a Ct product, which is the product of concentration and exposure time in oz-h/ft^3 or g-h/m^3. This parameter only signifies that if the exposure time is increased, then less amount of fumigant is needed to observe similar effects for insect control as long as it results in the same Ct product. In the application of phosphine fumigation, longer fumigation period is more effective

even at low concentrations as compared to higher concentrations and short fumigation period (Phillips et al., 2014). The recommended phosphine concentrations in treating different insect species under three temperature levels is listed in Table 2.6.

Table 2.6 Average concentrations of phosphine (mg/L) required to give 100% mortality of all developmental stages of insects under experimental conditions (Proctor, 1994)

Temperature	15 °C		25 °C			30 °C	
Duration of exposure (days)	4	8	2	4	7	2	7
Weevil, *Sitophilus spp.*		>1.50	>3.0	1.65	0.32	>0.36	0.05
Lesser grain borer			1.6	0.18	0.02		
Cigarette beetle, *Lasioderma serricorne*	0.36	0.04	1.6	0.32	0.15	>0.36	0.17
Khapra beetle, *Trogoderma granarium*	>1.30	0.77	0.8	0.32	0.08	>0.36	0.17
Bean weevil, *Acanthoscelides obtectus*			3	0.32	0.15	0.36	0.09
Groundnut borer, *Caryedon serratus*				0.32	0.2	0.36	0.05
Cacao moth, *Ephestia elutella*		>1.50	3	0.09	0.05	0.15	0.05
Almond moth, *Ephestia cautella*	>1.30	0.77	1.6	0.03	0.02	0.05	
Mediterranean flour moth, *Ephestia kuehniella*	>1.30	0.77	1.6	0.03	0.02	0.05	
Indianmeal moth, *Plodia interpunctella*	1.3	0.18	1.6	0.03	0.02	0.05	
Red flour beetle	0.03		0.16	0.08	0.04	0.02	
Sawtoothed grain beetle, *Oryzaephilus surinamensis*	0.03		0.04			0.05	
Flat grain beetle, *Cryptolestes pusillus*			0.16	0.08	0.01	0.36	0.05
Rusty grain beetle				>0.08	0.04		
Australian spider beetle, *Ptinus ocellus (P. tectus)*	1.3	0.18	0.4	0.08	0.04		

2.2.3.3 Temperature and Wind Speed

Although phosphine tends to be effective at high temperatures due to increased insect activity and respiration, Daglish and Pavic (2008) found that increasing ambient temperature leads to a decrease in fumigant concentration due to increased sorption. The temperature of the ambient air can also affect the circulation of air currents inside a silo. Increasing ambient temperature creates a larger temperature difference with the grain inducing faster velocity of air currents. The air moves towards the direction of leakage points in the silo where it exists. By this principle, the leakage rate increases as temperature increases. Lower wind speed results in high phosphine concentration but less even distribution throughout the silo, and vice versa. Increasing wind speed

decreases the overall Ct-product. On the other hand, the relative humidity has no significant effect on fumigant concentrations (Plumier & Maier, 2018).

2.2.3.4 Recirculation rate

Recirculation rate refers to the velocity of air moving across the grain mass, which can also greatly affect fumigation efficacy. With higher recirculation rate, the fumigant becomes more well-distributed and makes more contact with the grain mass. However, the air is induced to move out the leaky holes in the silo walls, and thus, a higher recirculation rate also causes the fumigant to move faster towards the exit holes. Although the insects thriving near the silo wall and exit holes are more exposed to the fumigant, the average fumigant concentration maintained in the silo decreases up to the sublethal levels for insect inactivity (Plumier & Maier, 2018).

2.2.3.5 Sorption and Desorption

In several fumigation experiments, it was observed that phosphine loss was not only attributed to leakage. A certain portion of the gas is lost as it gains contact with the grain mass. The fumigant adheres to the grain surface under a process known as sorption, which also includes partially adhering to inner surfaces of the kernels (Darby, 2008). These two phenomena are collectively known as sorption. Losses due to sorption and leakage are critical problems associated with fumigation as these phenomena causes the decrease in the average phosphine concentration exposed to the infestation. The occurrence of sorption and leakage prior to completely killing the insects lowers the efficacy of fumigation. On the other hand, desorption refers to the release of sorbed gas from the grain when the relative quantity of phosphine in the air approaches a low level (Darby, 2008; Daglish & Pavic, 2008).

The amount of fumigant that can be sorbed by the grain is highly influenced by the grain type, relative fumigant quantity present in the grain, and kernel condition. In gases, a mathematical

expression known as the sorption isotherm provides information on the gas quantity in the solid object as compared to that in the air. The uptake of gas by the grain may be reversible or irreversible (Banks, 1989), but the relative amounts of these uptakes are still unknown. Reversible sorption is also known as physisorption, irreversible sorption as chemisorption. Sorption is primarily influenced by several factors including moisture content, exposure period, dose, particle size and composition, and previous fumigation applications (Redd et al., 2006). Aside from these factors, Berck (1968), chemisorption is also influenced by the physical form of the fumigated product, which may be in the form of whole or milled grains. According to Tkatchuk (1972), a small portion of the absorbed phosphine binds to protein and reacts to some vegetable oils during contact which inhibits this portion to be desorbed as other phosphorus compounds or to solidify as residues within the grain. The interaction of a fumigant with the grain constituents is an important aspect that needs to be understood to justify the resulting gas isotherms.

Dumans (1980) studied the sorption and desorption of phosphine in stored wheat and corn. Fumigation of soft winter wheat and field corn was done by introducing 0.5 and 5 mg of phosphine per kilogram of the commodity in a 240-mL gas adsorbing bottles at 25 ℃, 45 ℃, and 85 ℃. After fumigation, the commodities were aerated and observed in a glass desorption chamber. A cold trap was used to collect the desorbed phosphine from the setup and a gas chromatograph was used to measure its quantity. Meanwhile, sorption was observed through the empty desorption chambers. The sorbed phosphine was found to be less than 3% in 24 hours for 50 µg of phosphine application. In this experiment, it was noted that desorption mostly took place during the first 2-3 days, following minimal desorption for the rest of the observation period. It was noted that even after 220 days of aeration, the desorption of phosphine was still occurring at a rate of parts per trillion. Throughout the duration of the experiment, about 10% of the initial phosphine residue was

adsorbed. The amount of sorbed phosphine is directly proportional to the fumigant concentration and duration of fumigation.

On the other hand, Rangaswamy (1985) conducted an experiment to determine the desorption pattern and behavior of phosphine desorption in wheat, raw polished rice, raw unpolished rice, and parboiled rice. These products were fumigated using a PhosFume® (Douglas Products) pellet packed and placed underneath the cereal and aerated after 2 weeks of exposure to phosphine. Prior to aeration, the amount of phosphine residue was measured and referred to as initial phosphine residue. The observation was done in a total of 60 days. Two methods, the Silver Nitrate Solution method and Detector Strip method, were employed to determine the amount of phosphine desorbed. The amount of phosphine remaining in these products per day was computed using the total quantity of phosphine in 60 days. The results were plotted to determine the relationship between the phosphine residue and a number of days of desorption. It was observed that linear relationship occurred for the first 19 days for all products except for the raw polished rice with linear relationship up to 9 days. It was also learned that first-order kinetics governed this linear relationship. Fluctuating phosphine residue was observed from 20 to 49 days, which was followed by a uniformly decreasing phosphine residue from 50 to 60 days for wheat, raw polished rice, and parboiled rice. For the raw unpolished rice, desorption was observed to be slowly decreasing until its 56th day.

In 2009, Daglish (2009) investigated the changes in phosphine sorption in wheat grains when stored at two temperatures (15 and 25 ℃) at 55% RH prior to fumigation. Wheat grains are commonly stored for several months prior to phosphine fumigation and this study was done to determine if the storage conditions can influence the fumigation efficacy of phosphine. In this study, wheat grains stored at a lower temperature exhibited a lower sorption rate than grains stored

at a higher temperature. However, phosphine is known to be more effective at higher temperatures where insect activity is high (Nayak & Collins, 2008). Thus, as a consequence of fumigation at lower temperature, it is recommended to lengthen the exposure period or increase the fumigant dose. It was also found that a longer storage period of wheat after harvest led to a decrease in sorptive capacity, which in turn resulted in an increase in the average phosphine concentration during fumigation (Daglish, 2009).

2.3 Application of Computational Fluid Dynamics (CFD) Model in Fumigation Studies

Computational Fluid Dynamics (CFD) is used in various industrial applications involving fluid flow. In the grain industry, CFD can be used to determine the behavior of fumigants inside a structural bin in pursuit of finding ways to increase fumigation efficacy. This application is governed by the fundamental laws of fluid mechanics – conservation of mass, momentum, and energy. By manipulating the equations associated with these laws, a set of coupled, non-linear partial differential equations are developed, which are then approximated in a computer software. These equations are too complex to solve directly in all but the simplest cases, but CFD computer software can approximate the full solution after reducing them to a large set of algebraic equations and solving those at discrete points. Rather than performing a large-scale experiment, CFD is able to reduce the number of experiments leading to a low-cost research alternative. However, it requires complex engineering expertise in the development and analysis of computer simulations.

In the study of Isa et al. (2016), a three-dimensional mathematical model was developed using FLUENT, a computational fluid dynamics (CFD) software, to determine the specific concentration of phosphine throughout a cylindrical silo at a given time. The simulation of phosphine fumigation in this storage facility was performed in two types of fumigation delivery:

fan-forced and tablet fumigations. The study also considered the position of leaky holes along the walls of the cylindrical silo and the degree of gas tightness indicated by the half-life pressure decay (HLP) for both types of fumigation. In the generated model for fan-forced fumigation, the phosphine concentration near the hole at position 1 (near the base of the silo) declines along the vertical axis of the silo, which prevented phosphine from reaching the headspace. Meanwhile, the desired level of phosphine concentration occurs for the fumigation with a hole near the headspace. This model indicates that fumigant concentration across the silo can be greatly influenced by the presence and position of leaky holes. Due to the incomplete distribution of phosphine throughout the silo, the stored-product pests would not be eradicated in a silo with a leak source near its bottom regardless of the length of fumigation. In terms of gas pressure, the silos with higher gas tightness (or higher HLP) have a higher gas pressure as compared to those with lower gas tightness (or lower HLP). This parameter affects the upward motion pace of phosphine since air molecules have initially occupied the pore spaces within the grains. On the other hand, the generated model for tablet fumigation shows that the desired level of phosphine concentration throughout the silo can be reached regardless of the position of leaky holes. It also shows that these leaky holes cause an even phosphine distribution. For both treatments in tablet fumigation, complete extinction of stored-product pests can be expected. In terms of gas pressure, the model shows a negligible difference in phosphine concentrations throughout the silo among those with different HLP values.

Meanwhile, Chayaprasert et al. (2010) developed a 3D Computational Fluid Dynamics (CFD) model using FLUENT software to determine the gas leakage rate in the fumigation at Hal Ross Flour Mill of Kansas State University, Manhattan, Kansas. This parameter was then used to estimate the gas Half-Loss Time (HLT) in the fumigation using methyl bromide and sulfuryl fluoride. The simulation was then compared to the available fumigation data from the study of

Chayaprasert et al. (2006). Although the previous research of Chayaprasert et al. (2008) already developed a fumigation model, this study developed another CFD model to simplify and improve the computation and model construction approach. The external flow simulations were reduced, and the milling equipment for the internal flow simulation was eliminated in the model. Meanwhile, the gas tightness of the structure was accounted for using the data from building pressurization tests. The simplified model gave an accurate prediction of the HLT values in comparison to the experimental values. It only indicates that the parameters used for the simplified modeling approach are valid for determining the HLT values.

Plumier et al. (2018) studied the venting and desorption process of phosphine from the wheat grains in silo storage. A computational model for the post fumigation of phosphine was developed and compared to the available data in operating a well-sealed grain silo situated in Lake Grace, Western Australia. It also based the computation from existing literature that developed fumigant desorption models. The effects of sorption were determined by observing the fumigant concentration lost. The equation used for the computation of fumigant concentration lost is only applicable for 1 mg/L application, 0.75 fill ratio at 25°C and 55% relative humidity. Aside from this consideration, temperature and moisture content were also accounted as these variables greatly influence the sorption process. The fumigant concentration lost due to the effect of silo leakage was also considered. Based on the computational model, phosphine concentration increases until it reaches its peak, which continually decreases thereafter until the end of fumigation. Phosphine concentration throughout the silo decreases as the temperature and wind speed increase which only indicates that the effectiveness of the fumigation process is also affected by the existing environmental conditions, especially by extreme weather events such as thunderstorms. It was concluded that the computational model gave satisfying results in the prediction of phosphine

concentrations throughout the silo and total Ct-product of the fumigation. The parameters, such as the environmental conditions and operational variables, considered in developing the model were accurate for the purpose and thus, can be used for future simulations of phosphine concentrations.

2.4 Sorption Isotherm

Sorption of any gaseous substance into a solid material is a natural phenomenon. An essential way to describe and determine the mobility of gas particles in a specific situation is to develop an isotherm curve, which can provide information on the retention of gas on a material at different concentrations (Limousin et al., 2007). Sorption isotherms can be categorized into different types depicting varying curve shapes. Figure 2.4 shows isotherm curves (Type I-V) based on Brunauer, Deming, and Teller (BDDT) developed in 1940, which mainly compose the International Union of Pure and Applied Chemistry (IUPAC) classification of sorption isotherms. In addition to the first five types of isotherm curves, IUPAC includes an additional classification, the Type VI isotherm. Type I sorption isotherm characterize microporous adsorbents; Type II and III are typically exhibited by microporous adsorbents with strong and weak adsorbate-adsorbent interactions, respectively; Types IV shows adsorption curve with hysteresis, which are typically mesoporous materials and commonly observed when capillary condensation is unlikely to happen; Type V also shows adsorption curve with hysteresis that is commonly observed when capillary condensation occurs during pore filling of micropores, and Type VI is an isotherm curve with steps, which is commonly exhibited by materials with strong fluid-surface forces (Aranovich & Donohue, 1998; Czepirski et al., 2000).

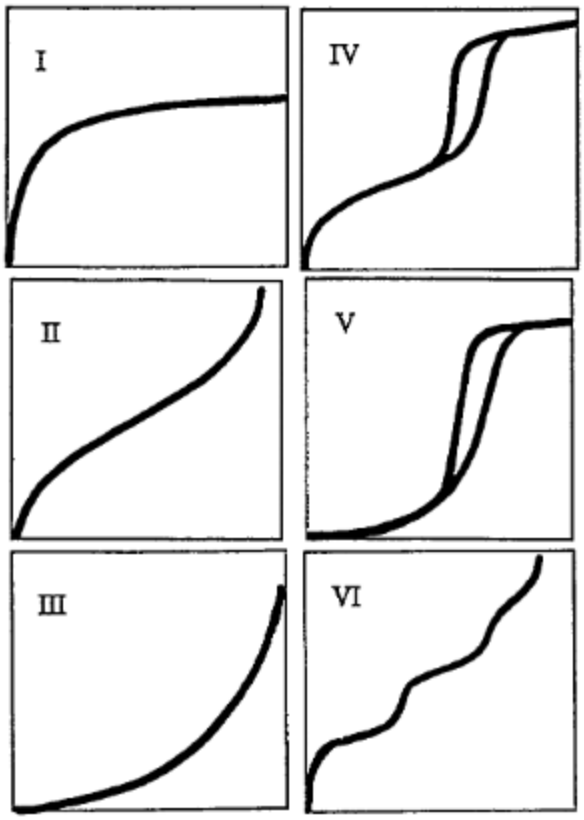

Figure 2.4 IUPAC classification of sorption isotherms for gas-solid equilibria

2.4.1 Semi-empirical Freundlich Isotherm

The semi-empirical Freundlich isotherm is given by an equation of sorbed fumigant as a function of the free fumigant concentration. It is expressed as:

$$c_s = ac_g^{\frac{1}{n}}$$

Where, c_s pertains to the concentration of the fumigant sorbed from the available concentration of fumigant in the air, c_g, and *a* and *n* are empirical parameters. The constant, *n*, has a value close to 1. Its deviation from 1 is related to the category of sorption process happening wherein a value of less than 1 means multi-molecular adsorption layer while a value greater than 1 indicates a uni-molecular layer (Winteringham & Harrison, 1946). This equation is used in computing concentrations in systems in equilibrium. The value of *a* changes with time for non-equilibrium

systems. Specifically, the values of *a* and *n* for phosphine treating wheat are 0.049, and 0.89 at 20 ℃ (Noack et al., 1983); 0.040 and 1.0 at 25 ℃ (Sato & Suwanai, 1974).

2.4.2 Langmuir Isotherm

The Langmuir isotherm depicts the Type I isotherm curve which is typically exhibited by microporous adsorbents such as zeolites and activated carbons. It assumes that the sorption phenomenon occurs in monolayer on a homogeneous surface. This is one of the most commonly used isotherm equation as it fits to a wide array of adsorption cases. Its main assumptions include 1) Adsorption is localized at specific sites on the material's surface and the saturation coverage means total occupancy of these localized sites, 2) only one molecule can be adsorbed by each site, 3) Neighboring adsorbed molecules do not interact with each other and surface is energetically homogeneous, and 4) phase transitions do not occur (Czepirski et al., 2000). Equilibrium concentration in the non-linear Langmuir isotherm model is expressed as:

$$q_e = \frac{q_{max} K_L C_e}{1 + K_L C_e}$$

where, q_{max} (mg/kg) is the monolayer sorption capacity of wheat kernels; C_e is equilibrium PH_3 concentration (ppm); and K_L is sorption constant of this model (Langmuir, 1918). Non-linear Freundlich isotherm model is given by:

2.4.3 Redlich-Peterson isotherm

The Redlich-Peterson (R-P) Isotherm combines the effects in both the Freundlich and Langmuir isotherms in one equation. Its numerator comes from the Langmuir isotherm and at infinite concentration, it approaches Henry's isotherm, wherein surface adsorbent volume is proportional to partial pressure of adsorbate gas. It incorporates three parameters indicating a combination of adsorption mechanism described in Freundlich and Langmuir isotherms, which

does not follow single layer of adsorbed molecules (Brouers & Al-musawi, 2015; Rajahmundry et al., 2021). It is expressed as:

$$q_e = \frac{K_R C_e}{1 + A_R c_e^g}$$

Where q_e is the amount of adsorbate over adsorbent at equilibrium (mg/g); K_R (L/g) and A_R are R-P isotherm constants; C_e is adsorbent concentration (mg/l); and g is an exponent indicating adsorbent heterogeneity (0 to 1). R-P isotherm has linear dependence on adsorbate concentration due to its numerator and has exponential function in its denominator. Thus, it can represent a wide array of adsorbate concentration at equilibrium for homogenous or heterogeneous systems.

2.5 Chlorine Dioxide as a Potential Fumigant Alternative

Chlorine dioxide (ClO_2) is a strong oxidizer, may be present in aqueous or gaseous form, and is known for its high oxidation property and antimicrobial activity against bacteria, viruses, and fungi. ClO_2 has 19 electrons and acts as free radical with an oxidation potential of 0.95 V. Due to presence of unpaired electrons, it is highly reactive with substances that can lose electrons. Based on this, ClO_2 can receive 5 electrons to reduce it to chloride. It can react with sulfuric substances, reactive organic substances, and amino acids (Li, 2019). Its aqueous form has been used for disinfecting drinking water without formation of trihalomethanes or chloramine (Shirasaki et al., 2016). ClO_2 can be applied at 200 ppm for processing equipment sanitation and at most 3 ppm for raw fruit and vegetable sanitation (US Food and Drug Administration, 1998; Tan et al., 2021). It is a yellowish to yellowish-green gas that smells like chlorine and has about 0.124 nm molecule size which is much smaller in comparison to that of microorganisms' cells (2-5 µm) (Lorcheim, 2013). Furthermore, the gaseous form of ClO_2 is more effective compared to its aqueous form. For instance, gaseous ClO_2 can distribute in an enclosed space without the need of water and mechanical agitators or conveyors to move products to be treated. It is more suitable to

use for low-moisture products like cereal grains. It also can reduce the wastewater that is usually produced when aqueous ClO_2 is used (Tan et al., 2021).

2.5.1 Stored-Product Insect Mortality

Several studies have investigated the efficacy of ClO_2 against various stored-product insect species (summarized in Table 2.7). These studies prove that chlorine dioxide gas is effective in killing and decreasing adult progeny production of various stored-product insect species that are either susceptible or resistant to phosphine.

In 2012, Channaiah et al. evaluated ClO_2 gas in killing eggs, larvae, and adults of red flour beetle and confused flour beetle. Each life stage was exposed to ClO_2 gas concentrations of 248.4, 331.2, 413.9, and 496.6 g/m^3 for 1.53, 2.07, 1.80 and 1.68 h, respectively. The presence of food (5g of wheat flour) was also compared to that without food. These gas concentration and time produced gas dosages (ct products) of 380.1, 685.6, 745.0, and 834.4 g-h/m^3. For young larvae of both insect species, the highest dosage treatment resulted in complete mortality in the absence of wheat flour. About 0 to 31% mortality was observed from old larvae of both species with or without wheat flour. At dosages of 745.0 and 834.4 g-h/m^3, adults of *T. confusum* were entirely killed with or without flour, but for red flour beetle, these dosages only achieved complete adult mortality when flour was absent. This study concluded that confused flour beetle is more susceptible to ClO_2 than red flour beetle. Insect survival was favored in the presence of wheat flour.

Sensitivity of Indian meal moth at different life stages were studied by Han et al. (2016). This study found that complete mortality can be obtained after exposing Indian meal moth to 100 ppm for 48 h or 200 ppm for 24 h for all life stages (egg, larvae, pupae, and adults). At 50 and 100 ppm, sensitivity of Indian meal moth was egg > larva > pupa; at 200 ppm, the order of sensitivity

changed to egg > pupa > larva. It was also observed that ClO_2 can impair subsequent life stage as the ClO_2-exposed larvae did not pupate and emerge into adults. Kumar et al. (2015) argued that the oxidative stress brought by ClO_2 was responsible for mortality of Indian meal moth larvae upon exposure. This oxidative stress results from the imbalance of synthesis and breakdown of reactive oxygen species (ROS) or irreparable ROS damage. Reactive oxygen species (ROS) is generated whenever ClO_2 reacts to material such as microbes and releases one reactive oxygen from its molecule (Young, 2016). ROS can cause damage to cellular building blocks such as protein, lipids, and DNA. Results of this study also discovered that ClO_2 exposure to insects generates ROS in cell lines of Indian meal moth, resulting to oxidative stress that significantly impaired the insect's immune responses. The amount of ROS produced was dependent on ClO_2 concentration. An interesting finding showed that addition of vitamin E (as an antioxidant) can quench ROS activity and prevent cell death. Furthermore, denaturation of proteins due to ClO_2 exposure caused the loss of spreading behavior of hemocytes which is essential for insect cellular immune responses. Sublethal doses of ClO_2 caused hemolysis, rupture of red blood cells, making the insect susceptible to microbial infection. It was speculated that this oxidative stress does not only affect immune responses of Indian meal moth but also alter its physiological systems (Kumar et al., 2015). Another study showed that oxidative stress caused by lethal ClO_2 treatment was the main factor in killing red flour beetle. Furthermore, generated ROS exceeded antioxidant activities of this beetle and two antioxidant enzymes, superoxide dismutase and thioredoxin-peroxidase, were up-regulated after exposure to lethal ClO_2 concentration. The upregulation of these enzymes indicates that the insect immune response is to detoxify the generated ROS (Kim et al., 2015). Another study of Han et al. (2017) worked on understanding effect of release of ROS due to ClO_2 exposure on lipid peroxidation of phospholipids, mainly in polyunsaturated fatty acids (PUFAs),

which are linked to the production of cytotoxic reactive aldehyde products (ie. MDA and 4-hydroxynonenal) (Grune et al., 2010). In this study, it was found that lipid peroxidation in the larval fat body of Indian meal moth increased after ClO_2 exposure in a dose-dependent manner and reduced expression of calcium-independent cellular phospholipase A_2, a protein that has an essential role in repairing damaged fatty acids in phospholipids.

Han et al. (2018) noted differences in sensitivity of various stored-product insect species such as maize weevil, khapra beetle, bean weevil, and red flour beetle to ClO_2 gas treatment. In their study, maize weevil, khapra beetle, and bean weevil were effectively killed at 100 ppm ClO_2 after 24 h of exposure. Higher concentration or longer exposure period was required in controlling populations of red flour beetle. Only 78.33% mortality of red flour beetle in this study was achieved at 200 ppm treatment for 48 h exposure. It was speculated that this result may be attributed to an induced reduction of respiration of red flour beetle. This is in contrast with the results in Xinyi et al. (2017) wherein 200 ppm ClO_2 for 24 h was effective in killing red flour beetle.

In the study of E et al. (2017), adults of five stored-product insect species (red flour beetle, sawtoothed grain beetle, maize weevil, lesser grain borer, and rice weevil), both phosphine-susceptible laboratory strains and phosphine-resistant field strains, were exposed to 200 ppm (0.54 g/m^3) ClO_2 gas in vials with (10 g) or without (0g) wheat kernels at an average temperature of 24.8 ± 0.6 °C. Longer exposure times were needed to achieve complete mortality of adults of these five insect species when wheat was present in the vials. A 99% mortality (LD_{99}) for red flour beetle, sawtoothed grain beetle, maize weevil, lesser grain borer, and rice weevil can be attained in vials with wheat after exposure to dosages of 14.79-22.57, 8.20-8.41, 10.66-14.53, 15.79-21.60, and 7.67-12.20 g-h/m^3, respectively. Vials without wheat resulted in complete mortality for red flour

beetle, maize weevil, and lesser grain borer at dosages of 6.51-8.66, 5.79-10.26, and 11.46-23.17 g-h/m^3, respectively. The LD_{99} values for rice weevil and sawtoothed grain beetle were not computed as mortality results for these species were close to or at 100% at all exposure times. Adult progeny production was also investigated between control and treated samples. For lesser grain borer, a dosage range of 10.07 to 18.11 g-h/m^3 resulted in 99% adult progeny reduction. For red flour beetle and sawtoothed grain beetle, adult progeny production was not observed for both control and treated samples, whereas for maize weevil and rice weevil, adult progeny production was only observed in control samples. In 2018, E et al. investigated the influence of temperature and food during ClO_2 exposure of 520 ppm or 1.40 g/m^3 for 2 to 12 h. Results in this study showed that phosphine-resistant and -susceptible strains were similar in susceptibility to ClO_2 at this concentration. Warmer temperatures (averaging 32.8 ± 0.5°C in this study) favored efficacy of ClO_2 against the same five insect species since lower dosage values were needed to achieve 50% mortality. The presence of wheat in vials containing the insects caused a delay in mortality, which was speculated that ClO_2 reacted to active sites within the kernels. As ClO_2 flows through wheat kernels, the active sites on the surface of kernels are oxidized. Once fully oxidized, excess gas molecules accumulate and increase in concentration through time with continuous gas inflow, thus reaching a lethal concentration against insects (Simpson, 2005; E et al., 2017). Among these five insect species, it was observed that sawtoothed grain beetle was the most susceptible while lesser grain borer and maize weevil species were the least susceptible to ClO_2 regardless if wheat kernels were present or absent in vials.

Kim et al. (2019) investigated the efficacy of ClO_2 against larvae and adult stages of Indianmeal moth and adult stage of maize weevil in rice grain bags. Results of this study showed that Indianmeal moth larva did not reach 100% mortality after exposure to 200 ppm ClO_2 gas for

24 h for all monitored locations in the rice grain bags (inner and outer sections of top, middle, bottom layers). Adult Indianmeal moth had a uniform mortality of 100% at all monitored locations after exposure to the same treatment as its larva immediately after fumigation. Adult maize weevil had 100% mortality only at the outer section of the rice grain bags about 3 days after exposure to the same treatment. This study concluded that variation in fumigation efficiency depends on storage position and insect species and life stage wherein fumigation efficiency was reported to be highest near the surface of the grain bag where the gas penetrated first.

2.5.2 Effects on Wheat Quality

Few published studies have evaluated the effect of chlorine dioxide (ClO_2) treatment on stored wheat and wheat-based product quality. In the study of Han et al. (2018b), wheat viability was found to be influenced by ClO_2 gas exposure at varying concentrations and durations. At 100 ppm ClO_2 gas for 12 h, wheat viability significantly decreased with only 48% of the wheat seeds growing into normal seedlings after the germination test while the untreated wheat seeds had an 81% germination rate. At 200 ppm ClO_2 gas exposure for 6 h, significant reduction in germination rate of wheat seeds from 89% (untreated) to 73% (treated) was observed. The same treatment led to a reduced germination rate of 32.7% when duration was extended up to 48 h. Residues in wheat seeds were also examined in this study. Chlorine dioxide (mg/kg of grain) was not detected immediately after treatment as well as on the 1^{st} and 10^{th} day after treatment of 200 ppm ClO_2 for 24 h. Chlorine (0.7 mg/kg wheat) and chlorite (1.3 mg/kg wheat) were detected after treatment, which significantly reduced after one day to 0.2 mg/kg wheat and 0.4 mg/kg wheat, respectively. During the 10^{th} day, no chlorine and chlorite residue were detected. Other than wheat, several research studies measured low residue levels of free chlorine dioxide (less than 0.4 mg/kg fruit),

chlorite (less than 0.4 mg/kg fruit), and chloride (less than 9.9 mg/kg fruit) for ClO_2-treated commodities such as tomatoes, apples, cantaloupe, strawberries, and oranges.

Early reports claimed that Agene, commercially produced for bleaching and aging flour, was replaced by ClO_2 as wheat flour improver in the U.S. after vast number of experiments on feeding animals, and humans showed the absence of acute toxicological effects (Meredith et al., 1956; Moran et al., 1953). However, the applied concentration of ClO_2 in these animal feeding tests (30 ppm) was lower than the applied concentration from the previously mentioned studies wherein complete mortality of stored-product insect pests were observed. Moran et al. (1953) explained the interaction of ClO_2 with flour chemical composition. The oxidative process starts with the unsaturated fatty acids of flour which includes a certain level of polymerization. Tocopherols or vitamin E of wheat flour was decreased by approximately 70% when treated with ClO_2.

In order to commercialize the use of ClO_2 in reducing populations of stored-product insect pests, further evaluation of this potential fumigant is critical in terms of grain and grain-based product quality and safety. It is important to test the treated grains for flour quality as this is the main product derived from wheat. Aside from quality parameters, the cost associated with its utilization in a large-scale setting should be feasible for grain storage managers. Understanding ClO_2 behavior within enclosed structure will help in future modelling studies focusing on optimization of fumigation practices once this chemical. Kim et al. (2019) stated research studies related to circulation of ClO_2 gas should be understood in order to achieve similar laboratory-scale fumigation effectiveness in large-scale setting. Channaiah et al. (2012) emphasized the need for establishment of baseline dosages that could effectively kill different stored-product insect pests at all life stages, which are commonly found in grain storage and processing facilities. Achieving

complete insect mortality should be accompanied by less alteration in grain quality and viability and low residue levels (Han et al., 2018b).

Table 2.7 Efficacy of gaseous ClO_2 treatment on stored-product insect species

Insect Species	Insect life stage	Conditions	Food/Grain	Mortality Rate	Reference
Red flour beetle *(Tribolium castaneum* (Herbst))	Egg	496.6 g/m^3 for 1.68 h	Wheat Flour	Without flour: 9.3% With 5 g flour: 5.5%	Channaiah et al. (2012)
	Young larvae	496.6 g/m^3 for 1.68 h	Wheat Flour	Without flour: 100.0% With 5 g flour: 18.9%	
	Old larvae	496.6 g/m^3 for 1.68 h	Wheat Flour	Without flour: 18.8% With 5 g flour: 4.0%	
	Adult	496.6 g/m^3 for 1.68 h	Wheat Flour	Without flour: 100.0% With 5 g flour: 100.0%	
Confused flour beetle (*Tribolium confusum* (Jacquelin du Val))	Egg	496.6 g/m^3 for 1.68 h	Wheat Flour	Without flour: 11.1% With 5 g flour: 5.6%	
	Young larvae	496.6 g/m^3 for 1.68 h	Wheat Flour	Without flour: 100.0% With 5 g flour: 37.2%	
	Old larvae	496.6 g/m^3 for 1.68 h	Wheat Flour	Without flour: 31.3% With 5 g flour: 14.7%	
	Adult	413.9 g/m^3 for 1.80 h	Wheat Flour	Without flour: 100.0% With 5 g flour: 100.0%	
Red flour beetle (*Tribolium castaneum*)	Adult	400 ppm for 6 h with heat treatment for 6 h		95%	Kim et al. (2015)
Red flour beetle	Adult	1.40 g/m^3 (520 ppm) for 8 h	Wheat	*Susceptible strain:* 98.3% DAT 1 100% DAT 5 *Resistant strains* AB1: 100.0% DAT 1 & 5 CF: 100.0% DAT 1 & 5	E et al. (2018)
Saw-toothed grain beetle	Adult	1.40 g/m^3 (520 ppm) for 4 h	Wheat	*Susceptible strain:* 94.9% DAT 1 100.0% DAT 5 *Resistant strains* AB2: 92.3% DAT 1 100.0% DAT 5	

Lesser grain borer	Adult	1.40 g/m^3 (520 ppm) for 8 h		*Susceptible strain:* 94.9% DAT 1 100.0% DAT 5 *Resistant strains:* CS: 96.8% DAT 1 100.0% DAT 5 RL: 96.2% DAT 1 100.0% DAT 5	
Maize weevil	Adult	1.40 g/m^3 (520 ppm) for 8 h		*Susceptible strain:* 84.6% DAT 1 *Resistant strain* TX: 89.3% DAT 1 100.0% DAT 5	
Rice weevil	Adult	1.40 g/m^3 (520 ppm) for 8 h		*Susceptible strain:* 100.0% DAT 1 & 5 *Resistant strain* TX: 77.8% DAT 1 100.0% DAT 5	
Indian meal moth	Adult	200 ppm for 24 h	Rice	All locations in rice bag: 100.0% DAT 0 100.0% DAT 3 100.0% DAT 5	Kim et al. (2019)
	Larvae	200 ppm for 24 h	Rice	Top 0.0% DAT 0 5.0 – 6.7% DAT 3 11.7 – 20.0% DAT 5 Middle 0.0% DAT 0 0.0% DAT 3	

				1.7 - 5.0% DAT 5 Bottom 0.0 - 1.7% DAT 0 1.67 - 5.00% DAT 3 3.3 - 5.0% DAT 5
Maize weevil (*Sitophilus zeamais*)	Adult	200 ppm for 24 h	Rice	Top 10.0 - 20.0% DAT 0 80.0 - 85.0% DAT 3 95.0 - 98.3% DAT 5 Middle 0.0 - 26.7% DAT 0 30.0 - 53.3% DAT 3 55.0 - 66.7% DAT 5 Bottom 0.0 - 1.7% DAT 0 13.3 - 23.3% DAT 3 28.3 - 60.0% DAT 5

2.6 References

Andrews, A.S, Annis, P.C., Newman, C.R., (1994) Sealed storage technology on Australian farms. In: Stored Product Protection, Proceedings of 6th International Working Conference on Stored-product Protection. Canberra, Australia, 17-23 April 1994, (Edited by Highley, E., Wright, E.J. Banks, H.J., and Champ B.R) pp. 27 - 36.

Aranovich, G., & Donohue, M. (1998). Analysis of adsorption isotherms: Lattice theory predictions, classification of isotherms for gas–solid equilibria, and similarities in gas and liquid adsorption behavior. Journal of colloid and interface science, 200(2), 273-290.

Arthur, F. & Subramanyam, B. (2012). Chemical control in stored products. Stored Product Protection, 95-100.

Banks, H. J. (1986). Sorption and desorption of fumigants on grains: mathematical descriptions. Pesticide and Humid Tropical Grain Storage Systems: Proceedings of an International Seminar, 14, 179-93.

Banks, H., & Annis, P. (1984). Importance of Processes of Natural Ventilation to Fumigation and Controlled Atmosphere Storage. Developments in Agricultural Engineering Controlled Atmosphere and Fumigation in Grain Storages, 299–323. doi: 10.1016/b978-0-444-42417-4.50032-3

Banks, H. and B. Ripp. 1984. Sealing of grain storages for use with fumigants and controlled atmospheres. Proceedings of the 3rd International Working Conference on StoredProduct Entomology. 375-390.

Bell, C. (2000). Fumigation in the 21st century. Crop Protection, 19(8-10), 563–569. doi: 10.1016/s0261-2194(00)00073-9

Boina, D. R., & Subramanyam, B. (2012). Insect management with aerosols in food-processing facilities. Insecticides – Advances in Integrated Pest Management, 195-212.

Brooker, D. B., Bakker-Arkema, F. W., & Hall, C. W. (1992). Drying and storage of grains and oilseeds. New York: Van Nostrand Reinhold.

Channaiah, L., Wright, C., Subramanyam, B., & Maier, D. E. (2012, October). Evaluation of chlorine dioxide gas against eggs, larvae, and adults of Tribolium castaneum and Tribolium confusum. In Proceedings, 9th International Conference on Controlled Atmosphere and Fumigation in Stored Products (pp. 15-19).

Chayaprasert, W., Maier, D. E., & Subramanyam, B. (2010). A simplified and improved modeling approach for the structural fumigation process using computational fluid dynamics. 10th International Working Conference on Stored Product Protection, 237-242.

Chen, Z., Schlipalius, D., Opit, G., Subramanyam, B., & Phillips, T. W. (2015). Diagnostic Molecular Markers for Phosphine Resistance in U.S. Populations of Tribolium castaneum and Rhyzopertha dominica. Plos One, 10(3). doi: 10.1371/journal.pone.0121343

Cohen, S., & Popp, F. (1997). Biophoton emission of the human body. Journal of Photochemistry and Photobiology B: Biology, 40(2), 187–189. doi: 10.1016/s1011-1344(97)00050-x

Collins, P. J. (2006). Resistance to chemical treatments in insect pests of stored grain and its management. Pest Resistance to Pesticides and Control Measures, 277-282.

Cook, S., & Maier, D. (2016, October 20). Grain Operations: Fumigating stored grain in sealed silos. Retrieved January 26, 2020, from https://www.world-grain.com/articles/10251-grain-operations-fumigating-stored-grain-in-sealed-silos

Czepirski, L., Balys, M. R., & Komorowska-Czepirska, E. (2000). Some generalization of Langmuir adsorption isotherm. Internet Journal of Chemistry, 3(14), 1099-8292.

Daglish, G. J., Collins, P. J., Pavic, H., & Kopittke, R. A. (2002). Effects of time and concentration on mortality of phosphine-resistant Sitophilus oryzae (L) fumigated with phosphine. Pest Management Science, 1015-1021.

Daglish, G. J., and Pavic, H. (2008). Effect of phosphine dose on sorption in wheat. Pest Management Science, 64(5), 513-518.

Daglish, G. J., & Pavic, H. (2009). Changes in phosphine sorption in wheat after storage at two temperatures. Pest Management Science, 65(11), 1228–1232. doi: 10.1002/ps.1814

Dhuyvetter, K. C., Harner, J. P., Tajchman, J., & Kastens, T. L. (2007). The economics of on-farm storage. Kansas State University. Retrieved from https://bookstore.ksre.ksu.edu/pubs/MF2474.pdf

Dumas, T. (1980). Phosphine sorption and desorption by stored wheat and corn. Journal of Agricultural and Food Chemistry, 28(2), 337–339. doi: 10.1021/jf60228a043

E, X., Subramanyam, B., & Li, B. (2017). Responses of phosphine susceptible and resistant strains of five stored-product insect species to chlorine dioxide. Journal of Stored Products Research, 72, 21-27.

E, X., Li, B., & Subramanyam, B. (2018). Toxicity of chlorine dioxide gas to phosphine-susceptible and-resistant adults of five stored-product insect species: Influence of temperature and food during gas exposure. Journal of economic entomology, 111(4), 1947-1957.

Environmental Protection Agency. (2018, November 28). Methyl Bromide. Retrieved from https://www.epa.gov/ods-phaseout/methyl-bromide

Environmental Protection Agency. (1998). Reregistration Eligibility Decision (RED): AL & MG Phosphide. Retrieved from https://archive.epa.gov/pesticides/reregistration/web/pdf/0025red.pdf

Environmental Working Group. (2011). EPA Proposes to Phase Out Fluoride Pesticide. Retrieved from https://www.ewg.org/news/testimony-official-correspondence/epa-proposes-phase-out-fluoride-pesticide

Fields, P. (2006). Alternatives to chemical control of stored-product insects in temperate regions. Alternative Methods to Chemical Control, 653-662.
Hagstrum, D. W., Reed, C., & Kenkel, P. (1999). Management of stored wheat insect pests in the USA. Integrated Pest Management Reviews, 4, 127-142.

Food and Agriculture Organization. (2002). Fumigation for the control of insect pests in storage. Retrieved from http://www.fao.org/3/x5048e/x5048E0q.htm

Grune, T., Zarkovic, N., & Kostelidou, K. (2010). Lipid peroxidation research in Europe and the COST B35 action 'Lipid Peroxidation Associated Disorders'. Free radical research, 44(10), 1095-1097.

Han, G. D., Kwon, H., Kim, B. H., Kum, H. J., Kwon, K., & Kim, W. (2018). Effect of gaseous chlorine dioxide treatment on the quality of rice and wheat grain. Journal of Stored Products Research, 76, 66-70.

Hu, Q., & Zhang, Z. (2019). Application of Dubinin–Radushkevich isotherm model at the solid/solution interface: A theoretical analysis. Journal of Molecular Liquids, 277, 646-648.

Iconomou, D., Athanasopoulos, P., Arapoglou, D., Varzakas, & Christopoulou, N. (2006). Cereal Quality Characteristics as Affected by Controlled Atmospheric Storage Conditions. American Journal of Food Technology, 1(2), 149–157. doi: 10.3923/ajft.2006.149.157

Isa, Z., Farrell, T., Fulford, G., & Kelson, N. (2016). Mathematical modelling and numerical simulation of phosphine flow during grain fumigation in leaky cylindrical silos. Journal of Stored Products Research, 67, 28–40. doi: 10.1016/j.jspr.2016.01.002

Jayas, D. S., & White, N. D. (2003). Storage and drying of grain in Canada: low cost approaches. Food Control, 14(4), 255–261. doi: 10.1016/s0956-7135(03)00014-8

Kaleta, A., & Grnicki, K. (2013). Criteria of Determination of Safe Grain Storage Time – A Review. Advances in Agrophysical Research. doi: 10.5772/52235

Kaloudis, E., Bantas, S., Athanassiou, C. G., Agrafioti, P., & Sotiroudas, V. (2018). Modeling the distribution of phosphine in cylindrical grain silos with CFD methods for precision

fumigation. 12th International Working Conference on Stored Product Protection (IWCSPP), 711-718.

Kim, B. H., Han, G. D., Kwon, H., Chun, Y. S., Na, J., & Kim, W. (2019). Chlorine dioxide fumigation to control stored product insects in rice stored in a room. Journal of Stored Products Research, 84, 101527.

Koçak, E., Schlipalius, D., Kaur, R., Tuck, A., Ebert, P., Collins, P., & Yılmaz, A. (2015). Determining phosphine resistance in rust red flour beetle, Tribolium castaneum (Herbst.) (Coleoptera: Tenebrionidae) populations from Turkey. Turkish Journal of Entomology, 39(2). doi: 10.16970/ted.17464

Konemann, C. E., Hubhachen, Z., Opit, G. P., Gautam, S., & Bajracharya, N. S. (2017). Phosphine Resistance in Cryptolestes ferrugineus (Coleoptera: Laemophloeidae) Collected from Grain Storage Facilities in Oklahoma, USA. Journal of Economic Entomology, 110(3), 1377–1383. doi: 10.1093/jee/tox101

Lawrence, J., & Maier, D. E. (2011). Development and Validation of a Model to Predict Air Temperatures and Humidities in the Headspace of Partially Filled Stored Grain Silos. Transactions of the ASABE, 54(5), 1809–1817. doi: 10.13031/2013.39820

Lee, K. (2018). How do grain silos work?. Retrieved from https://sciencing.com/grain-silos-work-4927013.html

Li, B. (2019). Effects of chlorine dioxide and ozone gases against immature stages of stored-grain insects. Kansas State University.

Limousin, G., Gaudet, J. P., Charlet, L., Szenknect, S., Barthes, V., & Krimissa, M. (2007). Sorption isotherms: A review on physical bases, modeling and measurement. Applied geochemistry, 22(2), 249-275.

Lorcheim, K. (2013).The myths and misconceptions of chlorine dioxide gas.Retrieved from https://www.alnmag.com/article/2013/09/myths-and-misconceptions-chlorine-dioxide-gas.

Magan, N., Aldred, D., Mylona, K., & Lambert, R. J. (2010). Limiting mycotoxins in stored wheat. Food Additives & Contaminants: Part A, 27(5), 644–650. doi: 10.1080/19440040903514523

Manickavasagan, A., Jayas, D. S., White, N. D. G., & Jian, F. (2006). Thermal Imaging of a Stored Grain Silo to Detect a Hot Spot. Applied Engineering in Agriculture, 22(6), 891–897. doi: 10.13031/2013.22243

Mason, L. J. & Obermeyer, J. (2010). Stored grain insect pest management. Stored Product Pests, E-66-W, 1-5.

McKenzie, B. A., & Fossen, L. V. (2005). Managing dry grain in storage. Retrieved from https://www.extension.purdue.edu/extmedia/AED/AED-20.html

Meredith, P., Sammons, H. G., & Frazer, A. C. (1956). Studies on the effects of treatment with chlorine dioxide on the properties of wheat flour. I.—The chemical composition of protein of treated flours. Journal of the Science of Food and Agriculture, 7(5), 361-370.

Morales-Quiros, A., Campabadal, C., Maier, D. E., Lazzari, S. M., Lazzari, F. A., & Phillips, T. W. (2019). Chilled Aeration to Control Pests and Maintain Grain Quality during Summer

Storage of Wheat in the North Central Region of Kansas. Applied Engineering in Agriculture, 35(4), 657–688. doi: 10.13031/aea.13252

Moran, T., Pace, J., & McDermott, E. E. (1953). Interaction of chlorine dioxide with flour: Certain chemical aspects. Nature, 171(4342), 103-106.

National Agricultural Statistics Service. (2020, January). Grain Stocks. Retrieved from https://www.nass.usda.gov/Publications/Todays_Reports/reports/grst0120.pdf

National Pesticide Information Center. (2017). Sulfuryl Fluoride. Retrieved from http://npic.orst.edu/factsheets/sfgen.html

Nayak, M. K., & Collins, P. J. (2008). Influence of concentration, temperature, and humidity on the toxicity of phosphine to the strongly phosphine resistant psocid Liposcelis bostrychophila Badonnel (Psocoptera: Liposcelididae). Pest Manag Sci, 64, 971-976.

Nayak, M. K., Holloway, J. C., Emery, R. N., Pavic, H., Bartlet, J., & Collins, P. J. (2012). Strong resistance to phosphine in the rusty grain beetle,Cryptolestes ferrugineus(Stephens) (Coleoptera: Laemophloeidae): its characterisation, a rapid assay for diagnosis and its distribution in Australia. Pest Management Science, 69(1), 48–53. doi: 10.1002/ps.3360

Nevada State Department of Agriculture. (2005). Fumigation: the use of poisonous and lethal fumigants. Retrieved from http://agri.nv.gov/uploadedFiles/agrinvgov/Content/Plant/PEST/Study_Manuals/New%20C4%20fumigation%20Manual-full.pdf

Newman, C., Newman, J., Cheng, H., Ren Y. (2012). Investigation of thermosiphon pipes to distribute phosphine gas through grain silos from a ground level introduction point. In: Navarro S, Banks HJ, Jayas DS, Bell CH, Noyes RT, Ferizli AG, Emekci M, Isikber AA, Alagusundaram K, [Eds.] Proc 9th. Int. Conf. on

Controlled Atmosphere and Fumigation in Stored Products, Antalya, Turkey. 15 – 19 October 2012, ARBER Professional Congress Services, Turkey pp: 557-570

Newman, C. J. E.1990. Specification and design of enclosures for gas treatment. Fumigation and Controlled Atmosphere Storage of Grain. 108-130.

Noack. S. Rcichmuth, C., & Wohlgemuth. R. (1983). PH,-Rlickstlinde bei Vorratsschutzbegasungen in Abhlingigkeit von der Konzentration. Einwirkuogszeit und Lagerdauer oach der Begasung. Zeitschrift flir Lebensmitel-Untersuchung und -Forschung. 177. 87-93,

Opit, G. P., Phillips, T. W., Aikins, M. J. & Hasan, M. M. (2012). Phosphine resistance in Tribolium castaneum and Rhyzopertha dominica from stored wheat in Oklahoma. Journal of Economic Entomology, 105(4), 1107-1114.

Phillips, T. W., Thoms, E. M., DeMark, J., & Walse, S. (2014). Fumigation. Retrieved from https://entomology.k-state.edu/doc/finished-chapters/s156-14-may29.pdf

Phillips, T. W., & Throne, J. E. (2010). Biorational Approaches to Managing Stored-Product Insects. Annual Review of Entomology, 55(1), 375–397. doi: 10.1146/annurev.ento.54.110807.090451

Plumier, B., Maier, D. E., Ren, Y., & Schramm, M. (2018). Use of a 3D finite element model for post fumigation phosphine movement analysis. 12th International Working Conference on Stored Product Protection (IWCSPP), 355-361.

Proctor, D.L. (1994). Grain storage techniques: Evolution and trends in developing countries. Retrieved from http://www.fao.org/3/T1838E/T1838E00.htm

Rangaswamy, J. R. (1985). Phosphine residue and its desorption from cereals. Journal of Agricultural and Food Chemistry, 33(6), 1102–1106. doi: 10.1021/jf00066a021

Reddy, P. V., Rajashekar, Y., Begum, K., Leelaja, B. C., & Rajendran, S. (2006). The relation between phosphine sorption and terminal gas concentrations in successful fumigation of food commodities. Pest Management Science, 63(1), 96–103. doi: 10.1002/ps.1298

Reed, C., Wright, V. F., Pedersen, J. R., & Wongo, L. (1989). Wheat quality deterioration caused by insects and molds during the first months of storage on farms and in country elevators in Kansas. Journal of the Kansas Entomology Society, 62(4), 563-574.

Sato. K., & Suwanai, M. (1974). Adsorption of hydrogen phosphide to cereal products. Applied Entomology and Zoology, 9. 127-132.

Schroth, E., Muir, W.E., Jayas, D.S., White, N.D.G., & Abramson, D. (1998). Storage limit of wheat at 17% moisture content. Canadian Agricultural Engineering, 40(3), 201-205.

Shelton, D. P., & Jones, D. D. (1998, September). Management – the key to maintaining stored grain quality. Retrieved from https://lancaster.unl.edu/ag/crops/inservice/manage-i98.html

Shi, W., Jiao, K., Liang, Y., & Wang, F. (2016). Efficient detection of internal infestation in wheat based on biophotonics. Journal of Photochemistry and Photobiology B: Biology, 155, 137–143. doi: 10.1016/j.jphotobiol.2015.12.016

Shirasaki, Y., Matsuura, A., Uekusa, M., Ito, Y., & Hayashi, T. (2016). A study of the properties of chlorine dioxide gas as a fumigant. Experimental animals, 15-0092.

Simpson, G. D. 2005. Practical chlorine dioxide. Volume 1, Greg D. Simpson & Associates, Colleyville, TX.

Sinha, R. N. (1961). Insects and mites associated with hot spots in farm stored grain. The Canadian Entomologist XCIII(8):609-621.

Tan, J. N., Hwang, C. A., Huang, L., Wu, V. C., & Hsiao, H. I. (2021). A p ilot-scale evaluation of using gaseous chlorine dioxide for decontamination of foodborne pathogens on produce and l ow-moisture foods. Journal of Food Safety, e12937.

Tilley, D. R., Casada, M. E., & Arthur, F. H. (2006). Heat treatment for disinfestation of empty grain storage bins. Journal of Stored Products Research, 43(3), 221-228. doi: 10.1016/j.jspr.2006.04.005

Tkachuk, R. (1972). Phosphorous residues in wheat due to phosphine fumigation. Cereal Chemistry, 49, 258-267.

U.S. Department of Agriculture. (2006, September). Fumigation Handbook. Retrieved from https://www.ams.usda.gov/sites/default/files/media/FumigationHB.pdf

U.S. Department of Agriculture. (2003, April 1). Methyl Bromide Phaseout Proceeds: Users Request Exemptions. Retrieved from https://www.ers.usda.gov/amber-waves/2003/april/methyl-bromide-phaseout-proceeds/

U.S. Department of Agriculture. (2015). Stored grain insect reference. Washington, D.C.: Federal Grain Inspection Service.

U.S. Food and Drug Administration. (1998).Guidance for industry: Guide tominimize microbial food safety hazards for fresh fruits and vegetables.Retrieved from https://www.fda.gov/regulatory-information/search-fda-guidance-documents/guidance-industry-guide-minimize-microbial-food-safety-hazards-fresh-fruits-and-vegetables.

Utah Department of Agriculture. (1996). Fumigation and stored commodities pest control: pesticide application and safety training study guide. Retrieved from https://ag.utah.gov/documents/FumigationAndStoredCommoditiesStudyGuide.pdf

Warrick, C. (2010). Sealed silos — take the pressure test. Retrieved from http://storedgrain.com.au/wp-content/uploads/2013/06/Cropping_grain-storage.pdf

Winteringham, F.P.W. & Harrison, A. (1946). The sorption of methyl bromide by wheat. Journal of the Society of Chemical Industry, 65, 140-149.

Young, R. O. (2016). Chlorine dioxide (ClO2) as a non-toxic antimicrobial agent for virus, bacteria and yeast (Candida albicans). Int J Vaccines Vaccin, 2(6), 00052.

Chapter 3 - Sorption Kinetics and Equilibrium Isotherms of Phosphine Gas into Wheat Kernels

Abstract

A laboratory study was undertaken to investigate equilibrium phosphine (PH_3) gas sorption into wheat kernels. Six PH_3 concentrations (400, 700, 1000, 1500, 2000, 2400 ppm) were applied to gas-tight fumigation flasks containing wheat kernels (1/2 filling ratio) and concentrations through time were monitored until it reached equilibrium by injecting headspace gas samples in a gas chromatograph fitted with a flame photometric detector. Fumigation flasks were held at 25°C in an environmental chamber. Kinetic data showed that the sorption process was time-dependent and occured in two phases – an initial faster adsorption phase followed by a phase with a slower sorption rate as the grain and phosphine reached equilibrium. Pseudo-first and pseudo-second order models were fitted to PH_3 concentrations versus time experimental data. The pseudo-first order model provided better estimates and was used for the sorption isotherm analysis. Langmuir, Freundlich, and Redlich-Peterson sorption isotherm models were fitted to the plot of equilibrium headspace gas concentration versus sorbed PH_3 quantity. All three models had low standard error of prediction = 0.46-0.47. Higher equilibrium concentration was observed with increase in initial phosphine concentration, indicating that maximum adsorption capacity of wheat kernels was still not met by equilibrium points of lower concentrations applied to the flasks. Highest daily sorption percentage was observed for the first 24 h for 400 ppm treatment and after 48 h for all remaining treatments, and decreased through time for all concentration levels. Phosphine sorption kinetics and its total sorbed quantity at equilibrium is significant in determining the rate and maximum quantity of phosphine uptake in wheat.

3.1 Introduction

Hydrogen phosphide (PH_3), also known as phosphine, is a widely used fumigant for the disinfestation of stored wheat grains due to ease and versatility in application, relatively low cost, and high toxicity among various insects and other pests (Friedemann et al., 2020; Kaur and Nayak, 2015). However, an alarming development of genetically based phosphine resistance have been discovered in major species of stored product insects, which could be highly attributed to overuse and improper fumigation practices. The widespread use of phosphine in wheat fumigation has been exacerbated by the regulated phase-out of methyl bromide that depletes the ozone layer (Wang et al, 2020). A certain level of resistance to phosphine was detected in lesser grain borer (Ryzopertha dominica) (Afful et al., 2017), red flour beetle (Tribolium castaneum) (Opit et al., 2012), khapra beetle (Trogoderma granarium) (Yadav et al., 2020), rice weevil (Sitophilus oryzae) (Holloway et al., 2016), and rusty grain beetle (Cryptolestes ferrugineus) (Nayak et al., 2013). These insect pests have the ability to feed on and contaminate stored grains through secretion. Insect infestation remains as a major threat to stored grains used for food and sowing due to resulting yield losses (Belhamel et al., 2020; Astuti et al., 2019). Hence, the lack of economical and feasible fumigant alternatives and development of insect resistance pose a significant problem on the sustainability of phosphine as a fumigant across the globe, specifically in USA, Australia, India, Morocco, Pakistan, China, and Europe (Agrafioti et al., 2020).

To achieve a successful fumigation, lethal phosphine concentration must be held constant long enough to kill the insect pests at varying life stages. Fumigation becomes more challenging when dealing with resistant insect pest species since higher concentrations and longer fumigation periods are required. One of the common fumigation practices is monitoring of phosphine concentration using analog (glass tubes) or digital sensors that require air sample from the

fumigation chamber (Brabec et al., 2019). Inefficient and inaccurate phosphine concentration monitoring leads to unsuccessful fumigation of stored product facilities. Existing monitoring methods are tedious and difficult to implement as only trained applicators can perform the air sampling that is done multiple times for the entire fumigation period. Oftentimes, the sampling interval is once per day or even less, which is incomparable to an ideal real-time monitoring. Increasing the sampling trial and points would still be insufficient to determine the actual phosphine concentration across the fumigated facility as only limited areas are sampled at specific time. Thus, accurate spatio-temporal phosphine distribution cannot be developed using these analog or digital sensors (Agrafioti et al., 2020). In several studies, computational fluid dynamics (CFD) modeling was done to create a detailed view of the phosphine distribution within the bulk of wheat grains under certain environmental conditions and structural configurations. CFD models could predict gas concentrations, pressures, velocities, and temperatures within the grain bulk in real time applications (Mills et al., 2000).

Apart from leakage, sorption reduces the available phosphine gas in the air, leading to sublethal exposure of insects to phosphine. Leakage can be minimized by providing adequate sealing of fumigation structures, whereas sorption remains to be an uncontrollable factor due to the inherent strong adsorption characteristics of wheat. Amount of sorbed phosphine is dependent on the length of exposure, temperature, moisture, and dose (Daglish and Pavic, 2008). Experimentally, phosphine sorption in stored wheat has been studied by Berck (1968), Dumas (1980), Soma et al. (1996), Xiaoping et al. (2004), Reddy et al. (2007), Daglish and Pavic (2008, 2009), but all of these studies did not provide equilibrium data. Thermodynamic equilibrium between the intergranular gas and the sorbed gas within a porous medium is reached when zero net transfer between the gas and porous medium is achieved (Darby, 2008). Sorption equilibrium

and kinetics are necessary to fully understand the interactions between wheat and phosphine and to accurately account the sorption capacity of wheat in phosphine fumigation modeling. The maximum capacity of wheat to adhere and absorb phosphine, as well as the time to reach equilibrium are still unknown. Sorption equilibrium data and published insect toxicity data would be helpful in estimating the minimum effective dose of phosphine during wheat fumigation to achieve insect lethal concentrations. Darby (2008) argued that sorption equilibrium data would provide a stronger modeling framework in fumigation studies.

The objective of this study was to establish sorption kinetic and isotherm models that describe phosphine uptake and capacity in wheat kernels at equilibrium. Specific objectives were to determine the effect of initial concentration on the terminal concentration at which wheat and phosphine reached equilibrium and on cumulative and daily sorption percentage through time.

3.2 Materials and Methods

3.2.1 Material

Organic hard red winter wheat purchased from Heartland Mill (Marienthal, KS, USA) was used as an adsorbent in this study. Moisture content (MC), in % wet basis (w.b.) of wheat samples was measured in accordance with ASAE 352.2. Bulk density of wheat samples was measured using a Winchester cup arrangement (Seedburo Equipment Co., Des Plaines, IL, USA) wherein samples were allowed to fall from a hopper into a 1-pint cup (4.732 x 10-4 m^3) placed 10 cm below the hopper. The heap of wheat samples exceeding the edge of cup was scraped off using a wooden scraper. Bulk density of wheat samples was computed as the ratio of wheat kernel mass (g) and cup volume (m^3). True density of wheat samples was measured using a gas (helium) pycnometer (Quantachrome Ultrapyc 1200e, Odelzhausen, Germany) wherein helium gas was purged into the stainless-steel cylindrical vessel containing wheat kernels and expressed as ratio of wheat kernel

mass (g) and actual kernel volume (mL). The average moisture content, bulk density, and true density of wheat kernels were 12.56%w.b., 742.89 kg/m^3, and 1397.47 kg/m^3, respectively. PH_3 gas sourced from a pressurized cylinder (10,000 ppm, 1% nitrogen) acted as an adsorbate in this study.

3.2.2 Fumigation Procedure

A pressurized cylinder containing PH_3 gas (10,000 ppm, 1% nitrogen) was purchased from Matheson (Manhattan, KS), which was then fitted with a stainless-steel regulator, a thin rubber hose pipe, and a syringe needle. In a fume hood, PH_3 gas was withdrawn from the cylinder into a gas tight Tedlar® PVF film bag (CEL Scientific Corporation, Cerritos, CA) serving as a source bag for easy and safe gas transfer into the fumigation flasks that served as fumigation chambers. Prior to withdrawal of PH_3 gas, excess air in the Tedlar® PVF film bag was evacuated using an air pump fitted with a thin rubber hose pipe and a syringe needle for leakage test. Only the Tedlar® PVF film bags that remained crumpled and did not spread after the leakage test were used. An airtight Erlenmeyer flask with a glass port fitted with a rubber septum attached to its lid (1094 mL) was filled with wheat in ½ filling ratio (by volume). A specific amount of air was withdrawn from the flasks prior to injection of PH_3 gas. The same amount of the 10,000 ppm phosphine was injected through the rubber septum using a gas-tight syringe. The airtight flask was transferred back to the environmental chamber wherein the desired temperature (25 °C) was held constant. Treatments were done in triplicates.

3.2.3 Dilution of PH_3 concentration

To achieve the desired PH_3 gas concentration in the glass jars, the high-concentration source PH_3 gas was diluted with known quantity of air. The volume of wheat in the flask was accounted in the computation of the quantity of 10,000-ppm phosphine to be injected in the glass

chambers. The actual glass chamber volume to be considered is equal to the total glass jar volume minus the volume of the materials inside and volume occupied by rubber stopper fitted into its mouth. Initially, the glass flask contained air and wheat samples only. Before injection of 10,000-ppm phosphine, the same quantity of air was withdrawn using a gas-tight syringe. The injection volume of PH_3 was computed using equation 1.

$$\boldsymbol{V_i(mL)} = \frac{\boldsymbol{V_a * C_t}}{\boldsymbol{C_{cylinder}}} \quad (3\text{-}1)$$

where V_i is the injection volume of 10,000 ppm PH_3 gas, V is the actual glass jar volume (mL), C_t is the target PH_3 gas concentration in the jar (ppm), and $C_{cylinder}$ is the PH_3 gas concentration in the pressurized cylinder (10,000 ppm). Table 3-1 shows the computed injection volumes of 10,000 ppm PH_3 gas.

3.2.4 Sorption Equilibrium Measurement

Phosphine concentration in the headspace through time was measured by withdrawing 15 µL of gas sample from the glass jar using a Hamilton® 25 µL gas tight syringe at specific time intervals (2 h interval for the first 6 h, then every after 24 h) for 18 days. The gas sample concentration was quantified via gas chromatography using an Agilent 7820A gas chromatograph equipped with flame photometric detector (GC-FPD) (Agilent Technologies, Santa Clara, CA, USA) set in phosphorous mode and a J&W HP-5 capillary column (30 m length x 0.32 mm diameter x 0.25 µm film thickness). The response was plotted in a chromatogram and used to compute for the concentration in the flask. Each sampling measurement involved flask shaking to ensure representative withdrawal of headspace gas (Darby, 2008). Percentage daily loss of PH_3 was also computed for all treatments.

3.2.5 Quantitative Gas Chromatographic Analysis of PH_3 concentrations

The headspace gas sample concentration was quantified via gas chromatography. The GC-FPD system was connected to air, hydrogen, and helium pressurized cylinders with 99.99% ultra-high purity. Helium gas served as the carrier gas, while air and hydrogen served as the detector gases. Gas purifiers were separately installed between the three gas cylinders and GC to filter common contaminants (ie. oxygen, hydrocarbons, and moisture) from the carrier and detector gases. Use of gas purifiers lengthens column life and maintains instrument performance. The column flow rate was set to 5.75 mL/min. Setpoint flows were 100 mL/min for air, 75 mL/min for H_2 gas, and 60 mL/min for helium gas. Heated zone conditions were as follows: inlet temperature of 200 °C, isothermal oven temperature of 100 °C, and detector temperature of 200 °C.

A standard curve (also known as calibration curve) was generated by plotting the concentrations determined using the gas chromatograph. An empty inert Tedlar® PVF film bag contained the diluted gas (1,000 ppm PH_3) used in generating the standard curve. The ratio of 10,000-ppm phosphine gas and ambient air injected into the Tedlar® PVF film bag to achieve the desired phosphine concentration (1,000 ppm) was 1 PH_3 : 9 ambient air. Diluted gas samples of 5, 10, 15, 20, and 25 µL in triplicates were injected into the GC-FPD. In the generated chromatogram, the area under the peak response curve for each injection was used to plot a standard curve. The corresponding response areas versus injection volumes were plotted in a graph. A linear equation in the form of $y = mx + b$, wherein y is the GC-FPD detector response, m is the slope, x is the PH_3 concentration and b is the y-intercept was fitted to the curve. The R^2 value was computed to determine the performance of GC-FPD, syringe, and injections in determining PH_3 gas concentration. A low value of R^2 signifies inconsistent injection volumes or loose, worn-out syringe.

3.2.6 Sorption Kinetics

Sorption kinetics of phosphine into wheat kernels were examined in this study. Using the headspace gas measurements through time, sorbed quantity of PH_3 gas was computed as the difference between the initial PH_3 concentration and instantaneous PH_3 concentration at a given time. The sorbed quantity of PH_3 gas was plotted against time (h). Non-linear Pseudo-First (equation 3-2) and Pseudo-Second Order (equation 3-3) kinetic models were fitted to this graph. Non-linear Pseudo-First Order kinetic model is expressed as:

$$q_t = q_e(1 - e_1^{-1k_1 t}) \quad (3\text{-}2)$$

where, q_t (mg/kg) and q_e (mg/kg) are the sorption capacity of wheat kernels at time t (h) and at equilibrium, respectively; and k_1 (h^{-1}) is the rate constant of this model (Ammendola et al., 2017). Non-linear Pseudo-Second Order kinetic model is expressed as:

$$q_t = \frac{k_2 q_e^2 t}{1 + k_2 q_e t} \quad (3\text{-}3)$$

where, k_2 (kg mg^{-1} h^{-1}) is the rate constant of this model (Dursun & Kalayci, 2005).

3.2.7 Sorption Isotherm

Langmuir, Freundlich, and Redlich-Peterson sorption isotherm models were used to evaluate equilibrium isotherm of PH_3 gas into wheat kernels. The predicted equilibrium headspace concentration (x-variable) was plotted against sorbed PH_3 gas (y-variable) and then fitted with the above-mentioned models. Equilibrium concentration in the non-linear Langmuir isotherm model is expressed as:

$$q_e = \frac{q_{max} K_L C_e}{1 + K_L C_e} \quad (3\text{-}4)$$

where, q_{max} (mg/kg) is the monolayer sorption capacity of wheat kernels; C_e is equilibrium PH_3 concentration (ppm); and K_L is sorption constant of this model (Langmuir, 1918). Non-linear Freundlich isotherm model is given by:

$$q_e = K_F C_e^{\frac{1}{n}} \tag{3-5}$$

where, K_F is the sorption constant of this model; and 1/n indicates adsorption intensity (Freundlich, 1906). Redlich-Peterson isotherm model is given by:

$$q_e = \frac{AC_e}{1+BC_e^g} \tag{3-6}$$

where, A, B, and g are isotherm constant, model constant, and model exponent of Redlich-Peterson equation; and g value should be between 0 and 1. If g becomes 1, this equation reduces into Langmuir isotherm equation, whereas if g is 0, it reduces into Henry's Law (Rangabhashiyam et al., 2014).

3.2.8 Data Analysis

The fitted sorption kinetic and isotherm models were evaluated using standard error of prediction (SEP), residual plot, and Akaike information criterion (AIC) to determine the accuracy of predictions.

$$SEP = \sqrt{\frac{\sum(Y-Y\prime)^2}{N}} \tag{3-7}$$

where Y and Y' are the experimental and predicted sorption capacity values, respectively; and N is the number of observation points.

$$AIC = 2k - 2\ln(\hat{L}) \tag{3-8}$$

where k is the number of estimated parameters in the model and $\hat{L}$ is the maximum value of the likelihood function for the model. TableCurve 2D v5.01 (Systat Software, San Jose, CA) was used to approximate the time needed to reach certain concentration of specific percentage from

its initial concentration value using the response y. All treatments were conducted in triplicates, while flask measurements were done in duplicates.

3.3 Results and Discussion

In this study, the effects of initial PH_3 headspace concentration (ppm) on phosphine sorption in hard red winter wheat kernels were investigated. Sorption kinetics and isotherms of this system were also studied.

3.3.1 Adsorption Kinetic Analysis

Non-linear regression analysis was performed by fitting adsorption kinetic models to experimental data of sorbed PH_3 gas in hard red wheat kernels. Parameters of Pseudo-first order and Pseudo-second order kinetic models were estimated by minimizing the sum of squared residuals. Figure 3.1 shows the non-linear plots of Pseudo-first order and Pseudo-second order kinetic models fitted to the experimental data of phosphine sorption capacity through time. Table 3.1 lists the kinetic model parameters, Akaike information criteria (AIC) and standard error of prediction (SEP) values obtained at six different initial concentrations. In terms of SEP, Pseudo-second order kinetic model obtained lower AIC and SEP values for all models fitted at different initial concentrations, which indicates that this model has lower response prediction errors or residuals for the experimental data. Figure 3.2 and 3.3 show the residual plots of pseudo-first order and pseudo-second order kinetic model estimates. In comparison, the pseudo-first order kinetic model had residual plots of scattered points for first half of points with distinct concave upward at the end of the plot. Meanwhile, the pseudo-second order model produced residual plots with more evidence of random scatter in some 2^{nd}-order plots, but patterns are still apparent in most cases. However, the predicted equilibrium sorbed PH_3 quantity (q_e) was overpredicted as it exceeds the initial concentration applied to the flasks. Only the pseudo-first order model resulted in reasonable

predicted q_e values that did not exceed the initial PH_3 concentrations. It is also in harmony with the experimental sorption data through time as indicated by its SEP. Thus, the pseudo-first order kinetic model predicted values were used for PH_3 sorption isotherm plots. The predicted q_e values for both models showed that as initial concentration increased, the sorbed quantity of PH_3 in wheat kernels also increased. This observation suggests that at lower concentrations, the maximum capacity of wheat kernels were not achieved and thus, the final sorbed quantity at the end of experiment still increased with increase in applied concentration. As observed in Figure 3.1, faster rate of sorption were observed for the first 48 hours, which gradually decreased through time as it reached near equilibrium. From pseudo-first kinetic model estimates, sorbed quantities at equilibrium after applying approximately 400, 700, 1000, 1500, 2000, and 2400 ppm initial concentrations were 1.10, 1.93, 2.88, 4.15, 5.23, and 6.35 mg PH_3 per kg wheat kernels, respectively. Darby (2008) stated that faster sorption rate indicated by steeper initial slope from the finite-volume fumigant concentration curve was a result of PH_3 gas diffusing into the intergranular space prior to entry into sorption sites of the exterior and interior parts of wheat kernels. The faster initial phase of PH_3 sorption represents the reversible binding, which is referred as physisorption. Quantity of phosphine sorbed by means of physisorption may be desorbed through rise in temperature, decrease in atmospheric pressure, long period of aeration using inert gases, or extraction with solvents. (Berck & Gunther, 1970). The concentration through time with less steep slopes and more curvature corresponds to the slower irreversible binding of PH_3 to wheat kernels. Irreversible binding occurred as phosphine may react with components of wheat kernels (Hwaidi et al., 2015; Daglish & Pavic, 2009).

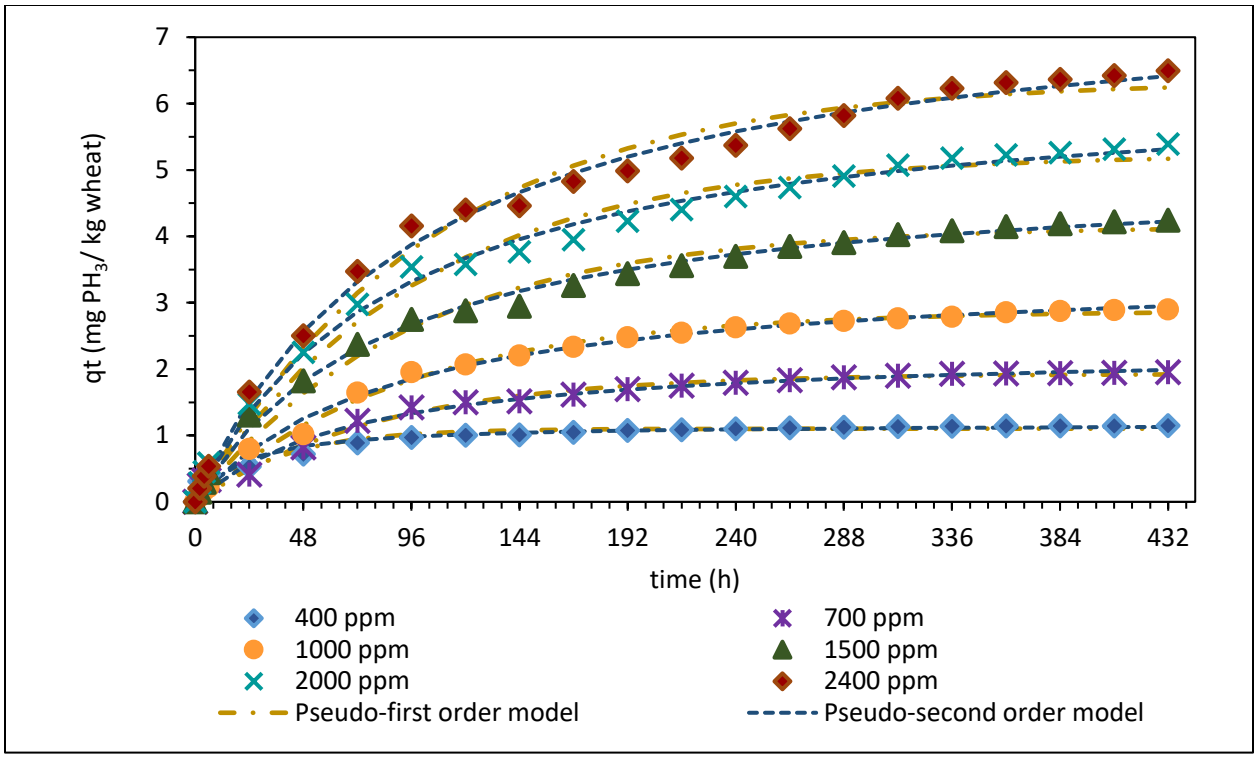

Figure 3.1 Sorption kinetics of phosphine gas in hard red winter wheat at different initial concentrations fitted to Pseudo-first order and Pseudo-second order models.

Table 3.1 Sorption kinetic model parameters, AIC, and SEP for phosphine in hard red winter wheat

Model	Temperature (°C)	Parameter	Initial Concentration (ppm)					
			400	700	1000	1500	2000	2400
Pseudo-first order	25	q_e (mg kg^{-1})	1.10	1.93	2.88	4.15	5.23	6.35
		k_1 (h^{-1})	0.03	0.01	0.01	0.01	0.01	0.01
		AIC	-96.4	-99.81	-115.8	-75.9	-62.3	-80.7
		SEP	0.10	0.09	0.06	0.16	0.21	0.23
Pseudo-second order	25	q_e (mg kg^{-1})	1.18	2.31	3.54	5.06	6.41	7.89
		k_2 (kg mg^{-1} h^{-1})	0.04	0.01	0.003	0.002	0.002	0.001
		AIC	-110.0	-102.3	-118.0	-102.6	-84.9	-58.1
		SEP	0.07	0.08	0.06	0.08	0.13	0.14

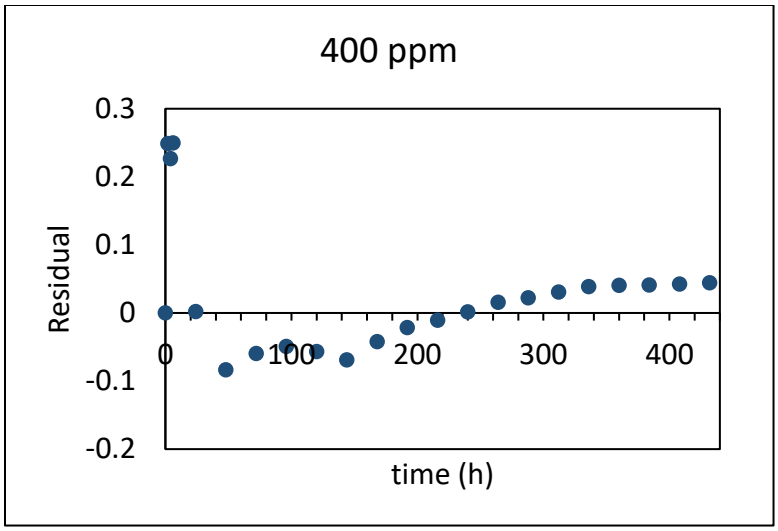
400 ppm
0.3
0.2
0.1
0
-0.1
-0.2
Residual
0
100
200
300
400
time (h)

(a)

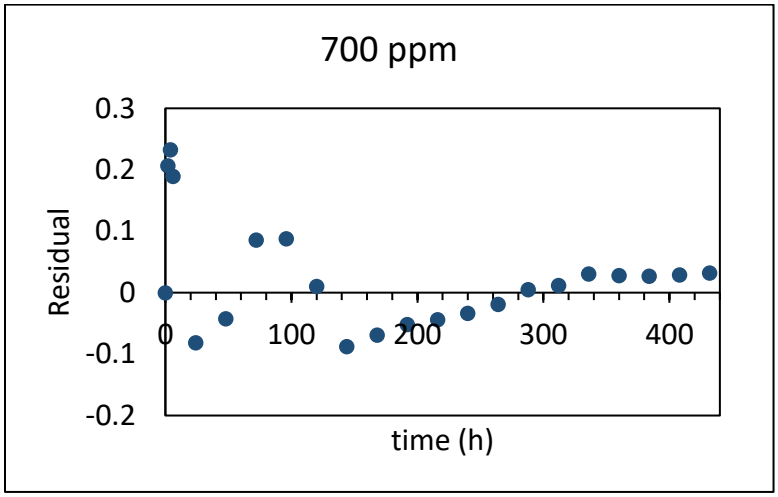
700 ppm
0.3
0.2
0.1
0
-0.1
-0.2
Residual
0
100
200
300
400
time (h)

(b)

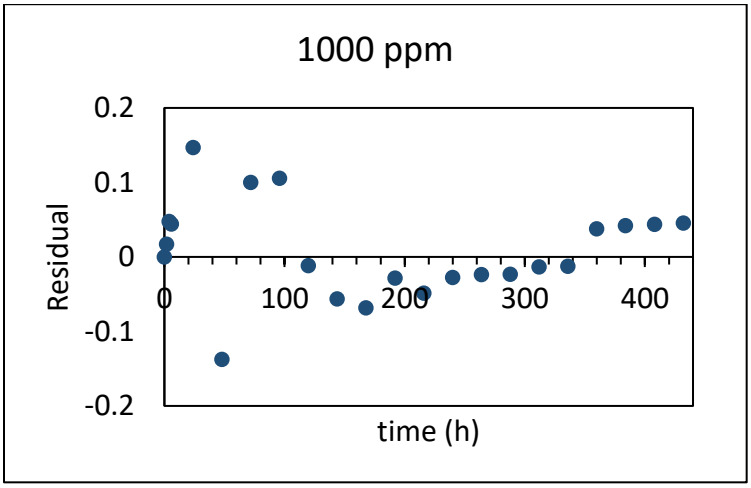
1000 ppm
0.2
0.1
0
-0.1
-0.2
Residual
0
100
200
300
400
time (h)

(c)

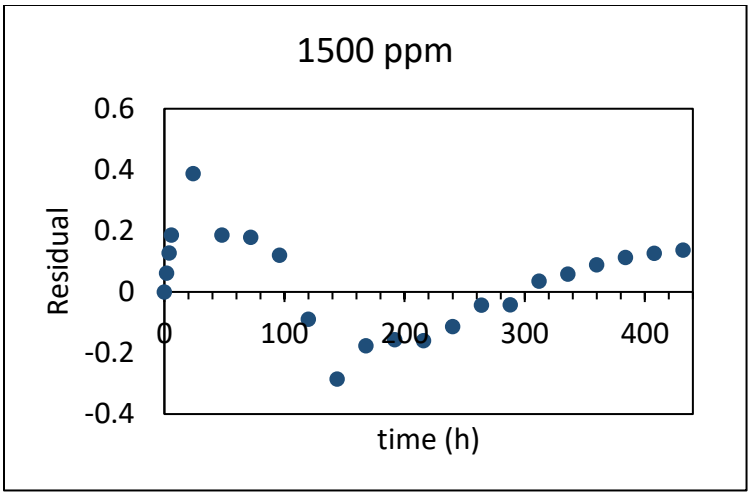

(d)

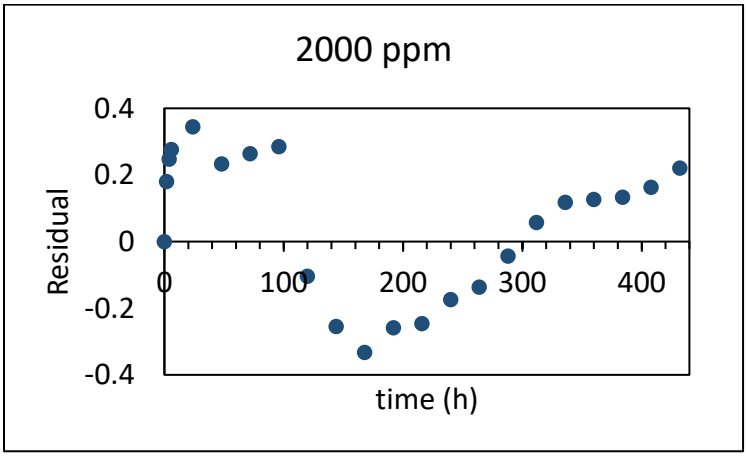

(e)

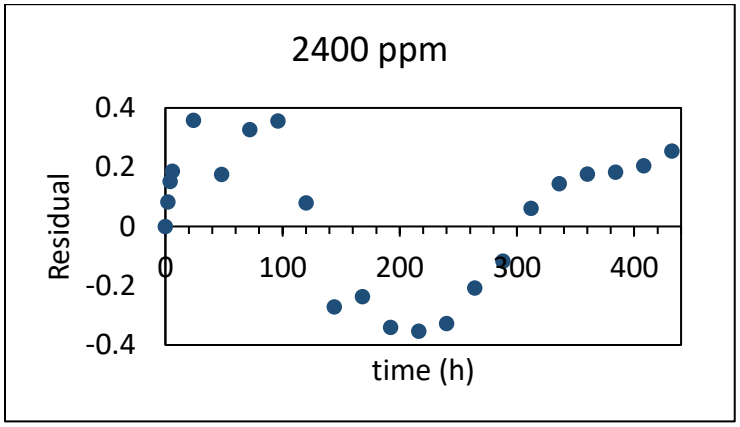

(f)

Figure 3.2 Residual plots of pseudo-first order kinetic model estimates: (a) 400 ppm, (b) 700 ppm, (c) 1000 ppm, (d) 1500 ppm, (e) 2000 ppm, and (f) 2400 ppm

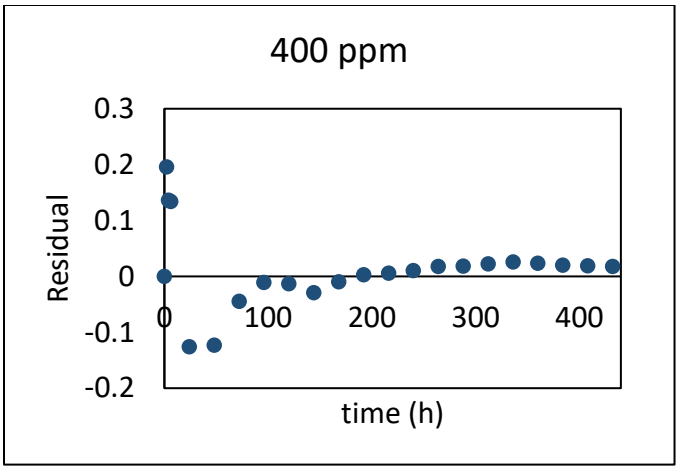
400 ppm
0.3
0.2
0.1
0
-0.1
-0.2
Residual
0
100
200
300
400
time (h)

(a)

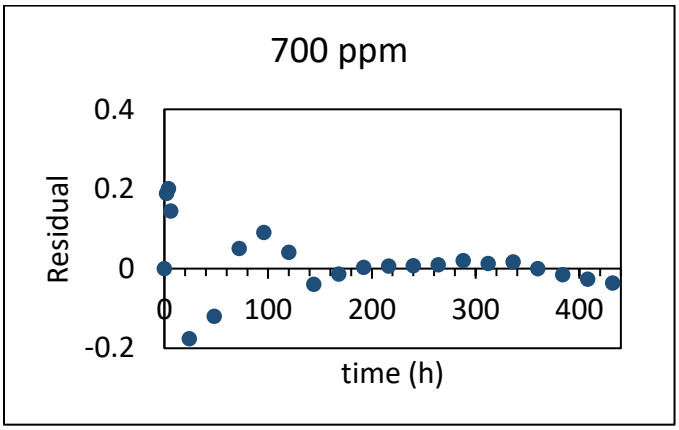
700 ppm
0.4
0.2
0
-0.2
Residual
0
100
200
300
400
time (h)

(b)

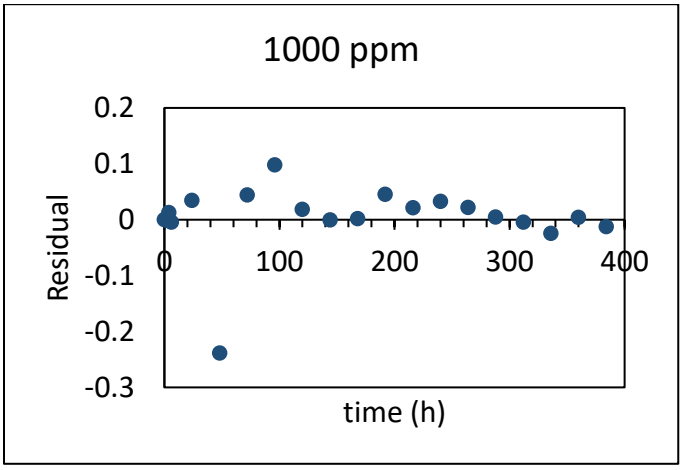
1000 ppm
0.2
0.1
0
-0.1
-0.2
-0.3
Residual
0
100
200
300
400
time (h)

(c)

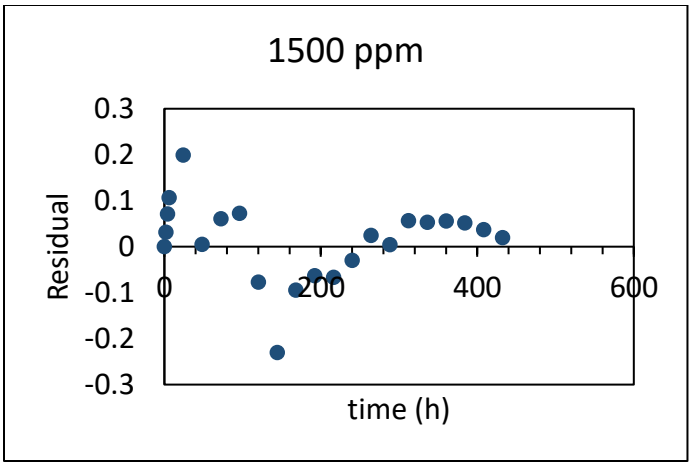

(d)

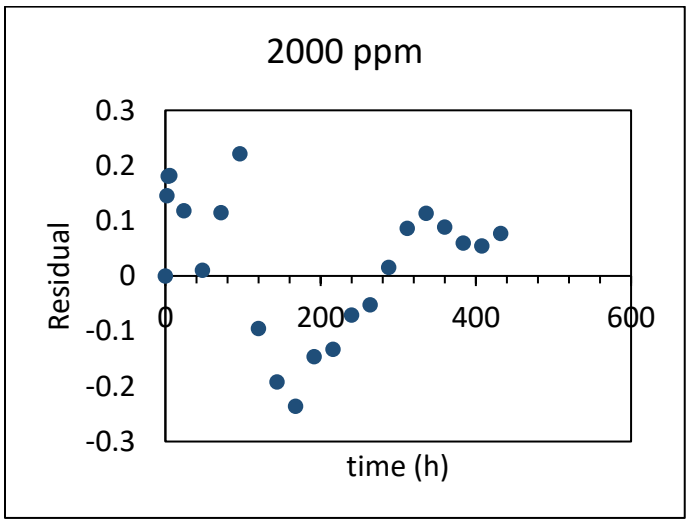

(e)

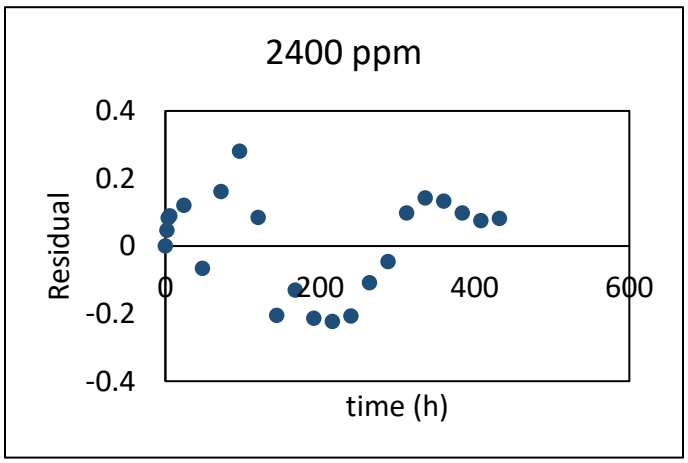

(f)

Figure 3.3 Residual plots of pseudo-second order kinetic model estimates: (a) 400 ppm, (b) 700 ppm, (c) 1000 ppm, (d) 1500 ppm, (e) 2000 ppm, and (f) 2400 ppm

3.3.2 Effect of Initial Concentration on Sorption

Figure 3.4 shows the daily and cumulative PH_3 sorption percentages throughout the fumigation of wheat kernels. It was observed that peak PH_3 sorption percentages occurred after approximately 24 hours for 400 ppm and approximately 48 hours for 700, 1000, 1500, 2000, and 2400 ppm. Highest daily PH_3 percentages for 400, 700, 1000, 1500, 2000, and 2400 were 31.6%, 18.6%, 17.2%, 16.6%, 16.2%, and 15.4%, respectively. Cumulative PH_3 sorption percentage provides information about the time before an initial concentration falls below 50%, 75%, and 90% of its value. Using TableCurve 2D v5.01, time to reach these mentioned points was obtained and summarized in Table 3.2. It was observed that as applied concentration increased, the time needed to fall to 50%, 75%, and 90% of its value also increased. Darby (2008) explained that finite-volume sorption experiments (similar to this study) often result in experimental data with higher scatter at the start of data gathering. This scatter may be due to the unavoidable admixing of subsequent traces of gas left in the syringe. As fumigant gas (99% pure phosphine) was administered to the fumigation flask with the use of a gas-tight syringe at varying concentrations (low to high) and withdrawal of this gas from the flasks was done subsequently using the same gas-tight syringe. Although scatter may happen during finite-volume flask experiments, it gradually minimizes as the gap in between syringe uses becomes longer and frequency of usage occurs as a slower pace, thus allowing the gas enough time to dissipate. Also, injection of gas was done from low to high concentrations to minimize the effect of traces of previous injection to the next injection.

Table 3.2 Time needed for initial PH_3 concentration to fall specified percentage of its value

Treatment	Time to reach (h)		
	50%	75%	90%
400 ppm	25.97	56.59	107.49
700 ppm	58.31	118.81	207.39
1000 ppm	66.47	134.61	230.86
1500 ppm	70.19	144.72	262.20
2000 ppm	73.07	151.57	280.62
2400 ppm	78.84	164.83	314.76

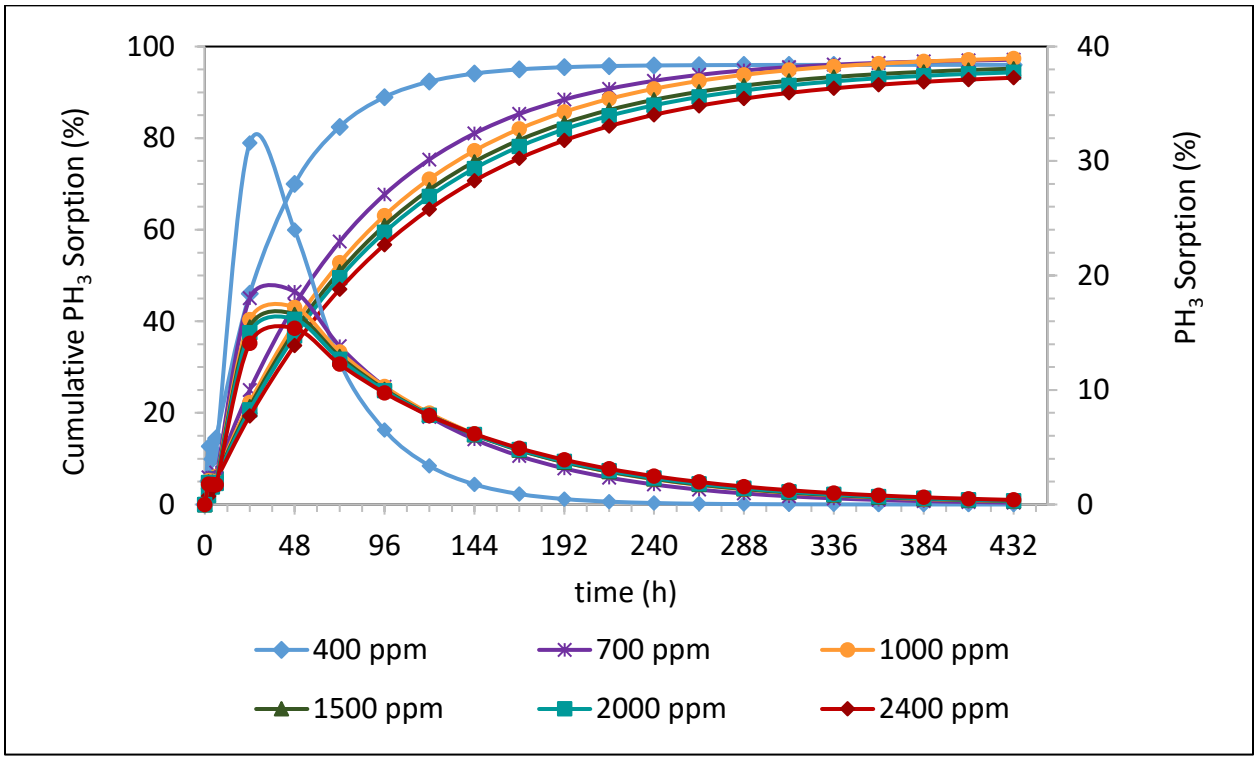

Figure 3.4 Cumulative and PH_3 sorption percentages in hard red winter wheat at 25°C through the entire fumigation experiment.

3.3.4 Sorption Isotherm Analysis

Sorption isotherm models were fitted to the experimental data of PH_3 concentrations until it reached equilibrium using non-linear regression analysis. Non-linear evaluation of these sorption isotherm models was done to optimize estimated isotherm model parameters giving the smallest possible sum of squared residuals. Langmuir, Freundlich, and Redlich-Peterson sorption isotherm

models were used to evaluate experimental sorption equilibrium data of PH_3 at 25°C. Figure 3.5 illustrates non-linear plots of Langmuir, Freundlich and Redlich-Peterson models fitted to experimental equilibrium PH_3 headspace concentration (ppm) versus sorbed PH_3 concentration (mg/kg wheat). All model parameters and their corresponding AIC and SEP are reported in Table 3.3. As observed in Figure 3.5, it is evident that the plots of Langmuir, Freundlich, and Redlich-Peterson fit well with the experimental data. Only at 400 and 1000 ppm treatments that the model was not close in predictions. In terms of AIC, lowest AIC of -4.8 was obtained from both Freundlich sorption isotherm model. In terms of SEP, lowest SEP value of 0.46 was obtained from both Freundlich and Redlich-Peterson sorption isotherm models. All models had residual plots with no distinct pattern, thus these models were appropriate for predicting sorbed quantity using headspace gas concentration at equilibrium. The Langmuir sorption isotherm model suggests that the sorption occured in a monolayer coverage and wheat kernels have identical sorption sites that are energetically equivalent. Meanwhile, Freundlich sorption isotherm model is applicable to model the sorption process on heterogenous surfaces that are characterized by various coexisting structural and chemical surface properties (Ayawei et al., 2017). It is also applicable to model phosphine-wheat system as the heterogeneous surface of wheat results from its different constituents such as protein, starch, lipid, vitamin, and minerals. The majority of nutrients (such as lipid, protein, vitamin, and minerals) and other undesirable components (such as phytic acid) are usually located along the external tissues of cereal grains (Liu, 2007). Furthermore, Freundlich also assumes, in this case, that wheat kernels have exponential distribution of active sites Ayawei et al., 2017). In the study of Suresh and Neethirajan (2015), a 3D visualization of the vertical cross-section of wheat kernel was generated, showing its structural features such as pores, protein assemblies, starch granules, and biopolymer matrices. The generated 3D visualization showed

potential sites where PH_3 gas can further penetrate during the sorption process. Interestingly, Ayawei et al. (2017) explained that at high concentrations of adsorbate, the Redlich-Peterson sorption isotherm model reduces into a Freundlich sorption isotherm model. As the Redlich-Peterson sorption isotherm model is linearly dependent on concentration in its numerator and exponentially dependent in its denominator, which altogether represents a wide range of adsorption equilibrium at varying concentrations of adsorbate, it is said to be applicable for both homogeneous or heterogeneous surfaces. The sorption rate results in this study were limited to phosphine-wheat system with a ½ filling ratio of wheat at 25 °C. Hence, other wheat filling ratios and temperatures should be investigated for sorption isotherm analysis to gain better understanding of the adsorption capacity of wheat kernels at different fumigation conditions.

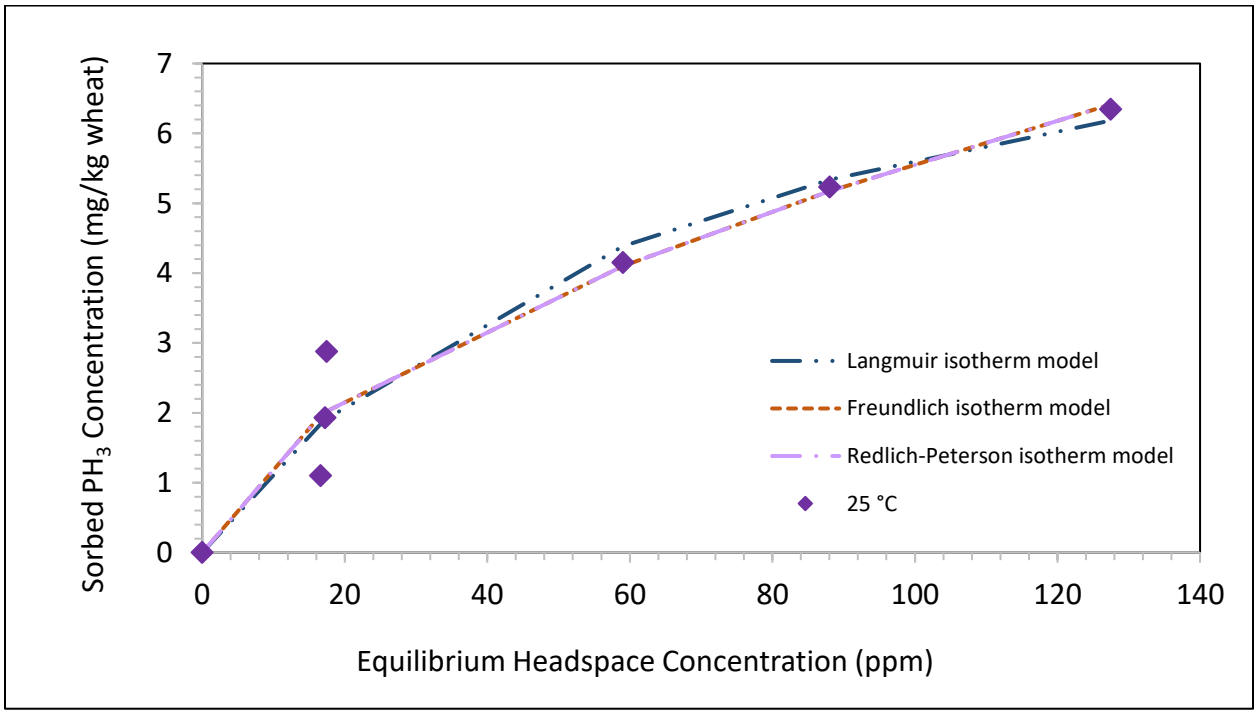

Figure 3.5 Sorption isotherms of phosphine gas in hard red winter wheat at two temperatures (25 °C and 30 °C) fitted to Langmuir, Freundlich, and Redlich-Peterson isotherm models.

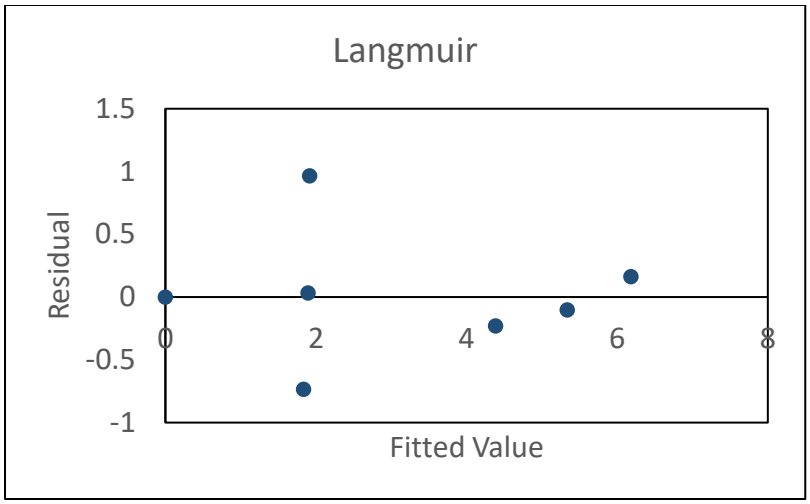

(a)

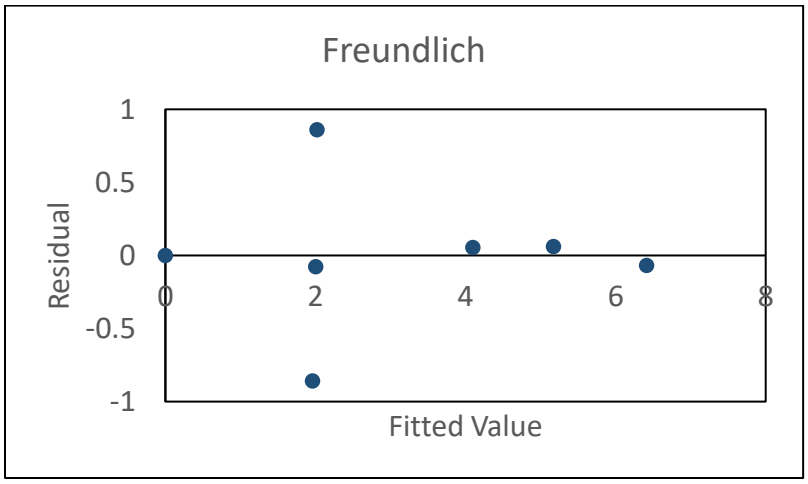

(b)

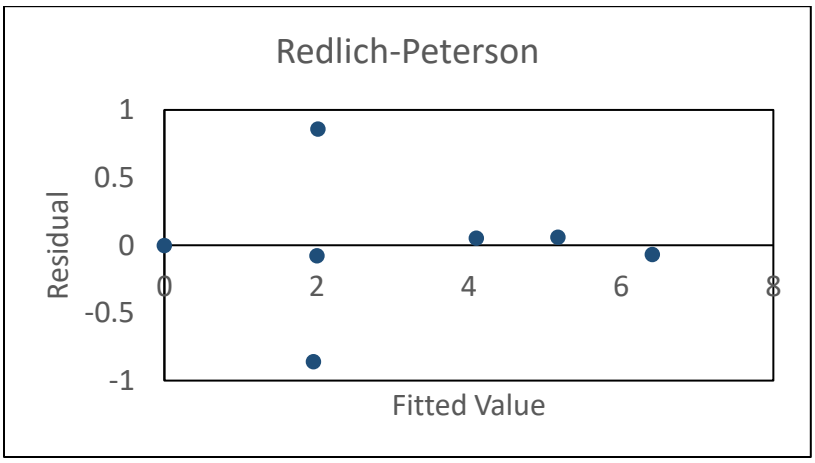

(c)

Figure 3.6 Residual plots of sorption isotherm estimates: (a) Langmuir model, (b) Freundlich model, and (c) Redlich-Peterson model.

Table 3.3 Sorption isotherm model parameters for phosphine in hard red winter wheat

Model	Parameter	Value
Langmuir	q_{max} (mg/kg)	9.57
	K_L	0.01
	AIC	-4.5
	SEP	0.47
Freundlich	K_F	0.38
	1/n	0.58
	AIC	-4.8
	SEP	0.46
Redlich-Peterson	g	0.42
	B	2708.1
	A	1037.5
	AIC	-2.8
	SEP	0.46

3.4 Summary and Conclusion

The kinetics of sorption of PH_3 into wheat kernels and resulting equilibrium isotherms were analyzed. Headspace gas concentrations over time in a finite-volume flask were measured using a gas chromatograph fitted with flame photometric detector. Flasks were fumigated at six PH_3 concentrations and held at 25°C for 18 days. Non-linear regression analyses were performed to describe the concentrations through time.

Based on the results of this study, conclusions were:

1. The sorption of PH_3 into wheat kernels occurred in two phases for all treatments. First, a rapid sorption phase indicated by steeper slopes at the start of the process followed by gradual decrease in sorption rate as concentration nears its equilibrium.
2. The pseudo-first order model fit well to the experimental data of sorbed PH_3 concentration through time. Pseudo-second order overpredicted endpoint values that are not applicable to the analysis as it also exceeds the known initial concentrations.

3. Equilibrium concentrations at the headspace and sorbed quantities of PH_3 into wheat kernels can be described by Langmuir, Freundlich, and Redlich-Peterson sorption isotherm models.
4. An increase in adsorption capacity with increasing applied concentration indicates that the maximum wheat adsorption capacity was still not reached at equilibrium points of lower concentrations applied to fumigation chambers.

3.5 References

Afful, E., Elliott, B., Nayak, M., & Phillips, T. (2017). Phosphine Resistance in North American Field Populations of the Lesser Grain Borer, Rhyzopertha dominica (Coleoptera: Bostrichidae). Journal of Economic Entomology, 111(1), 463-469. https://doi.org/10.1093/jee/tox284

Agrafioti, P., Kaloudis, E., Bantas, S., Sotiroudas, V., & Athanassiou, C. G. (2020). Modeling the distribution of phosphine and insect mortality in cylindrical grain silos with Computational Fluid Dynamics: Validation with field trials. Computers and Electronics in Agriculture, 173, 105383.

Ammendola, P., Raganati, F., & Chirone, R. (2017). CO2 adsorption on a fine activated carbon in a sound assisted fluidized bed: Thermodynamics and kinetics. Chemical Engineering Journal, 322, 302-313.

ASAE International (1988), Method S352.2- Moisture Measurement-Unground Grain and Seeds. American Society of Agricultural and Biological Engineers, St. Joseph, Michigan

Astuti, L., Rizali, A., Firnanda, R., & Widjayanti, T. (2020). Physical and chemical properties of flour products affect the development of Tribolium castaneum. Journal Of Stored Products Research, 86, 101555. doi: 10.1016/j.jspr.2019.101555

Ayawei, N., Ebelegi, A. N., & Wankasi, D. (2017). Modelling and interpretation of adsorption isotherms. Journal of chemistry, 2017.

Belhamel, C., Boulekbache–Makhlouf, L., Bedini, S., Tani, C., Lombardi, T., & Giannotti, P. et al. (2020). Nanostructured alumina as seed protectant against three stored-product insect pests. Journal Of Stored Products Research, 87, 101607. doi: 10.1016/j.jspr.2020.101607

Berck, B. (1968). Sorption of phosphine by cereal products. Journal Of Agricultural And Food Chemistry, 16(3), 419-425. doi: 10.1021/jf60157a009

Berck, B., & Gunther, F. A. (1970). Rapid determination of sorption affinity of phosphine by fumigation within a gas chromatographic column. Journal of Agricultural and Food Chemistry, 18(1), 148-153.

Brabec, D., Campbell, J., Arthur, F., Casada, M., Tilley, D., & Bantas, S. (2019). Evaluation of Wireless Phosphine Sensors for Monitoring Fumigation Gas in Wheat Stored in Farm Bins. Insects, 10(5), 121. doi: 10.3390/insects10050121

Daglish, G. J., & Pavic, H. (2008). Effect of phosphine dose on sorption in wheat. Pest Management Science: formerly Pesticide Science, 64(5), 513-518.

Daglish, G. J., & Pavic, H. (2009). Changes in phosphine sorption in wheat after storage at two temperatures. Pest Management Science: formerly Pesticide Science, 65(11), 1228-1232.

Darby, J. A. (2008). A kinetic model of fumigant sorption by grain using batch experimental data. Pest Management Science: formerly Pesticide Science, 64(5), 519-526.

Dumas, T. (1980). Phosphine sorption and desorption by stored wheat and corn. Journal of agricultural and food chemistry, 28(2), 337-339.

Dursun, A. Y., & Kalayci, C. S. (2005). Equilibrium, kinetic and thermodynamic studies on the adsorption of phenol onto chitin. Journal of hazardous materials, 123(1-3), 151-157.

Freundlich, H. M. F. (1906). Over the adsorption in solution. J. Phys. chem, 57(385471), 1100-1107.

Friedemann, A., Andernach, L., Jungnickel, H., Borchmann, D., Baltaci, D., & Laux, P. et al. (2020). Phosphine fumigation – Time dependent changes in the volatile profile of table grapes. Journal Of Hazardous Materials, 393, 122480. https://doi.org/10.1016/j.jhazmat.2020.122480

Holloway, J., Falk, M., Emery, R., Collins, P., & Nayak, M. (2016). Resistance to phosphine in Sitophilus oryzae in Australia: A national analysis of trends and frequencies over time and geographical spread. Journal Of Stored Products Research, 69, 129-137. doi: 10.1016/j.jspr.2016.07.004

Hwaidi, M., Collins, P. J., Sissons, M., Pavic, H., & Nayak, M. K. (2015). Sorption and desorption of sulfuryl fluoride by wheat, flour and semolina. Journal of Stored Products Research, 62, 65-73.

Kaur, R., & Nayak, M. K. (2015). Developing effective fumigation protocols to manage strongly phosphine-resistant Cryptolestes ferrugineus (Stephens) (Coleoptera: Laemophloeidae). Pest. Manag. Sci. 71: 1297–1302.

Langmuir, I. (1918). The adsorption of gases on plane surfaces of glass, mica and platinum. Journal of the American Chemical society, 40(9), 1361-1403.

Liu, K. (2007). Laboratory methods to remove surface layers from cereal grains using a seed scarifier and comparison with a barley pearler. Cereal chemistry, 84(4), 407-414.

Mills, K. A., Wontner-Smith, T. J., Bartlett, D. I., & Harral, B. B. (2000). A new positive pressure system for combating dilution during phosphine fumigation of bulk grain. In Proceeding International Conference Controlled Atmosfphere and Fumigation in (pp. 405-420).

Nayak, M., Holloway, J., Emery, R., Pavic, H., Bartlet, J., & Collins, P. (2012). Strong resistance to phosphine in the rusty grain beetle,Cryptolestes ferrugineus(Stephens) (Coleoptera: Laemophloeidae): its characterisation, a rapid assay for diagnosis and its distribution in Australia. Pest Management Science, 69(1), 48-53. doi: 10.1002/ps.3360

Opit, G. P., Phillips, T. W., Aikins, M. J., & Hasan, M. M. (2012). Phosphine resistance in Tribolium castaneum and Rhyzopertha dominica from stored wheat in Oklahoma. Journal of Economic Entomology, 105(4), 1107-1114.

Rangabhashiyam, S., Anu, N., Nandagopal, M. G., & Selvaraju, N. (2014). Relevance of isotherm models in biosorption of pollutants by agricultural byproducts. Journal of Environmental Chemical Engineering, 2(1), 398-414.

Soma, Y., Kishino, H., & Akagawa, T. (1996). Sorption of phosphine in cereal grains and beans. Research Bulletin of the Plant Protection Service (Japan).

Suresh, A., & Neethirajan, S. (2015). Real-time 3D visualization and quantitative analysis of internal structure of wheat kernels. Journal of Cereal Science, 63, 81-87.

Vanitha Reddy, P., Rajashekar, Y., Begum, K., Chandrappa Leelaja, B., & Rajendran, S. (2007). The relation between phosphine sorption and terminal gas concentrations in successful fumigation of food commodities. Pest Management Science: formerly Pesticide Science, 63(1), 96-103.

Wang, K., Liu, M., Wang, Y., Song, W., & Tang, P. (2020). Identification and functional analysis of cytochrome P450 CYP346 family genes associated with phosphine resistance in Tribolium castaneum. Pesticide Biochemistry And Physiology, 168, 104622. doi: 10.1016/j.pestbp.2020.104622

Xiaoping, Y., Zhanggui, Q., Daolin, G., & Wanwu, L. (2004, August). Adsorption of phosphine by wheat, paddy and corn. In Proceedings of the International Conference on Controlled Atmosphere and Fumigation in Stored Products. Gold-Coast Australia (pp. 8-13).

Yadav, S., Srivastava, C., & Sabtharishi, S. (2020). Phosphine resistance and antioxidant enzyme activity in Trogoderma granarium Everts. Journal Of Stored Products Research, 87, 101636. doi: 10.1016/j.jspr.2020.101636.

Chapter 4 - Chlorine Dioxide Gas Kinetics and its Effects on Wheat Kernel and Flour Quality

Abstract

Chlorine dioxide (ClO_2) gas, known for its high oxidation and penetration capacity, is a potential alternative fumigant to control stored-product insect pest population. In the present study, hard red spring wheat (*Triticum aestivum* L.) kernels were exposed to varying levels of gaseous ClO_2 concentrations (200, 300, 400, and 500 ppm) and held in a gas-tight bucket assembly for 24 h after achieving desired concentration. Three vials containing 20 unsexed adults of lesser grain borer (*Rhyzopertha dominica* (Fabricius)) were placed at top, middle, and bottom layers of wheat mass during fumigation for insect mortality assessment. ClO_2 treatment achieved complete insect mortality and highest adult progeny reduction at 500 ppm across all vial locations. Increased mortality was observed with increasing ClO_2 concentration. Significant reduction (37.8-51.1%) in germination rate resulted after exposure to 300-500 ppm. In terms of flour color, lightness value significantly increased ($p < 0.05$) after treatment of 200-500 ppm. The pH value of wheat flour had significant reduction ($p < 0.05$) from 6.2 to 6.1 after 500 ppm treatment. In terms of pasting characteristics, peak and final viscosities of ClO_2-treated wheat flour at 200-500 ppm significantly decreased ($p < 0.05$) from 3303.7 to 3073.3 cP and from 3515.0 to 3208.3 cP, respectively. No significant difference ($p > 0.05$) was observed in other investigated flour quality and functionality parameters, including falling number, trough viscosity, breakdown viscosity, starch damage, and mixolab dough behavior properties. Overall, ClO_2 treatment at 500 ppm is effective in killing adult lesser grain borers without negatively affecting wheat flour quality parameters but affects wheat kernel viability.

4.1 Introduction

Wheat is one of the major staple food crops that ranks third in terms of annual production, planted acreage, and gross farm receipts in the U.S. next to corn and soybeans. In total, 1.6 billion bushels of wheat from 37.2 million acres of harvested land was recorded for marketing year 2021-2022 in the U.S. (USDA, 2022). Wheat production varies in quantity from year to year depending on several factors including environmental conditions, and planting and harvesting practices. Storing grains during over-production is a strategic way to meet the demand for wheat during under-production seasons (Neethirajan et al., 2007).

During storage, insect infestation is a major constraint that threatens both quantity and quality of the wheat supply. Insect pests can feed on and contaminate wheat kernels with excretion or dead body parts, which could further lead to mycotoxin contamination. Fumigation is a method to reduce insect pest populations that involve the application of toxic chemical gas into the bulk grain. With the phase-out of methyl bromide and increasing insect resistance development to phosphine, there is a need to find suitable alternatives to these commonly used fumigants for insect pest control for bulk stored grains (Kim et al., 2019).

Chlorine dioxide (ClO_2) is a potential fumigant that can effectively kill various stored-product species. Its efficacy has been proven in controlling adult populations of both susceptible and laboratory strains of the red flour beetle (*Tribolium castaneum*), saw-tooted grain beetle (*Oryzae surinamensis*), and lesser grain borer (*Ryzopertha dominica*) (E et al., 2018). Although mortality assessment results for these insect species is promising, it is important to evaluate the effects of ClO_2 on wheat kernel and flour characteristics as these aspects determine its processability into food products. Few published studies have evaluated the effect of chlorine dioxide (ClO_2) treatment on stored wheat and wheat-based product quality. In the study of Han et

al. (2018), wheat viability was found to be influenced by ClO_2 gas exposure at varying concentrations and durations. At 100 ppm ClO_2 gas for 12 h, wheat viability significantly decreased with only 48% of the wheat seeds growing into normal seedlings after the germination test while the untreated wheat seeds had an 81% germination rate. At 200 ppm ClO_2 gas exposure for 6 h, significant reduction in germination rate of wheat seeds from 89% (untreated) to 73% (treated) was observed. The same treatment led to a reduced germination rate of 32.67% when duration was extended up to 48 h. Residues in wheat seeds were also examined in this study. Chlorine dioxide (mg/kg of grain) was not detected immediately after treatment as well as on the 1^{st} and 10^{th} day after treatment of 200 ppm ClO_2 for 24 h. Chlorine (0.70 mg/kg wheat) and chlorite (1.27 mg/kg wheat) were detected after treatment, which significantly reduced after one day to 0.23 mg/kg wheat and 0.44 mg/kg wheat, respectively. During the 10^{th} day, no chlorine and chlorite residue were detected.

The objective of this study was to determine ClO_2 kinetics during fumigation of wheat kernels at desired concentrations with a non-continuous source of ClO_2 and to evaluate its effects on mortality of lesser grain borers and wheat kernel and flour properties after treatment.

4.2 Materials and Methods

4.2.1 Chlorine dioxide fumigation

ClO_2 gas was produced by a custom-built ClO_2 generator from Pure Line Treatment Systems, LLC (Chicago, Illinois, USA) housed inside a trailer, located next to the O.H. Kruse Feed Technology Innovation Center on the K-State campus. It is composed of a pump, bucket, gas monitor, and purging system. This system can produce 99% pure ClO2 gas, which was then diluted with ambient air in the bucket. Inside the gas-tight bucket, a circular perforated hose at its bottom served as the entry point of gas to ensure even gas distribution. The gas-tight bucket was half-filled

(~ 8.25 kg) with hard red spring wheat (MC = 8.8%w.b.) that had not been fumigated before. After the optical sensor converter (Control 4000, Optek, Germantown, Wisconsin, USA) set to detect ClO_2 concentrations displayed the desired concentrations (200, 300, 400, 500 ppm), the valve was closed and pump was shut down. No ClO_2 gas was entering at this point into the bucket. Achieving the exact target ClO_2 concentration was difficult. Hence, resulting peak concentrations were above the target concentrations. ClO_2 concentration was monitored for up to 24 hours prior to venting. Temperature and humidity measurements inside the trailer were recorded using HOBO© data loggers (Model U10-003, Onset Computer Corp., Bourne, Massachusetts, USA).

4.2.2 Insect mortality and progeny production assessment

Three snap cap vials (diameter = 23 mm, height = 55 mm, 250 µm, wire-meshed top and bottom) containing 20 unsexed adults of lesser grain borers (*Rhyzopertha dominica*) and about 10 g of organic hard red spring wheat (8.8% w.b.) were placed vertically at top, middle, and bottom sections of wheat mass during ClO_2 treatment. The mesh screens allowed ClO_2 diffusion through the vials and prevented insects from escaping during the treatment. Two similar vials were placed outside the bucket for the entire duration of treatment, which served as control treatment. After treatment, vials were kept in an environmental chamber at 28°C and 65% r.h. Mortality was assessed after 5 days from treatment as delayed toxic effects may happen after ClO_2 treatment. Dead insects were counted, and mortality was computed as the percentage of dead insects out of the initial number of insects in each vial. After mortality assessment, both live and dead adult insects, wheat kernels, and grain dust were placed into flat bottom vials with meshed snap caps, which were held at 28°C and 65% r.h. for 30 days to determine adult progeny production. The culture of this insect species was reared in 0.95L glass jars supplemented with approximately 250

g of diet and held at 28°C and 65% R.H in an environmental chamber. Culture jars consisted of wire mesh screens plus filter papers in the metal lids.

4.2.3 Chlorine dioxide kinetics

Concentration of ClO_2 for all treatments was monitored for 24 hours. ClO_2 Concentration data were plotted against time. Percentage loss in concentration was plotted against time. TableCurve 2D v5.01 (Systat Software, San Jose, CA) was used to find the best-fit model to the plot of average ClO_2 concentration versus time (starting only at the peak concentration adjusted to time zero).

4.2.4 Germination rate

ClO_2-treated and control wheat kernels were placed into petri dishes (diameter = 90 mm) lined with one piece of filter paper initially impregnated with 5 ml distilled water. Exactly 15 wheat kernels were placed into each petri dish. All petri dishes were covered with lid and wrapped with parafilm strip to prevent water loss through evaporation. Aluminum foil was used to wrap the entire petri dish to prevent light from passing through for four days at 22°C. Germination rate was computed as the percentage of germinated wheat kernels divided by the total number of wheat kernels.

4.2.5 Straight-grade flour milling

ClO_2-treated and control wheat samples (1.5 kg per replicate, 3 replicates) were tempered to reach 16%w.b for 24 h and then milled using a Chopin LabMill (Chopin, France). This mill was equipped with 6 roll pairs, specifically 2 break, 1 sizing, and 3 reduction rolls. The samples were fed at a rate of 5 g/sec for 1st break roll and 2.5 g/sec for all remaining rolls. Flour fractions from the break, sizing, and reduction setting were blended together to make straight-grade flour, which

were then subjected to flour quality analysis. Milling yields in this study were expressed in % as-is basis. Other milling fractions recovered were shorts and coarse and fine bran.

$$\%yield\ (as-is) = \frac{weight\ of\ milling\ fraction\ (g)}{weight\ of\ tempered\ wheat\ (g)} x\ 100$$

4.2.6 Proximate composition

The following methods were conducted in measuring moisture content (% wet basis), ash (%), fat (%), and fiber (%) of wheat flour samples were ASAE 352.2 (ASAE, 1988), AOAC 923.03, AOAC 922.06, and AOAC 962.09 (AOAC, 2019), respectively. Following AACC method 46-30.01, nitrogen (N) content of flour samples was determined and used to compute for its protein content which was equated to N x 5.7 for wheat flour. Nitrogen-free extract (%) was computed as 100 – (% ash + % crude fat + % protein + % moisture + % crude fiber). All proximate composition percentages were expressed in % as-is basis.

4.2.7 Flour analysis

4.2.7.1 Falling number

Falling number of wheat flour samples was measured using a Foss Alphatec^{TM} FN° machine (Eden Prairie, MN) in accordance with AACC method 56-81.04. About 7.0 ± 0.05 g of wheat flour (moisture corrected by varying the quantity) was placed in a viscometer tube and 25 ml distilled water was then added. This mixture of distilled water and sample were vigorously shaken to achieve a homogeneous suspension. A stirrer was placed into the viscometer tube and then the setup was placed into a boiling water bath. The instrument stirred the mixture and stirrer was released at the top section of the tube after 60 seconds of stirring. It was allowed to submerge by its own weight. Falling number was the length of time (s) from the start until the stirrer completely fell at the bottom.

4.2.7.2 Dough rheology

In accordance with AACC method 54-60.01, dough rheology assessment was done using MixoLab (Chopin, France) (AACC, 2010). The "Chopin+" protocol in 14% moisture basis was used during the test. Water absorption (%) of wheat flour samples were adjusted until C1 value reaches the range 1.10 ± 0.05 Nm after mixing for 8 mins. After reaching the desired C1, the test proceeded with the actual protocol that involves 80 rpm mixing speed, equilibrium point at 30°C for 8 mins, heating for 15 mins up to 90°C with 4°C/min rate, holding time of 7 mins at 90°C, cooling for 5 mins to reach 50°C at -4°C/min rate, and holding period at 50°C for 5 mins. From this test, values of C1, CS, C2, C3, C4, C5, development time, and absorption (%) were measured.

4.2.7.3 Pasting characteristics

A Rapid Visco Analyzer (RVA) Model-4 (Newport Scientific; Warriewood, NSW) was used to measure pasting properties of wheat flour samples, following STD2 of AACC method 76-21.02 (AACC, 2010). The test was done after wheat flour moisture adjustment to 14% moisture basis. The STD2 RVA analysis involved the following conditions: 1st stage (50°C, 0 s), 2nd stage (960 rpm, 0 s), 3rd stage (160 rpm, 10 s), 4th stage (50°C, 1 min), 5th stage (95°C, 8.5 min), 6th stage (95°C, 13.5 min), 7th stage (50°C, 21 min), and end of test at 23 mins. Time interval between measurements was 4 s. From this test, peak viscosity, breakdown viscosity, peak time, minimum viscosity, final viscosity, and pasting temperature values were recorded.

4.2.7.4 Flour color

A MiniScan EZ 4500 Colorimeter (HunterLab, Reston, VA) was used to measure color of wheat flour samples in terms of L* (-black to +white), a* (-green to +red), and b* (-blue to +yellow) color parameters.

4.2.7.5 Damaged starch

Damaged starch of wheat flour samples was measured using SDMatic (Chopin, France) in accordance with AACC method 76-33.01 (AACC, 2010). A solution was made consisting of 120 ml distilled water, 1.5 g citric acid, 3 g potassium iodide, and 1 drop of sodium thiosulphate. This solution was then placed into the reaction bowl. About 1 g of flour was placed in a plastic piece inserted to the SDmatic instrument. The solution was allowed to reach 35°C, then the instrument automatically vibrated to load the samples into the solution. Damaged starch values were recorded after 3 min.

4.2.7.6 pH

A calibrated pH meter (Extech PH100 ExStik, FLIR ExStik®, Nashua, NH, USA) was used to measure pH of wheat flour samples in accordance with AACC method 02-52.01 (AACC, 2010). About 10 g of wheat flour samples was mixed with 100 ml distilled water and this mixture was then mixed continuously for 15 min with a magnetic stirrer until combined homogeneously and free of lumps. Afterwards, mixture was left undisturbed for 10 mins. The pH meter was submerged into the decanted supernatant liquid to measure the pH of flour samples. The pH meter was calibrated prior to the test.

4.2.8 Data Analysis

Mortality was expressed as the percentage of dead insects out of the initial number of insects exposed to ClO_2 gas treatment. Mortality percentages were corrected using the control mortality following Abbott's formula as shown below (Abbott, 1925):

$$Corrected\ mortality\ (\%) = \left(1 - \frac{insect\ population\ after\ treatment}{insect\ population\ in\ control\ treatment}\right) * 100$$

First part of this study followed a one-way factorial treatment with 6 treatments (control, 200, 300, 400, 500, 500x2) for concentration monitoring and insect mortality assessment. Second

part of this study followed a one-way factorial treatment with 5 treatments (control, 200, 300, 400, 500) for wheat kernel and flour analyses. Treatments were conducted in triplicates. All data obtained from the experiment were analyzed using Statistical Analysis Software (SAS) 9.3 (SAS Institute, Cary, NC, USA). Analysis of variance (ANOVA) was used for treatment means comparison and Tukey's Honestly Significant Difference (HSD) was used to compare significant differences ($p < 0.05$) between treatment means.

4.3 Results and Discussion

4.3.1 Insect mortality and progeny production assessment

Table 4.1 shows mortality and adult progeny production for adults of lesser grain borer. After 5 days, complete mortality was achieved for all vial locations for insects treated with 500 ppm ClO_2 gas. Complete mortality was also observed for the top and bottom vials treated with 400 ppm ClO_2 gas, while its middle vial had a mortality of 96.7%. Other treatments, such as 200 and 300 ppm, did not achieve complete mortality across all vial locations. For 300 ppm, mortality of lesser grain borers ranged from 71.7 to 91.7% across the bucket, while for 200 ppm, it ranged from 91.7 to 96.7%. Mortality increased from lower to higher concentration both for top and bottom vial locations for all treatments. Adult progeny of Lesser grain borer was observed in both control and ClO_2-treatments. On average, about 96.7 of adult progeny were produced after 30 days at 28°C and 65% R.H. All treatments resulted in significant ($p < 0.05$) progeny reduction. However, 200 ppm treatment still resulted in high adult progeny production of about 39.7 to 48.7, which is about 48.3 to 59.0% of adult progeny reduction relative to the control treatment. In comparison to the control and 200 ppm treatments, significantly greater ($p < 0.05$) adult progeny reduction were observed for remaining treatments. The adult progeny reduction averaged from 92.1 to 97.2% for 300 ppm treatment; 96.2 to 97.2% for 400 ppm treatment; and 96.6 to 99.0% for 500 ppm

treatment. No treatment achieved complete adult progeny reduction, thus indicating reinfestation may happen even after complete mortality was achieved for 400 and 500 ppm treatments. Adult progeny production even after complete mortality at 400 and 500 treatment is caused by the possibility that the insects hatched eggs during fumigation as a stress response. These eggs are able to survive and continue its growth into adults (E et al., 2017). Greater progeny production at lower concentration (200 ppm treatment) signifies that lower mortality leaves more adults to produce progeny aside from the eggs hatched by the adult insects during fumigation. Hence, increase in mortality can also help in reduction of adult progeny production; however, eggs may be hatched by the insects during fumigation that can still survive as progeny given favorable development conditions and time.

Table 4.1 Corrected insect mortality and adult progeny production results for all ClO_2 gas treatments

Treatment	Mortality (%)			Number of Adult Progeny (% reduction relative to control treatment)		
Control	-			96.67 ± 8.50^{a}		
	Top	Middle	Bottom	Top	Middle	Bottom
200 ppm	71.7 ± 5.8^{bB}	91.7 ± 2.9^{A}	90.0 ± 0.0^{bA}	39.7 ± 17.8^{b} (59.0%)	50.0 ± 33.1^{b} (48.3%)	48.7 ± 12.5^{b} (49.7%)
300 ppm	91.7 ± 7.6^{a}	96.7 ± 2.9	95.0 ± 5.0^{ab}	2.7 ± 3.1^{c} (97.2%)	7.7 ± 2.5^{c} (92.1%)	3.0 ± 1.0^{c} (96.9%)
400 ppm	100 ± 0.0^{a}	96.7 ± 5.8	100 ± 0.0^{a}	2.7 ± 1.2^{c} (97.2%)	2.3 ± 2.1^{c} (97.6%)	3.7 ± 4.0^{c} (96.2%)
500 ppm	100 ± 0.0^{a}	100 ± 0.0	100 ± 0.0^{a}	3.3 ± 1.5^{c} (96.6%)	1.3 ± 1.2^{c} (98.6%)	1.0 ± 1.0^{c} (98.97%)
F	23.39	2.83	11.00	62.91	22.05	107.10
P	0.0003	0.1062	0.0033	<0.0001	<0.0001	<0.0001

Note: Different lowercase superscript letters differ significantly among different fumigation treatments ($P < .05$); Different uppercase superscript letters differ significantly among different location of insect vials at a specified fumigation treatment ($P < .05$).

4.3.2 Chlorine dioxide kinetics

Figure 4.2 shows the plot of ClO_2 gas concentration throughout the duration of all replications of all treatments. In this plot, since the system purged ClO_2 gas into the bucket from time zero, it took a finite time to reach the nominal concentrations. Peak concentrations for all treatments were not identical, but near the nominal concentrations due to the complexity of handling gas. Figure 4.3 shows the plot of concentration starting from the nominal concentration through the end of all treatments. Time zero in this plot starts at the point where the target concentration was achieved. Adjustment of nominal values to time zero was necessary as the time to reach the desired concentration varied across replicates and nominal concentrations do not lie at the same time points. After readjusting the time zero, the concentration values were then averaged through time to assess the rate of concentration loss after the source of ClO_2 gas was turned off. TableCurve 2.0 v5.01 was used to fit a model that could describe the change in ClO_2 concentration with time at different initial concentrations (200, 300, 400, and 500). Selection of best-fit model was done by choosing a model equation with a smaller number of coefficients for simplicity and has low standard error and low sum of squared residuals. Various model equations satisfied these selection criteria, but the simplest model that provided a good fit was chosen for this analysis. Model coefficients and goodness-of-fit indices of the best-fit model for the experimental data are listed in Table 4.2. The best-fit model is given below:

$$\ln(y) = a + bx$$

Wherein A and B are regression coefficients; x is the time in h; and y is the ClO_2 concentration at any given time. All fitted equations resulted to $p < 0.05$. Thus, selected model was significant in predicting the response y for all treatments. Both A and B coefficients for all equations resulted to $p < 0.05$, which indicate that both coefficients should be retained in the equation. This fitted model

resulted to low standard error ranging from 3.9 to 9.4. Shown in Figure 4.4 is the equivalent percentage of concentration loss through the entire treatments. In general, the concentration loss percentage was very similar for all treatments, with the maximum difference of about 12% for the 400 ppm treatment at 4 h of treatment. This deviation may be due to some differences in temperature across replications and treatments. The times required to reach specific concentration levels are listed in Table 4.3. Across all treatments, no significant difference ($P > 0.05$) was found for time needed to reach peak concentration. No significant difference ($P > 0.05$) was also found for time needed to reach 1^{st} and 2^{nd} half-lives and 90% concentration loss. On average, the peak concentration took about 1.5 to 1.9 h to fall at 50% of its value, about 2.9 to 3.6 h to fall at 25% of its value, and about 4.2 to 6.8 h to fall at 10% of its value. The decrease in concentration of ClO_2 gas may be explained by the initial oxidation of the active sites on the surface of kernels followed by its penetration to kernels once active sites were fully oxidized. Excess gas molecules accumulated after full oxidation of active sites in wheat kernels and increase in concentration through time with continuous gas inflow caused a lethal concentration against insects (Simpson, 2005; E et al., 2017). Aside from chemical reaction, decrease in concentration may also be attributed to mass transfer of ClO_2 molecules from headspace into the intergranular space as ClO_2 has a specific gravity of 1.6, which means it is heavier than air and naturally sinks by its weight (Ramsey & Mathiason, 2019).

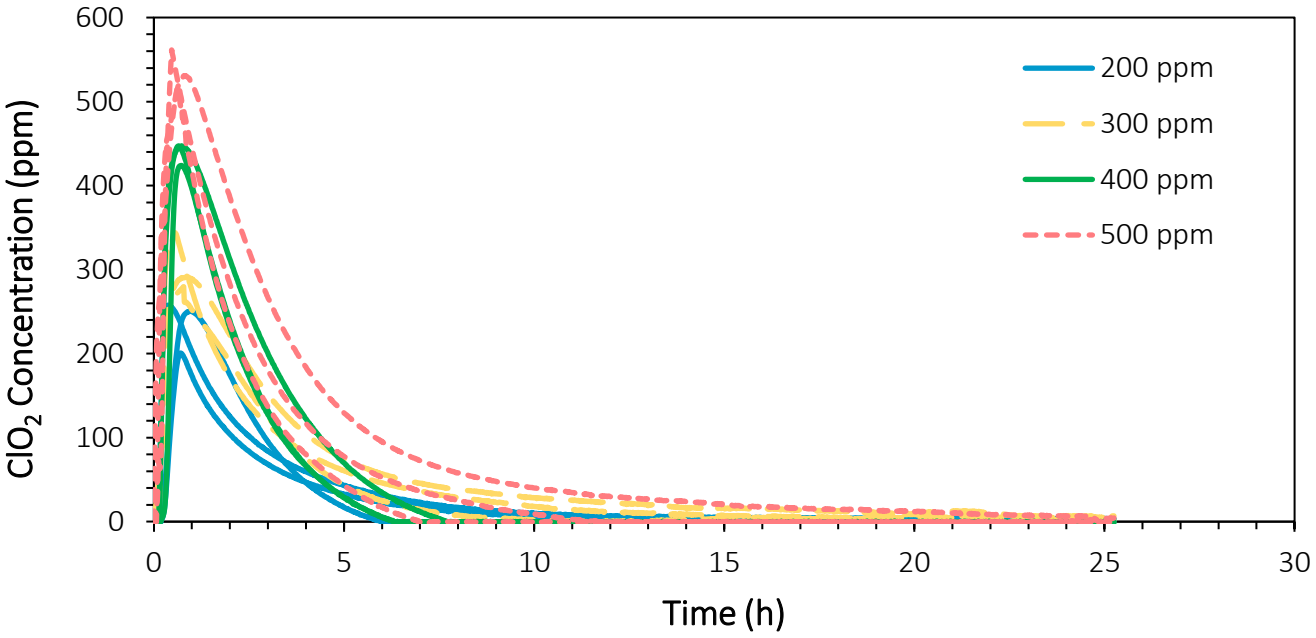

Figure 4.1 Concentration of ClO_2 over time for all replications of treatments

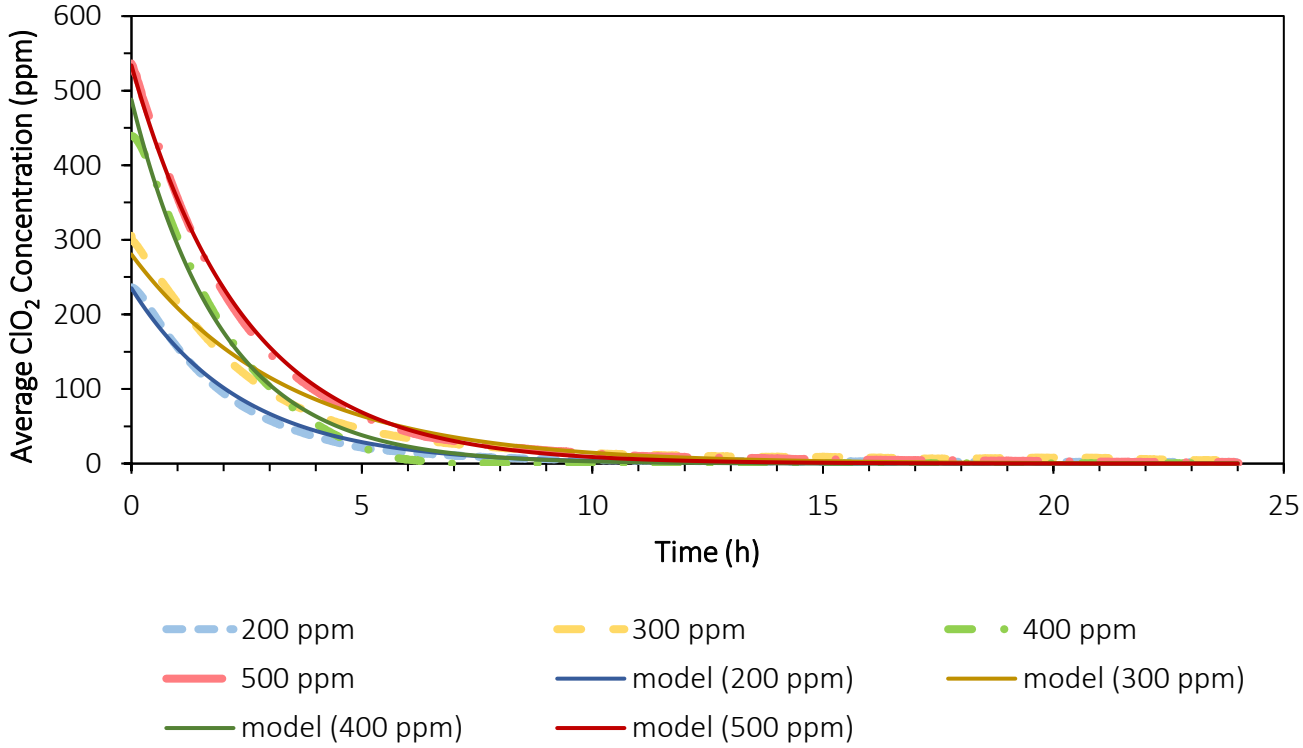

Figure 4.2 Average ClO_2 concentration over time for all treatments (adjusted time zero at nominal concentration)

Table 4.2 Model coefficients and goodness-of-fit indices generated from ClO_2 concentrations through time for each treatment

Treatment	Coefficients		Goodness-of-Fit Indices
	A	B	Standard Error
200 ppm	5.46	-0.42	3.92
300 ppm	5.64	-0.30	9.41
400 ppm	6.19	-0.51	7.39
500 ppm	6.28	-0.41	4.75

Note: A & B are coefficients obtained from model fitting; model coefficients and goodness-of-fit indices were obtained using TableCurve 2D v5.01

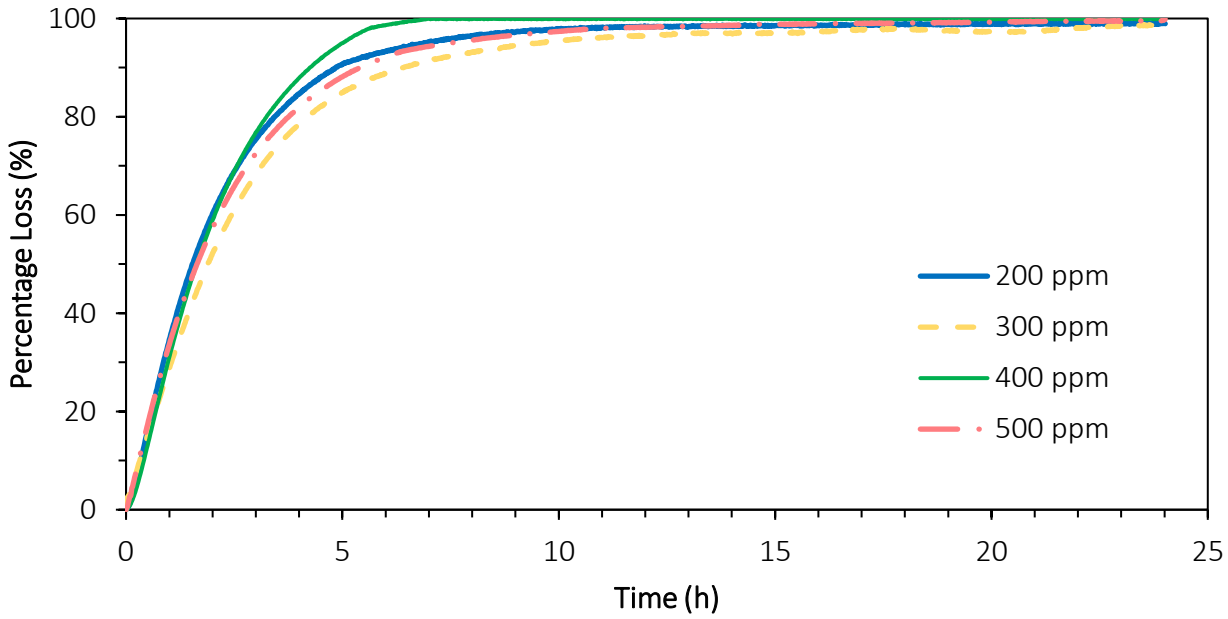

Figure 4.3 Percentage loss of ClO_2 gas through time for all treatments

Table 4.3 Time to reach nominal, 1st and 2nd half-life, and 90% loss in concentration for all treatments

Time to reach (h)	ClO2 gas treatment				F-value	P
	200 ppm	300 ppm	400 ppm	500 ppm		
Nominal concentration	0.7 ± 0.3	0.7 ± 0.2	0.7 ± 0.0	0.6 ± 0.2	0.19	0.9035
1st Half-life (50% concentration)	1.5 ± 0.1	1.9 ± 0.4	1.7 ± 0.3	1.7 ± 0.5	0.48	0.7030
2nd Half-life (25% concentration remaining)	3.1 ± 0.4	3.6 ± 0.5	2.9 ± 0.5	3.3 ± 0.9	0.89	0.4875
90% concentration loss	5.6 ± 0.7	6.8 ± 2.0	4.2 ± 0.6	5.7 ± 1.8	1.74	0.2369

4.3.3 Germination rate

The germination rate (%) of ClO_2-treated and control wheat kernels is illustrated in Figure 4.5. Both the control (91.1%) and 200 ppm treated flour (88.9%) recorded a significantly higher germination percentage compared to the remaining treatments. Meanwhile, the germination rates of 300 ppm (53.3%), 400 ppm (57.8%), and 500 ppm (40.0%) treated flours are not significantly different with each other. These results are in harmony with the findings of Han et al. (2018) wherein significant reduction in germination rate was observed in wheat kernels when it was subjected to ClO_2 gas treatment of 100 ppm for 12 h and 200 ppm for 6 h. Based on concentration data through time, ClO_2 concentration in this study fall from 200 to 100 ppm in less than 2 hours as the source has been stopped after hitting the desired concentration. Thus, its effect on germination at 200 ppm did not result to any significant difference. Germination rate is an important consideration since it indicates seed viability. Reduced germination rate may translate to lower expected emergence of wheat seeds planted, thus affecting crop stand, yield, and profitability. This decrease in germination may be attributed to the oxidative stress caused by excess in reactive oxygen species that can damage cellular components of wheat kernels such as protein and lipid (Kim et al., 2015). Further evaluation of biochemical components is needed to specify any disrupted structure or reduced activity of related enzymes upon exposure to ClO_2 gas treatment. Hence, in this case, germination results in this study suggests that ClO_2-treated at higher concentration (500 ppm for lesser grain borer) to achieve complete insect mortality would not be ideal for planting as it is expected to have more than 50% reduction in germination.

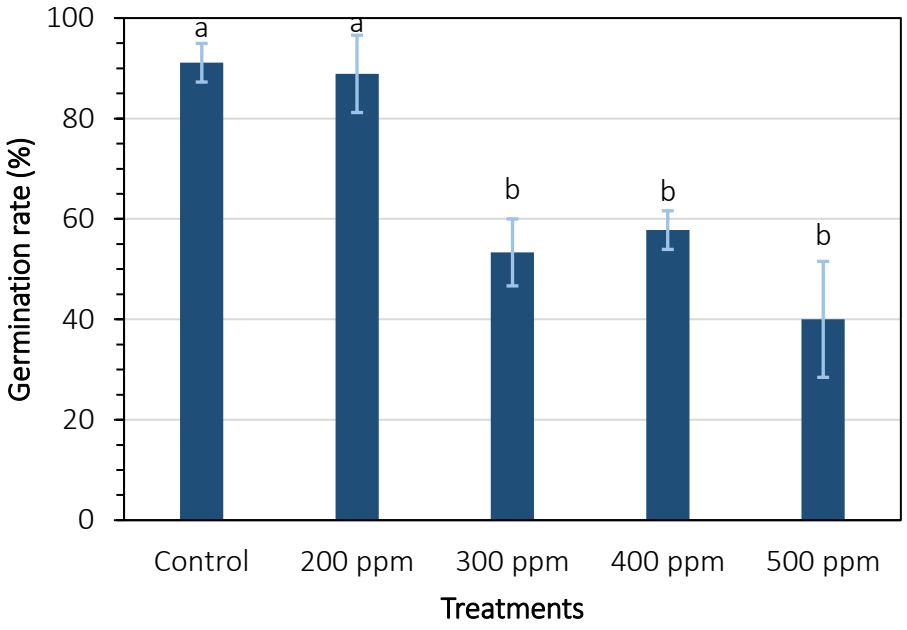

Figure 4.4 Germination rate (%) of ClO_2-treated and control wheat kernels

4.3.4 Milling outcomes

The milling outcomes of ClO_2-treated and control wheat samples milled using the Chopin Mill are summarized in Table 4.4. Milling outcomes indicate efficiencies in the separation of bran, germ, and endosperm separation. In milling, the target is to extract as much endosperm as possible with less bran percentage. On average, the yield of straight-grade flour, shorts, and bran ranged from 65.3-68.5%, 7.9-10.0%, and 22.1-23.1%, respectively. Highest applied concentration (500 ppm) was not significantly different to the control both in terms of flour and bran percentage. Only 300 ppm treatment deviated from the non-significant difference in terms of straight-grade flour percentage in comparison to the control, which may be due to slight deviation from tempering moisture addition and varying inevitable losses during flour milling operation across all treatments. All other treatments did not result to any significant difference in straight-grade flour. Bran percentage did not vary significantly across all treatments and control and the value ranged from

22.1 to 23.1 % as-is. However, shorts percentage was found highest for 500 ppm treatment. Bran friability may have been increased with increasing ClO_2 concentration as significantly higher fine bran as indicated by higher shorts percentage were recovered from 500 ppm treatment. However, bran percentage was comprised of both coarse and fine bran and, hence, may have resulted in a different trend than the shorts.

Table 4.4 Milling outcomes of ClO_2-treated and control wheat samples milled using Chopin Mill

Milling outcomes (% as-is)	Treatment					F	P
	Control	200 ppm	300 ppm	400 ppm	500 ppm		
Straight-grade Flour	67.1 ± 1.1^{ab}	67.6 ± 1.1^{ab}	68.54 ± 0.96^{a}	66.7 ± 1.1^{ab}	65.3 ± 0.3^{b}	4.84	0.0197
Shorts	7.9 ± 0.9^{b}	8.6 ± 0.4^{b}	8.25 ± 0.31^{b}	8.9 ± 0.3^{ab}	10.0 ± 0.1^{a}	8.93	0.0025
Bran	22.7 ± 1.2	22.1 ± 0.8	22.31 ± 0.50	22.9 ± 0.6	23.1 ± 0.1	0.88	0.5084

Note: Mean values with different superscript letters in the same row differ significantly among different fumigation treatments ($P < .05$).

4.3.5 Proximate composition, total starch, and damaged starch

Table 4.5 shows the proximate composition, total starch, and damaged starch contents of ClO_2-treated and control wheat kernels milled into straight-grade flour. No significant difference in the moisture content (MC) of resultant flour was recorded among treated flours. No specific trend was observed in terms of this significant difference. All treatments resulted to MC values higher than the usual MC for wheat flour (14%w.b.). Higher percentage of MC may be attributed to the reduced workflow setting of a laboratory-scale mill due to fewer number of rolls for the wheat kernels to pass through as compared to commercial milling facility, thus less heat transfer between rolls and wheat (Rivera et al., 2020). In terms of the protein content, both the control and 300 ppm treated flours recorded significantly lower protein contents (14.6% and 14.3%, respectively) compared to the 200 ppm, 400 ppm, and 500 ppm treated flours (15.2%, 15.2%,

15.0%, respectively). The control yielded a significantly lower ash content (0.4%) compared to the 300 ppm (0.5%) and 400 ppm (0.5%) treated flour.

The total starch of the untreated and treated straight-grade flour ranged from 59.4% to 72.0%. The 200 ppm treated flour recorded the highest starch content (72.0%) that is significant when compared to the starch content of the 300 ppm and 500 ppm treated flour, but insignificant when compared to the control and 400 ppm treated flour. Lastly, no significant differences were observed for the damage starch across all treatments and control, but the value ranged from 13.8 UCDc to 15.9 UCDc.

Table 4.5 Proximate Composition, total starch, and damaged starch contents of ClO_2-treated and control wheat kernels milled into straight-grade flour

Parameter	ClO_2 Gas Treatment				
	Control	200 ppm	300 ppm	400 ppm	500 ppm
Moisture (% w.b.)	14.0 ± 0.2^{a}	14.2 ± 0.1^{a}	14.5 ± 0.08^{a}	14.1 ± 0.05^{a}	14.3 ± 0.2^{a}
Protein (% as-is)	14.6 ± 0.2^{b}	15.2 ± 0.2^{a}	14.3 ± 0.06^{b}	15.2 ± 0.2^{a}	15.0 ± 0.1^{a}
Crude Fiber (% as-is)	0.2 ± 0.01^{ab}	0.2 ± 0.03^{ab}	0.2 ± 0.0^{b}	0.2 ± 0.04^{a}	0.2 ± 0.02^{ab}
Crude Fat (% as-is)	0.03 ± 0.05^{b}	ND	0.3 ± 0.03^{a}	ND	ND
Ash (% as-is)	0.4 ± 0.04^{b}	0.4 ± 0.06^{ab}	0.5 ± 0.08^{a}	0.5 ± 0.03^{a}	0.4 ± 0.03^{ab}
Nitrogen-free extract (% as-is)	68.9 ± 0.4^{c}	70.01 ± 0.3^{b}	70.3 ± 0.2^{b}	69.0 ± 0.2^{c}	71.0 ± 0.2^{a}
Total Starch (%)	65.5 ± 4.0^{abc}	72.0 ± 2.7^{a}	59.4 ± 2.7^{c}	70.6 ± 1.1^{ab}	64.1 ± 0.9^{bc}
Damaged Starch (UCD_c)	15.3 ± 0.6^{a}	15.9 ± 1.9^{a}	14.6 ± 0.3^{a}	13.8 ± 0.5^{a}	14.3 ± 0.4^{a}

Note: Mean values with different superscript letters in the same row differ significantly among different fumigation treatments ($P < .05$); ND – not detected.

4.3.6 Effects of ClO_2 treatment on flour properties

The rapid visco analyzer (RVA) characteristics of ClO_2-treated and control wheat kernels milled into straight-grade flour are summarized in Table 4.6. In this RVA test, the first stage comprised of loading the mixture of wheat flour and distilled water to the RVA instrument at above ambient temperature and mixed by the paddle. Hydration of starch occurred during this stage wherein water started penetrating starch granules and bonded to protein particles. At the start,

minimal swelling of starch granules was observed at temperatures below 50 °C and aggressive swelling occurred towards high temperature at which granules began to burst (Batey, 2007). After reaching the peak temperature, peak viscosity was measured at this point. Results showed that the control flour recorded the significantly highest peak viscosity (3303.7 cP) as compared to the 200 ppm, 300 ppm, and 400 ppm ClO_2-treated flour. The decrease in peak viscosity among flours produced from ClO_2-treated wheat kernels may be attributed to the possibility of glycosidic bond cleavage in its starch molecules and depolymerization of amylopectin (Balet et al., 2019). Chlorine dioxide acts as a monomeric free radical giving its oxidizing capacity (Simpson, 2005; Gomez-Lopez et al., 2009). According to Bashir and Haripriya (2016), these free radicals can cleave glycosidic bonds, thus causing starch polymers to decompose into macromolecules characterized by shorter chain lengths. After peak viscosity and temperature was reached, a decrease in viscosity was observed as the peak temperature was held for 2 min and lowest viscosity associated with this decrease is called the trough viscosity (Balet et al., 2019). No significant difference was observed for the trough viscosities and pasting temperatures across control and all ClO_2 treatments. Pasting temperature is the temperature at which viscosity of the mixture starts to rise. Thus, statistically similar pasting temperature among control and ClO_2-treated samples indicates similar minimum temperature required to cook these flour samples (Sandhu et al., 2007). The breakdown viscosities ranged from 527 cP to 927 cP with the control having the highest breakdown viscosity and 300 ppm-treated flour having the lowest. The breakdown viscosity is the difference between the peak viscosity and trough viscosity (viscosities measured at the start of peak temperature and end of holding time). Since trough viscosities of samples were not significantly different, the significant difference on breakdown viscosity is predominantly due to the difference in peak viscosity of the samples. Zaidul et al. (2007) explained that breakdown viscosity is associated with peak viscosity

that gives an idea about degree of swelling of starch granules with application of heat. Breakdown viscosity is a measure of starch granule disintegration and paste stability of flour-water mixture (Dengate, 1984). During holding time, swollen starch granules further burst, causing amylose to leach out into the mixture (Zaidul et al. 2007; Newport Scientific, 1995). The control flour also recorded the significantly highest final viscosity (3515 cP) compared to all other treated flours. The same is true for the setback viscosity (difference between peak and final viscosities) except when compared to the 400 ppm-treated flour. In the study of Li et al. (2012), it was explained that the decrease in setback viscosity of wheat flour may be due to high oxidation resulting to higher tendency of retrogradation. The lower setback viscosities of ClO_2-treated samples in comparison to control samples indicate lower tendency of starch granules to undergo retrogradation during cooling (Sandhu et al., 2007). Less retrogradation is desirable in terms of breadmaking as retrogradation significantly influences bread staling or crumb firming (Santos et al., 2008). Finally, the peak times of all sample ranged from 6.6 to 6.7 min.

Table 4.6 RVA characteristics of ClO_2-treated and control wheat kernels milled into straight-grade flour

RVA characteristics	ClO_2 Gas Treatment				
	Control	200 ppm	300 ppm	400 ppm	500 ppm
Peak Viscosity (cP)	3303.7 ± 27.4[a]	3003.0 ± 95.4[b]	2849.0 ± 49.0[b]	2984.3 ± 143.3[b]	3073.3 ± 68.3[ab]
Trough Viscosity (cP)	2376.3 ± 106.1[a]	2302.0 ± 15.4[a]	2278.0 ± 34.4[a]	2256.7 ± 61.0[a]	2236.0 ± 56.6[a]
Breakdown Viscosity (cP)	927.3 ± 127.6[a]	701.0 ± 81.0[ab]	571.0 ± 42.0[b]	727.7 ± 145.6[ab]	837.3 ± 100.1[ab]
Final Viscosity (cP)	3515.0 ± 22.6[a]	3286.0 ± 47.2[b]	3254.0 ± 33.3[b]	3300.3 ± 69.7[b]	3208.3 ± 33.1[b]
Setback Viscosity (cP)	1138.7 ± 83.8[a]	984.0 ± 35.8[b]	976.0 ± 32.7[b]	1043.7 ± 9.1[ab]	972.3 ± 59.2[b]
Peak Time (min)	6.6 ± 0.04[b]	6.7 ± 0.1[ab]	6.9 ± 0.04[a]	6.7 ± 0.2[ab]	6.6 ± 0.1[b]
Pasting Temperature (°C)	68.6 ± 0.1[a]	69.1 ± 0.5[a]	69.1 ± 0.4[a]	69.1 ± 0.5[a]	68.8 ± 0.4[a]

Note: Mean values with different superscript letters in the same row differ significantly among different fumigation treatments ($P < .05$).

Figure 4.5 shows Mixolab curves and Table 4.7 summarizes the Mixolab characteristics of the ClO_2-treated and control wheat kernels milled into straight-grade flour. This Mixolab test provides information about dough behavior of wheat flour samples as subjected to heating and mixing stresses. The parameters measured in this curve include C1 (maximum torque during mixing), CS (indicates dough consistency at the end of mixing time), C2 (relates to protein weakening caused by mechanical work and increase in temperature), C3 (relates to starch gelatinization), C4 (indicates starch gel stability), C5 (measure of starch retrogradation as the gel cools down), water absorption (percentage of water required to for the dough to reach a torque of 1.1 ± 0.05 Nm), stability time (time at which dough achieves consistent torque of 1.1 ± 0.05 Nm during mixing), and dough development time (time needed for dough to reach maximum torque). It is also a measure of protein and starch quality of wheat flour. Mixolab stages such as C2, C3,

C4, dough development time, and dough stability were found to be positively correlated with specific loaf volume (Banu et al., 2011; Dhaka et al., 2013). The control flour recorded the highest absorption (59.40 %) while the 500 ppm-treated flour recorded the lowest (55.37 %). The development time, stability, dough development, protein weakening, starch gelatinization, enzymatic and thermal breakdown, and starch retrogradation ranged from 8.73 to 9.37 min, 11.20 to 11.87 min, 1.12 to 1.15 Nm, 0.53 to 0.57 Nm, 0.9 to 1.65 Nm, 1.82 to 186 Nm, and 2.62 to 2.86 Nm, respectively. These results indicate that ClO_2 gas treatment did not alter the mixing properties relative to control samples. Similar C2 value also indicate that flour samples were similar in terms of protein quality even after ClO_2 gas treatment.

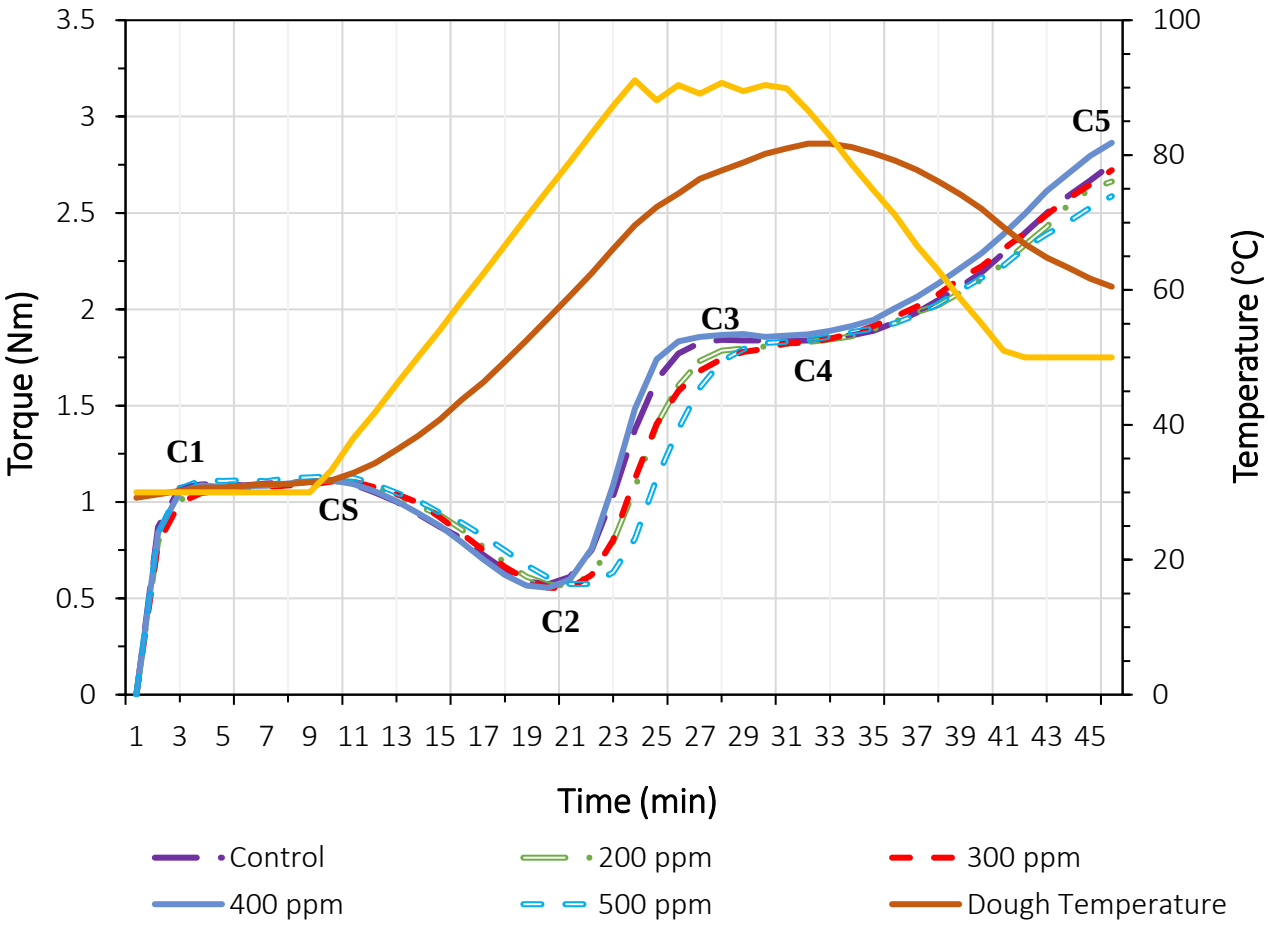

Figure 4.5 Mixolab curves of flour milled using wheat kernels treated with ClO_2 gas

Table 4.7 Mixolab characteristics of ClO_2-treated and control wheat kernels milled into straight-grade flour

Mixolab Characteristics	ClO_2 Gas Treatment				
	Control	200 ppm	300 ppm	400 ppm	500 ppm
Absorption (%)	59.4 ± 0.5[a]	57.40 ± 0.7[b]	58.57 ± 0.5[ab]	59.77 ± 0.9[a]	55.37 ± 0.8[c]
Development time (min)*	8.8 ± 0.3	9.37 ± 0.1	9.31 ± 0.5	8.91 ± 0.4	9.03 ± 0.4
Stability (min)*	11.3 ± 0.4	11.70 ± 1.0	11.87 ± 0.4	11.20 ± 0.7	11.67 ± 0.2
C1 - dough development (Nm)*	1.1 ± 0.02	1.12 ± 0.03	1.12 ± 0.01	1.12 ± 0.03	1.15 ± 0.01
Cs (Nm)*	1.1 ± 0.03	1.11 ± 0.03	1.09 ± 0.2	1.10 ± 0.04	1.13 ± 0.01
C2 - protein weakerning (Nm)*	0.6 ± 0.01	0.55 ± 0.02	0.53 ± 0.02	0.55 ± 0.01	0.56 ± 0.00
C3 - starch gelatinization (Nm)*	1.5 ± 0.3	1.07 ± 0.3	1.12 ± 0.4	1.65 ± 0.2	0.90 ± 0.1
C4 - enzymatic and thermal breakdown (Nm)*	1.8 ± 0.1	1.82 ± 0.01	1.82 ± 0.1	1.86 ± 0.01	1.84 ± 0.02
C5 - starch retrogradation (Nm)*	2.8 ± 0.1	2.73 ± 0.1	2.72 ± 0.2	2.86 ± 0.09	2.62 ± 0.05

Note: Mean values with different superscript letters in the same row differ significantly among different fumigation treatments ($P < .05$).
*no significant difference were found ($p > 0.05$); F-values: Development time – 1.38, Stability – 0.68, C1 – 0.84, Cs – 1.07, C2 – 3.47, C3 – 3.29, C4 – 0.37, and C5 – 1.41.

Shown in Table 4.8 are the color, pH, and falling number values of ClO_2-treated and control wheat kernels milled into straight-grade flour. The 500 ppm flour sample recorded the highest lightness (L*) value of 89.4 while the control recorded the lowest (86.4). In terms of the a* and b*, the control recorded significantly lower values (0.8 and 10.2, respectively) compared to the values of 200 ppm, 300 ppm, and 400 ppm treated flours. Since both a* and b* results were positive values, color of ClO_2-treated samples become less red and less yellow. Increasing concentration of ClO_2 gas treatment on wheat kernels led to brighter flour. In general, color results of ClO_2-treated samples were more acceptable in visual aspect as wheat flour normally undergoes chlorination for bleaching purposes. The brighter color of ClO_2-treated samples may be attributed to the reduced polyphenol oxidase activity due to exposure to ClO_2 gas, which in turn, decrease the level of enzymatic darkening. Moreover, ClO_2 gas exposure also causes break down of natural

yellow compounds such as carotenoid and flavone (Cheng et al., 2021). In terms of pH, the control recorded the highest pH (6.18) while the 500-ppm treated sample recorded the lowest (6.06). Meanwhile, there are no significant differences in the pH values of the control, 200 ppm, 300 ppm, and 400 ppm treated flours. The decrease in pH after ClO_2 gas treatment of 500 ppm in comparison to control sample may be attributed to the oxidation of lipid and starch upon exposure to ClO_2 gas treatment (Cheng et al., 2021). Lastly, the values of the falling number for the control, 200 ppm, 300 ppm, 400 ppm, and 500 ppm are 579.2, 539.5, 553.2, 558.3, and 528.8, respectively.

Table 4.8 Color, pH, and falling number of ClO_2-treated and control wheat kernels milled into straight-grade flour

Treatment	Color			pH	Falling number*
	L*	a*	b*		
Control	86.4 ± 0.5^{c}	0.8 ± 0.04^{c}	10.2 ± 0.2^{b}	6.28 ± 0.06^{a}	579.2 ± 36.0
200 ppm	87.5 ± 0.3^{bc}	1.0 ± 0.00^{ab}	11.2 ± 0.2^{a}	6.14 ± 0.03^{ab}	539.5 ± 19.9
300 ppm	87.9 ± 0.7^{b}	1.1 ± 0.03^{a}	11.8 ± 0.01^{a}	6.14 ± 0.02^{ab}	553.2 ± 37.5
400 ppm	88.5 ± 0.7^{ab}	1.0 ± 0.10^{a}	11.3 ± 0.7^{a}	6.11 ± 0.01^{ab}	558.3 ± 31.9
500 ppm	89.4 ± 0.4^{a}	0.9 ± 0.04^{bc}	10.9 ± 0.3^{ab}	6.06 ± 0.03^{b}	528.8 ± 13.0

Note: Mean values with different superscript letters in the same row differ significantly among different fumigation treatments ($p < .05$); *$F = 1.29$; $P = 0.3386$.

4.4 Summary and Conclusion

This study explored the efficacy of ClO_2 gas in killing adult lesser grain borers through purging ClO_2 gas and holding specific quantity of gas in the fumigation chamber for 24 hours and investigated its effects on wheat kernel and flour quality. ClO_2 gas purging assembly were used to fumigate gas-tight buckets half-filled with hard red spring wheat and vials containing adult lesser grain borers (located at top, middle, and bottom layers of wheat mass) at varying ClO_2 gas concentrations (200, 300, 400, and 500 ppm).

Based on the results of this study, conclusions were:

1. Statistically similar times (h) were needed to reach 1st and 2nd half-lives and 90% concentration loss for all treatments.
2. ClO_2 treatment was effective in killing adult lesser grain borers at 500 ppm treatment across all vial locations.
3. Adult progeny production at 500 ppm treatment indicated possibility of reinfestation even after complete mortality was achieved.
4. ClO_2 gas (300-500 ppm) reduced germination rate of wheat kernels; 200-500 ppm treatments increased lightness and decreased peak and final viscosities; and 500 ppm treatment reduced pH.
5. Flours from ClO_2-treated wheat kernels had comparable characteristics to the control sample in terms of falling number, trough viscosity, breakdown viscosity, starch damage, and mixolab dough behavior properties.

4.5 References

AACC International. (2010), Approved methods of analysis (11th ed.), Method 46-30.01, Crude Protein-Combustion method; Method 76-13.01, Total Starch Assay Procedure; Method 76-33.01, Damaged starch – Amperometric Method; Method 56-81.04, Determination of Falling Number; Method 76-21.02, General Pasting Method for Wheat or Rye Flour or Starch Using the Rapid Visco Analyzer; Method 54-60.01, Determination of Rheological Behavior as a Function of Mixing and Temperature Increase in Wheat Flour and Whole Wheat Meal by Mixolab; St. Paul, MN: AACC International.

AOAC International (2019, Official methods of analysis (21st ed.), Method 923.03 – Ash Determination; Method 922.06-Fat in flour acid hydrolysis method; Method 962.09 – Fiber

in Animal Feed and Pet Food, Association of Official Agricultural Chemists, Rockville, MD.

ASAE International (1988), Method S352.2- Moisture Measurement-Unground Grain and Seeds. American Society of Agricultural and Biological Engineers, St. Joseph, Michigan

Abbott, W. S. (1925). A method of computing the effectiveness of an insecticide. J. econ. Entomol, 18(2), 265-267.

Balet, S., Guelpa, A., Fox, G., & Manley, M. (2019). Rapid Visco Analyser (RVA) as a tool for measuring starch-related physiochemical properties in cereals: A review. Food Analytical Methods, 12(10), 2344-2360.

Banu, I., Stoenescu, G., Ionescu, V., & Aprodu, I. (2011). Estimation of the baking quality of wheat flours based on rheological parameters of the Mixolab curve. Czech journal of food sciences, 29(1), 35-44.

Bashir, M., & Haripriya, S. (2016). Physicochemical and structural evaluation of alkali extracted chickpea starch as affected by γ-irradiation. International journal of biological macromolecules, 89, 279-286.

Batey, I. L. (2007). Interpretation of RVA curves. The RVA handbook, 19-30.

Cheng, Z., Li, X., Hu, J., Fan, X., Hu, X., Wu, G., & Xing, Y. (2021). Effect of Gaseous Chlorine Dioxide Treatment on the Quality Characteristics of Buckwheat-Based Composite Flour and Storage Stability of Fresh Noodles. Processes, 9(9), 1522.

Dengate, H. N. (1984). Swelling, pasting, and gelling of wheat starch. Advances in Cereal Science and Technology (USA).

Dhaka, V., & Khatkar, B. S. (2013). Mixolab thermomechanical characteristics of dough and bread making quality of Indian wheat varieties. Quality Assurance and Safety of Crops & Foods, 5(4), 311-323.

Dobrin, D., Magureanu, M., Mandache, N. B., & Ionita, M. D. (2015). The effect of non-thermal plasma treatment on wheat germination and early growth. Innovative Food Science & Emerging Technologies, 29, 255-260.

E, X., Li, B., & Subramanyam, B. (2018). Toxicity of chlorine dioxide gas to phosphine-susceptible and-resistant adults of five stored-product insect species: Influence of temperature and food during gas exposure. Journal of economic entomology, 111(4), 1947-1957.

E, X., Subramanyam, B., & Li, B. (2017). Efficacy of ozone against phosphine susceptible and resistant strains of four stored-product insect species. Insects, 8(2), 42.

Han, G. D., Kwon, H., Kim, B. H., Kum, H. J., Kwon, K., & Kim, W. (2018). Effect of gaseous chlorine dioxide treatment on the quality of rice and wheat grain. Journal of Stored Products Research, 76, 66-70.

Kim, B. H., Han, G. D., Kwon, H., Chun, Y. S., Na, J., & Kim, W. (2019). Chlorine dioxide fumigation to control stored product insects in rice stored in a room. Journal of Stored Products Research, 84, 101527.

Li, M., Zhu, K. X., Wang, B. W., Guo, X. N., Peng, W., & Zhou, H. M. (2012). Evaluation the quality characteristics of wheat flour and shelf-life of fresh noodles as affected by ozone treatment. Food chemistry, 135(4), 2163-2169.

Neethirajan, S., Karunakaran, C., Jayas, D. S., & White, N. D. G. (2007). Detection techniques for stored-product insects in grain. Food control, 18(2), 157-162.

Newport Scientific (1995). Operation manual for the series 4 Rapid Visco Analyzer. Newport Scientific Pty. Ltd, 10-18.

Ramsey, C. L., & Mathiason, C. (2019). Novel Use of Chlorine Dioxide Granules as an Alternative to Methyl Bromide Soil Fumigation. Global Journal of Agricultural Innovation, 6, 000-000.

Sandhu, K. S., Singh, N., & Malhi, N. S. (2007). Some properties of corn grains and their flours I: Physicochemical, functional and chapati-making properties of flours. Food Chemistry, 101(3), 938-946.

Santos, E., Rosell, C. M., & Collar, C. (2008). Gelatinization and retrogradation kinetics of high-fiber wheat flour blends: A calorimetric approach. Cereal Chemistry, 85(4), 455-463.

Simpson, G. D. (2005). Practical chlorine dioxide. Foundations, Volume 1. Greg D. Simpson & Associates, Colleyville, TX.

US Department of Agriculture (USDA). (2022). Retrieved 23 July 2022 from https://www.ers.usda.gov/topics/crops/wheat/.

Zaidul, I. S. M., Yamauchi, H., Kim, S. J., Hashimoto, N., & Noda, T. (2007). RVA study of mixtures of wheat flour and potato starches with different phosphorus contents. Food Chemistry, 102(4), 1105-1111.

Chapter 5 - Summary and Recommendations

5.1 Summary

The first part of this thesis was conducted with the aim of establishing sorption kinetic and isotherm models for phosphine gas into wheat kernels that would provide essential information to phosphine sorption capacity of wheat and its rate of uptake during fumigation. Summary of results obtained from the first part of this thesis are below:

1. Sorption process of PH_3 into wheat kernels occurred in two phases for all treatments. First, a rapid sorption phase indicated by steeper slopes at the start of the process followed by gradual decrease in sorption rate as concentration nears its equilibrium.
2. Pseudo-first order model fitted well to the experimental data of sorbed PH_3 concentration through time. Pseudo-second order overpredicted endpoint values that are not applicable to the analysis as it also exceeds the known initial concentrations.
3. Equilibrium concentrations at the headspace and sorbed quantities of PH_3 into wheat kernels can be described by Langmuir, Freundlich, and Redlich-Peterson sorption isotherm models.
4. Increase in adsorption capacity with the increase in applied concentration indicates that maximum wheat adsorption capacity is still not reached at equilibrium points of lower concentrations applied to fumigation chambers.

The second objective of this thesis was to investigate chlorine dioxide as a potential fumigant alternative to phosphine in terms of its kinetics, insect mortality of a common stored-product species – lesser grain borer, and effects on wheat kernel and flour characteristics. Summary of results from the second part of this study are below:

1. The best-fit model for the ClO_2 concentration versus time is $\ln(y) = a + bx$. Model coefficients describing change in concentration for 24 h were estimated for all treatments.
2. No significant difference ($P > 0.05$) for the time needed to reach 1st and 2nd half-lives and 90% concentration loss for all treatments. On average, the peak concentration took about 1.5 to 1.9 h to fall at 50% of its value, about 2.9 to 3.6 h to fall at 25% of its value, and about 4.2 to 6.8 h to fall at 10% of its value.
3. ClO_2 treatment achieved complete insect mortality at 500 ppm across all vial locations. Increased mortality was observed with increasing ClO_2 concentration.
4. 200 ppm treatment resulted in the highest adult progeny production of about 39.7 to 48.7, which is about 48.3 to 59.0% of adult progeny reduction relative to the control treatment. The adult progeny reduction averaged from 92.1 to 97.2% for 300 ppm treatment; 96.2 to 97.2% for 400 ppm treatment; and 96.6 to 99.0% for 500 ppm treatment.
5. On average, straight-grade flour production of ClO_2-treated wheat kernels was about 65.3-68.5%.
6. Significant reduction (37.8-51.1%) in germination rate resulted after exposure to 300-500 ppm.
7. In terms of flour color, lightness value significantly increased ($P < 0.05$) after treatment of 200-500 ppm.
8. The pH value of wheat flour had significant reduction ($P < 0.05$) from 6.2 to 6.1 after 500 ppm treatment.

9. In terms of pasting characteristics, peak and final viscosities of ClO_2-treated wheat flour at 200-500 ppm significantly decreased ($P < 0.05$) from 3303.7 to 3073.3 cP and from 3515.0 to 3208.3 cP, respectively.
10. No significant difference ($P > 0.05$) was observed in other investigated flour quality and functionality parameters, including falling number, trough viscosity, breakdown viscosity, starch damage, and mixolab dough behavior properties.

5.2 Recommendations

For the phosphine-wheat study, the models developed in this study is limited to ½ filling ratio. Filling ratio would affect equilibrium headspace concentrations. Increasing filling ratio means addition of adsorbate that shares the phosphine molecules that adhere and adsorb into wheat. Hence, better understanding of phosphine-wheat sorption process through investigating effect of filling ratios on the developed kinetic and isotherm models. Although previous study of Daglish and Pavic (2008) discussed phosphine concentrations were relatively stable and minimal degradation occurred during their sorption experiment, degradation of this compound through time may also have influence on the final equilibrium concentration. Hence, it is essential to quantify the degree of degradation of phosphine in phosphine-wheat system through time.

For the chlorine dioxide study, the fumigation buckets were housed in a trailer that is not equipped with a temperature control. Hence, the temperature varies throughout 24 hours during day and night. The kinetic study of ClO_2 during wheat fumigation may be extended by investigating effect of controlled temperatures (within the range of usual temperatures when fumigation is done in actual grain bins) on the percentage of ClO_2 gas

concentration loss. Understanding ClO_2 behavior within enclosed structure will help in future modelling studies focusing on optimization of fumigation practices once this chemical. Studies related to circulation of ClO_2 gas should be understood to achieve similar laboratory-scale fumigation effectiveness in large-scale setting. In this way, influence of the high and low temperature on ClO_2 concentrations, as well as wheat kernel and flour quality may be explored. Another important direction for this research study is to investigate the effects of repeated ClO_2 gas treatments on wheat and wheat-based product quality as reinfestation may occur throughout transport and storage. Residue and sensory analyses are also recommended to ensure both safety and acceptability of the fumigated wheat and its derivatives such as wheat flour. In terms of efficacy of ClO_2 gas in reducing adult progeny production, investigating concentrations that could completely eradicate adult progeny production is critical. Further investigation on establishing baseline concentrations and dosages effective in controlling immature stages of insect species to prevent likelihood of reinfestation due to progeny production could be explored.